SAND 86-8179

MCDONNELL DOUGLAS CORPORATION

SOLAR ONE
BEAM CHARACTERIZATION SYSTEM
DESIGN DESCRIPTION AND REQUIREMENTS DOCUMENT

AUGUST 1986

PREPARED BY:
J.B. BLACKMON

APPROVED BY:
R.G. RIEDESEL

Prepared Under Sandia Contract 84-8173
Revised Under Sandia Contract 90-1523

MCDONNELL DOUGLAS ASTRONAUTICS COMPANY-HUNTINGTON BEACH
5301 Bolsa Avenue Huntington Beach, California 92647 (714) 896-3311

CONTENTS

APPENDICES

FIGURES

TABLES

PREFACE

This document is provided by the McDonnell Douglas Astronautics Company (MDAC) in accordance with Sandia National Laboratories Contracts 84-8173 and 90-1523. The purpose of this document is to provide a comprehensive description of the Solar One Beam Characterization System (BCS). Detailed descriptions are provided of BCS hardware, software, supporting analysis, operational sequences, and the fundamental principles involved. Additional information is presented in the "Beam Characterization System Operator/Users Manual" and in the computer program unit Development Folders.

Section 1
EXECUTIVE SUMMARY

1.1 INTRODUCTION

Early in the development of solar central receivers, it was recognized that some means of aligning, monitoring, and evaluating large numbers of heliostats would be required. To meet these objectives, a Digital Image Radiometer (DIR) was conceived in 1974 at McDonnell Douglas Astronautics Company as part of a company funded solar research and development program. This system was used to evaluate heliostats in desert tests conducted in 1974-1975 and in 1976-1977 at the Naval Weapons Center, as shown in Figure 1-1 and described in Reference 1. Results showed that total beam power, irradiance distribution, beam centroid, tracking accuracy, and overall mirror reflectivity were accurately and rapidly determinable.

An improved version was installed in late 1977 at the MDAC Huntington Beach Solar Energy Test Facility, and used to evaluate various mirror modules and heliostats. A similar device termed the Heliostat Beam Characterization System, was developed at Sandia Laboratories Central Receiver Test Facility in 1978, and used extensively in the evaluation of various heliostat designs (References 2 to 6).

The basic DIR approach was originally selected because it offered very high resolution; high acquisition rates; real-time visual monitoring; used passive targets; required little maintenance; and was the lowest cost system, when compared to use of calorimeters or arrays of moving or stationary point detectors mounted on the tower.

These advantages, coupled with the successful experience with the first DIR systems at MDAC and Sandia, led to the selection of the DIR as the Beam Characterization System at the Solar I 10MWe Pilot Plant in Daggett, California (Figure 1-2). Additional requirements imposed on this system involved automatic operation, sophisticated integration with other subsystems, and a variety of options for acquiring, storing and analyzing data, both on-line and off-line. The principal uses of this system are to provide an

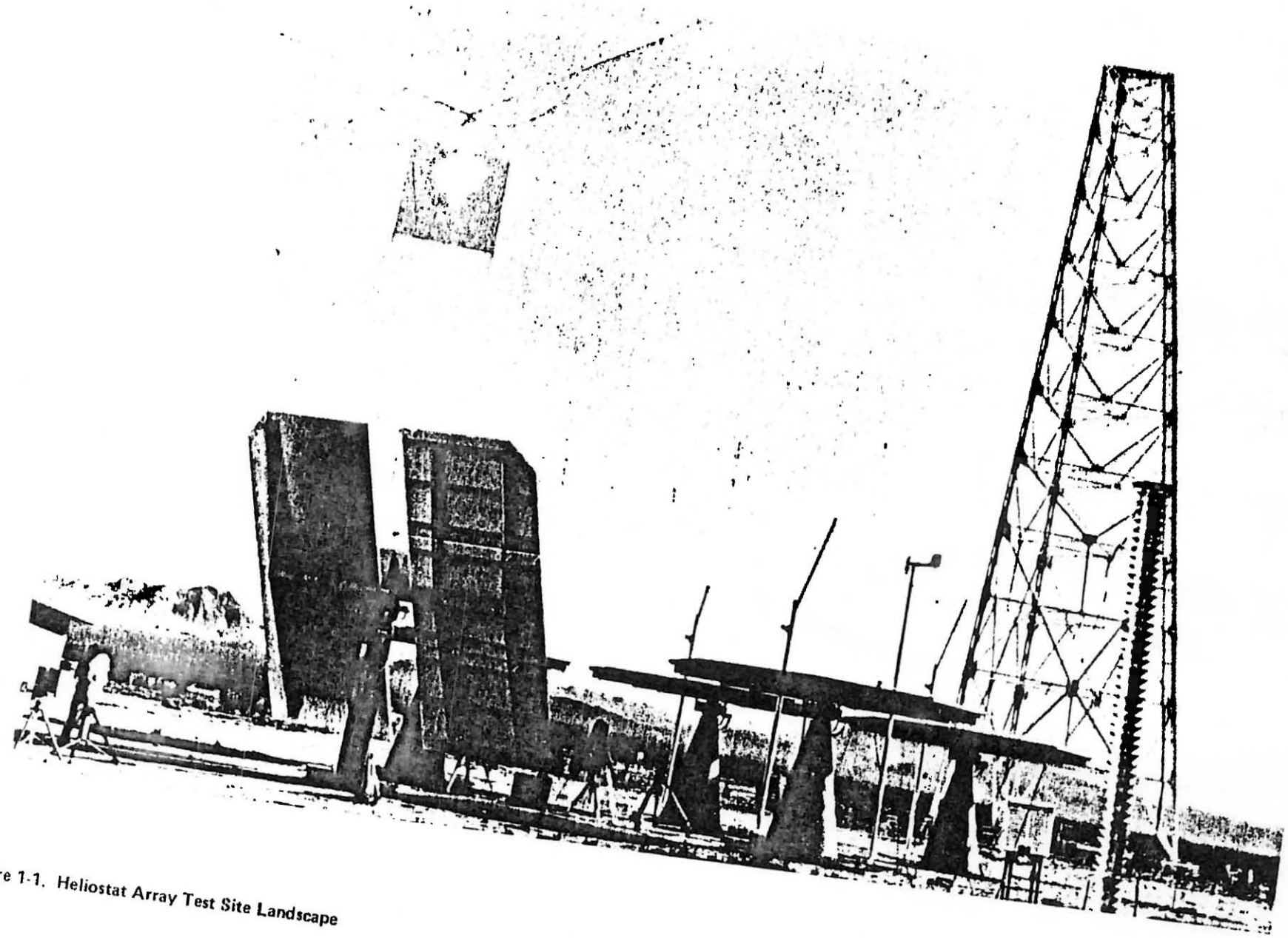

Figure 1-1. Heliostat Array Test Site Landscape

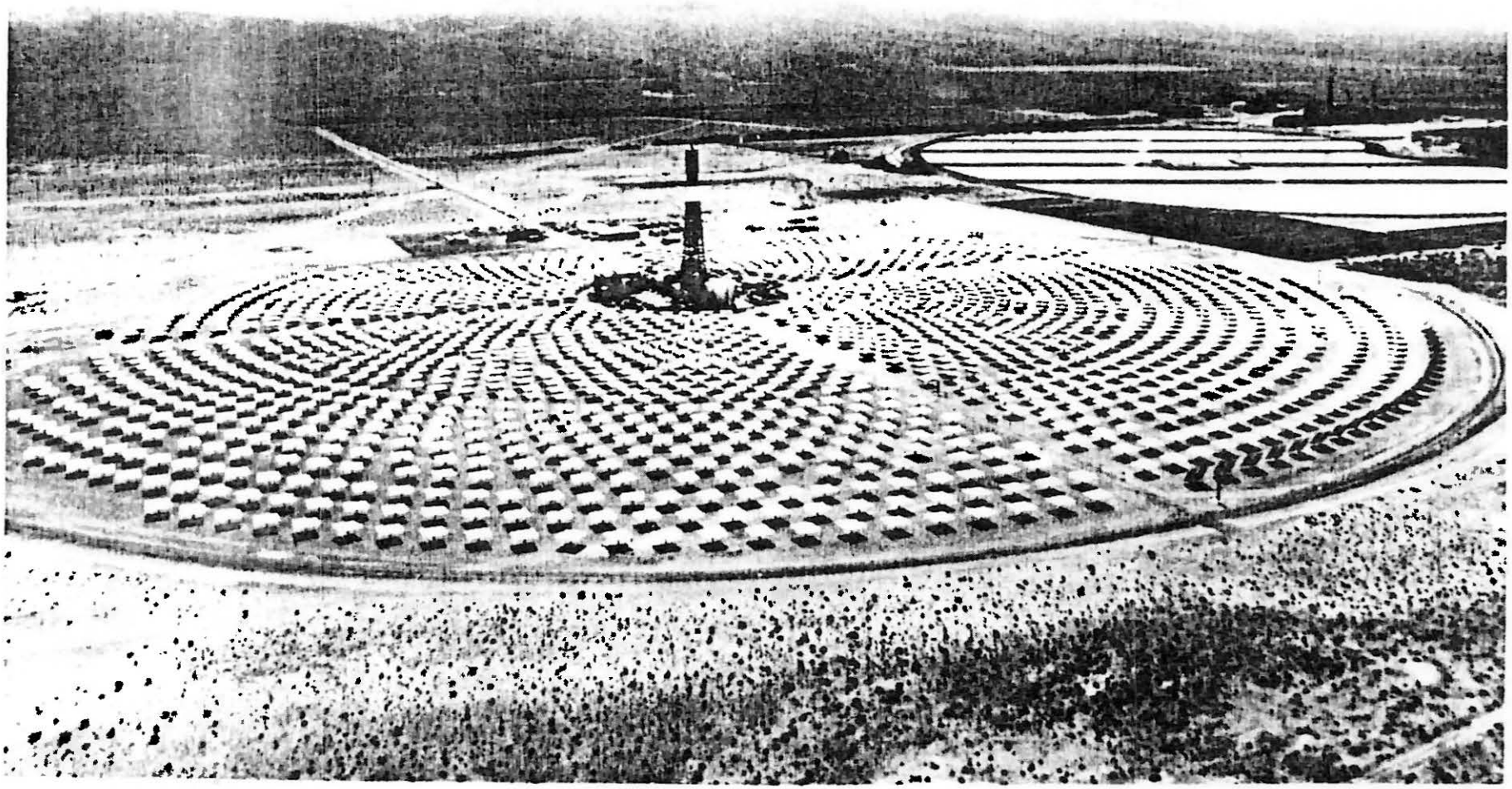

Figure 1-2. Aerial Photograph of Solar One Landscape

automatic update of heliostat tracking aimpoint biases, and to monitor heliostat optical performance. This system has been operational since September, 1982 (Reference 7). Improvements were made in 1983-84, such as the addition of a camera to track the sun and determine the solar radiance distribution simultaneous with each beam scan. The BCS now provides comparisons of observed beam shape with computer codes which use the solar radiance distribution data and theoretical heliostat optical characteristics to evaluate performance.

1.2 DESIGN

The basic requirement of the Solar One Beam Characterization Subsystem (BCS) is to characterize the reflected beam from a heliostat or mirror module, with respect to the beam size and shape, flux distribution, beam centroid, and beam power. The BCS is used to align and evaluate heliostats as part of the Pilot Plant functional and integrated acceptance test program, and provides operational support for collector subsystem realignment, performance evaluation, and maintenance throughout the plant operation. The BCS design requirements are defined by RADL Item 3-1, BCS Technical Objectives and Design Requirements, Reference 8. A summary of design requirements is given in Section 2. The overall system design principles and performance are described below.

The BCS is based on the Digital Image Radiometer (DIR) measuring and recording instrument and is shown in Figures 1-3 and 1-4. The basic BCS consists of four video cameras each of which views an elevated target mounted on the tower beneath the receiver. The video analog output signals are digitized to provide a measure of beam intensity incident on each target from a heliostat. The digitized intensity for a particular frame is correlated with absolute intensity measurements made nearly simultaneously by a calibration procedure utilizing three target mounted radiometers. The targets are flat structures painted with a high temperature white paint specifically selected for its near-Lambertian reflectance characteristics to minimize glare and provide uniform reflection over the target surface. Three radiometers are positioned about the center of the target within the area of a centered beam

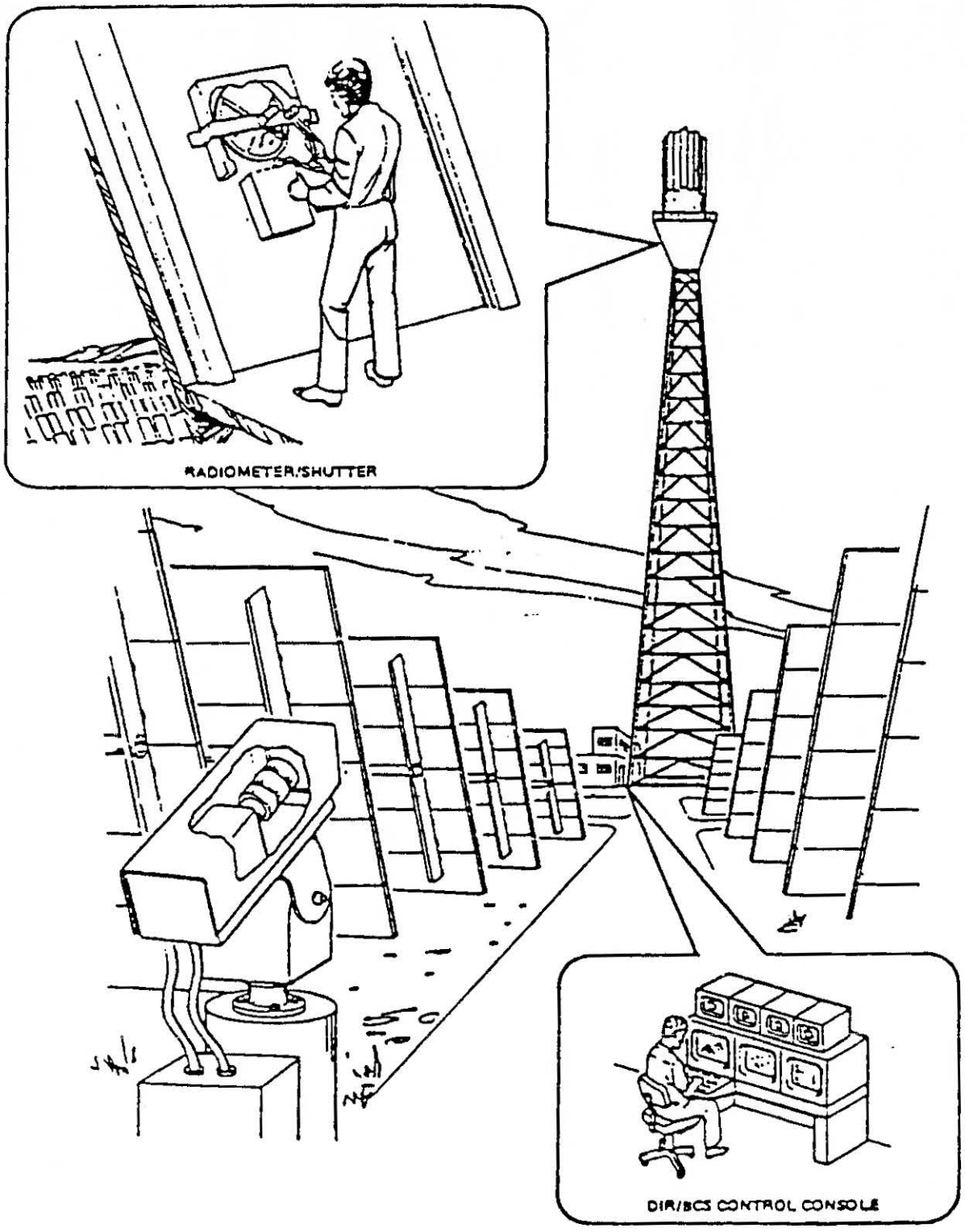

Figure 1-3. Digital Image Radiometer Beam Characterization Subsystem

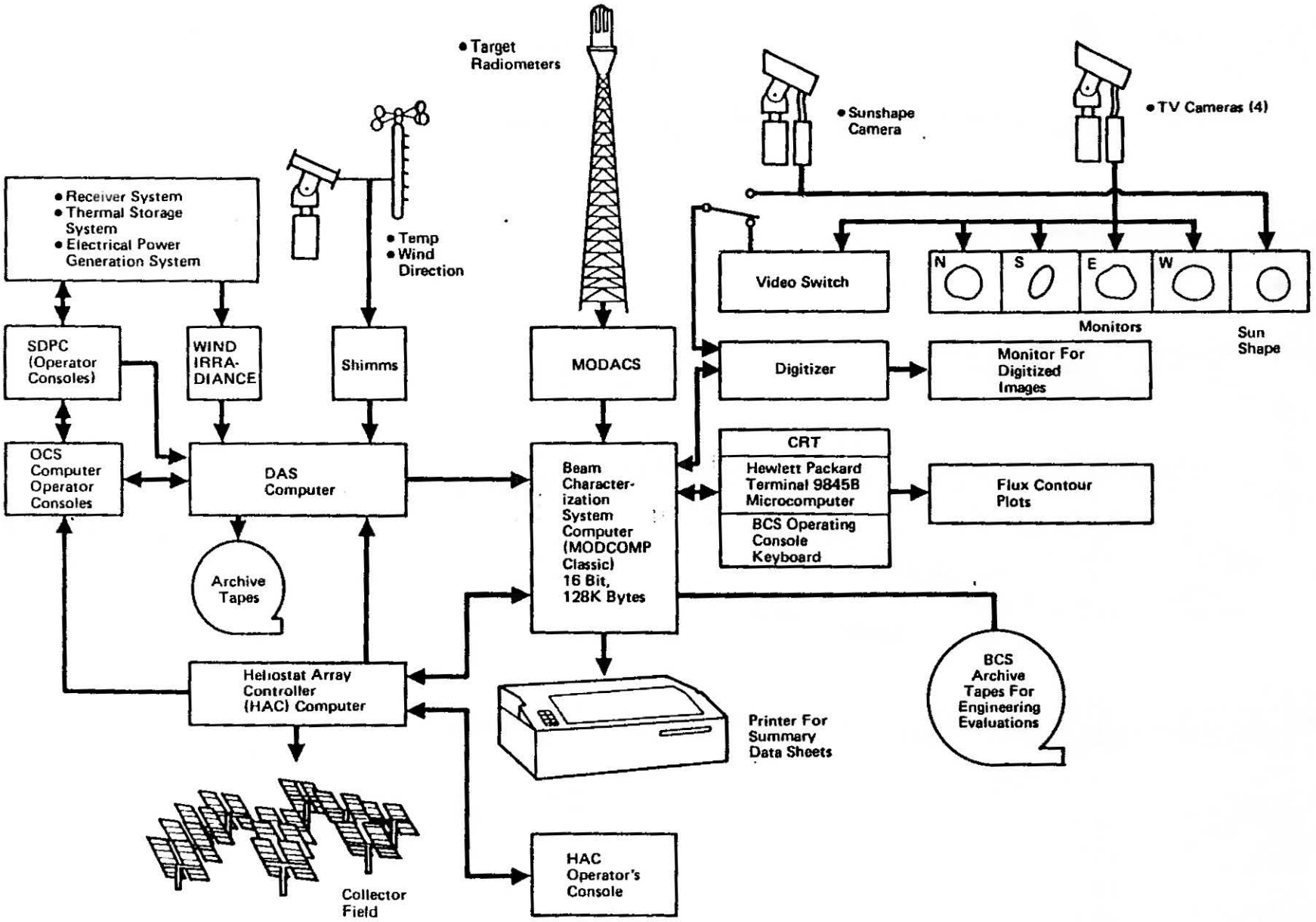

Figure 1-4. BCS Interface Block Flow Diagram Landscape

image so as to provide reflected beam irradiance measurements over some portion of the moderate to high intensity regions of the beam and thus improve the calibration curve accuracy.

Simultaneous measurements of the sun's radiance distribution are made with a specially modified video camera which tracks the sun. These data, coupled with the absolute measurements of incident irradiance, are used in computer codes which compare actual and theoretically ideal heliostat irradiance distributions. Additional radiometers located in the field as part of the data acquisition subsystem (DAS) determine incident solar irradiance, which is used to establish heliostat reflective efficiency as measured at the target.

Beam centroid data are obtained to establish heliostat aimpoints, which are then corrected as necessary by changing bias values in the Heliostat Array Controller (HAC) code. Supporting data on heliostat performance consist primarily of net power, tracking error variations, spillage power, overall power effectivity, and environmental conditions such as wind speed, direction, temperature, and solar irradiance. These data, coupled with displays of the beam contour on the target and, as required, solar radiance distribution, are provided for operator usage and engineering evaluation.

1.3 PERFORMANCE

The BCS measures up to 60 heliostats three times per day automatically. Centroid measurement accuracy is of the order of, and usually better than ± 2 inches, although wind induced heliostat movement can cause the standard deviation of beam centroid location to exceed this value. The corresponding angular error is approximately ± 0.15 mr. Beam power measurement accuracy is approximately $\pm 5\%$, with low wind, clear sky conditions (for beams located properly on the target).

Data required for heliostat bias updates, used to correct tracking errors, are subjected to a series of validity algorithms prior to being transmitted to the Heliostat Array Controller, to minimize operator review of the data.

The sunshape camera data for solar irradiance has been analyzed by Sandia National Laboratories and found to be in good agreement with similar data acquired by the Lawrence Berkeley Laboratory Circumsolar Telescope. Solar radiance data is acquired in 1/30 second during the last image grab of a particular beam on a target and is thus closedly correlated with heliostat beam data.

The following sections describe the design, operation, and principles of the BCS. Additional descriptive material is provided in the Appendices and in supporting publications referenced in the text.

Section 2
BCS PERFORMANCE REQUIREMENTS AND CAPABILITIES

Performance requirements and capabilities are provided in this section for (1) parameters to be measured by the BCS, (2) design requirements, (3) output data and analysis, and (4) environmental design conditions.

2.1 MEASURED PARAMETERS - BCS

The BCS is capable of measuring the following parameters:

- Absolute flux distribution (w/m^2)
- Relative flux distribution (non-dimensional)
- Reflected beam centroid from a heliostat relative to a specified location on the target
- Total power in beam
- Background power on target
- Net power in beam (total power minus background power)
- Incident irradiance on specific target-mounted radiometers
- Incident direct solar irradiance (provided through interface with Data Acquisition Subsystem)
- Characteristic pixel dimension (vertical and horizontal) relative to target, based on registration marks
- Position of target-mounted radiometers as video digitizer coordinates

The BCS provides the following data on hardware and instrumentation status and environmental conditions:

- Video camera dark current (determined by analog measurement or digitized output, for relay mask region)
- Target-mounted radiometer shutter position signal - automatic monitoring by BCS (use of shutter is optional, but currently shutters are kept open permanently)
- Ambient temperature - provided through interface with Data Acquisition System (DAS)
- Digitizer signal continuity and data integrity
- Excessive dynamic range indicator for cameras (BCS software controls iris to required level)

- Wind speed - provided through interface with Data Acquisition System (DAS)
- Solar irradiance

2.2 MEASURED PARAMETERS - SUNSHAPE CAMERA

The sunshape camera measurement capabilities include

- Measurement of solar radiance on a pixel-by-pixel basis by comparison of the relatively flat spectral response total intensity with simultaneous pyrheliometer readings
- Measurement of the solar disk diameter in pixels (x and y directions) for determination of characteristic pixel angle
- Selection of the best radiance vs angle curve for the sun by comparison of four radial distributions each of which is used to predict a total irradiance by volume integration
- Correlation of sun radiance data with a particular heliostat beam scan, time, and date

2.3 BCS DESIGN REQUIREMENTS

The BCS meets the following design requirements:

Configuration - The BCS is configured to provide beam data on all heliostats by using four video cameras in the field viewing four targets mounted on the tower beneath the receiver. The sunshape camera is located on the roof of the control building. It tracks the sun and determines solar radiance distribution. Video output signals from the four field cameras and the sunshape camera are processed by a single digitizer. Data acquisition, data reduction, and display are provided by the dedicated BCS computer.

Data Acquisition Rate - The data acquisition rate is determined by digitizer/computer processing rates and video camera scan rates. The scan rate is 60 frames per second, with a composite of 2 scans taken in 1/30 second framing the image. The digitizer resolution is 256x256 pixels.

Dynamic Range - Each of the BCS field cameras provides an unsaturated video input signal and digitizer output for the maximum irradiance on the target from the sum of (1) the beam from a single canted and focused heliostat, (2) the maximum solar irradiance directly incident on the target, and (3) the

maximum background irradiance as determined for nominal operating conditions and test periods.

The video cameras are capable of viewing the sun directly without damage. The sunshape camera is equipped with filters to obtain the requisite dynamic range.

The dynamic range is variable through software control of the iris for the field cameras, and manual adjustment for the sunshape camera.

Video Camera Placement - Cameras are emplaced in the field for an unobstructed view of each target face. Camera deflection is less than $\pm$ 0.2 milliradians for all operational wind and temperature conditions. Camera aimpoint is verified periodically by comparing target registration mark positions as viewed by the camera. Camera angle with respect to the target is determined to within $\pm$ 0.25° so that accurate coordinate transformations of the observed beam intensity distribution can be made as part of detailed beam profile evaluations. The sunshape camera is mounted on an equatorial tracker and adjusted for all-day tracking of the sun with minimum operator control.

BCS Camera Enclosure - The BCS camera enclosure is equipped with an antiglare tube and baffles to minimize glare from the sun, light reflections in the field, and the illuminated receiver. The enclosure is sealed and pressurized to 5 psig with dry nitrogen.

Sunshape Camera Enclosure - The sunshape camera enclosure maintains a constant temperature of 50 $\pm$ 2 degrees F, based on the camera requirements for constant dark current. The enclosure has an access door which allows convenient inspection and maintenance of the camera, and the camera can be easily removed. The enclosure is environmentally sealed against dust and moisture. Enclosure temperature measurements are provided by a clearly visible thermometer. The enclosure is thermally insulated and prevents condensation on the viewing window.

Target Configuration - Four targets are mounted beneath the receiver such that (1) receiver panel remove and replace operations are not adversely affected,

(2) the targets form an enclosure for equipment and personnel, and (3) all heliostats in a given quadrant of the field can project beams onto one target, without adverse beam spillage to the adjacent target.

Target Size - The targets are sized to be compatible with the reflected beam image from any heliostat within the view angle of each target.

Target Resolution - The BCS provides a characteristic distance between adjacent pixels of approximately 1.5 in. for the full beam image as observed on the target.

Target Surface Flatness - The target is designed and constructed to maintain flatness within $\pm$ 1 inch in 10 feet under all operational conditions, including wind and temperature, with a single heliostat beam incident on the target.

This flatness requirement corresponds to a maximum angular variation of the target surface with respect to the video camera of approximately $\pm$ 0.5 degrees and is compatible with the target paint relative reflectance requirements as a function of incident and reflected angles.

Target Registration Markings - The targets have registration markings a known distance apart to provide a measure of the characteristic dimensions for the horizontal and vertical pixels, and thus the characteristic pixel area. The registration markings are black, to provide maximum contrast, and are at the outer edges of the camera field of view, to provide an accurate measure. The physical distance between the markings is of the order of 25 ft (horizontal and vertical) and is measured to within $\pm$ 0.25%. The markings are black squares, with horizontal bases.

Target-Mounted Radiometers - Four radiometers are mounted on each target. Three radiometers having a range of approximately 0 to 50 suns are emplaced to measure heliostat incident beam flux. The radiometer dynamic range is compatible with the maximum beam flux from one or two heliostats and background flux. One radiometer is placed in the top corner of each target to measure the background radiation, but this capability is currently not used. This radiometer can be used as a spare. The time response of the radiometers

is 250 milliseconds full scale. Each radiometer can be continuously cooled to maintain a constant ambient temperature under maximum flux conditions but this has not been found to be necessary. The radiometers are mounted behind the target and have a field of view (FOV) consistent with each heliostat in the associated quadrant of the field. Radiometers are mounted such that the FOV can be manually increased or decreased. The nominal FOV is approximately 90° in azimuth and 45° in elevation, as viewed through the opening in the target.

The radiometer output is linear to within ± 1%. Calibration is verified both by vendor tests in the laboratory and system tests in the field with sunlight using a pyrheliometer, verified against a primary standard radiometer (e.g., Active Cavity Radiometer), under conditions simulating the geometric positioning behind the target. The calibration coefficient variation with angle has been determined and corrections are applied.

2.4 DATA AND ANALYSIS

The BCS provides output data in appropriate engineering units as summarized below.

Output Data

- Beam centroid error (mean ± standard deviation) relative to aimpoint
- Plot of the 90% isoflux power contour (both normalized and non-normalized) superimposed on the receiver configuration plot
- Receiver configuration plot as seen from each heliostat
- Net power in the beam (mean ± standard deviation)
- Power Effectivity - The ratio of net power in the beam to the theoretical net power for the incident solar irradiance condition
- Spillage power (percent) off of the receiver
- Data validity algorithms
- Irradiance and corresponding brightness (0-255 DIR numbers) used to generate calibration curves.
- Solar irradiance level
- Sun radiance as a radial distribution
- Wind speed
- Temperature

- Heliostat number
- Date and time
- Number of measurements for a bias update
- Date of last bias update

2.5 ENVIRONMENTAL DESIGN CONDITIONS

The BCS is designed to maintain structural integrity in any applicable combinations of environments as described in Pilot Plant Environmental Conditions (Overall Plant Design Description (OPDD), Appendix C, Revision 1).

2.5.1 Operational Limits

The BCS must meet performance requirements for the following conditions:

Environment	Level
Wind, including gusts	12 m/s maximum (27 mph)
Temperature	32°F to 122°F (0°C to 50°C)

2.5.2 Hail

The BCS camera enclosures and target are designed to survive hail conditions sited in "Pilot Plant Environmental Conditions" (OPDD, Appendix C, Revision 1).

2.5.3 Lightning

The Beam Characterization Subsystem has lightning protection consistent with the following guidelines:

Direct Hit. Total destruction of a video camera, target, electronics, or electrical cables subjected to a direct lightning strike is acceptable.

Adjacent Strike. Damage to a video camera adjacent to a direct lightning strike should be minimized within appropriate cost-risk limits.

Section 3
BCS HARDWARE DESCRIPTION

3.1 DESIGN OVERVIEW

The basic BCS consists of four video cameras each of which views an elevated target mounted on the tower beneath the receiver. The video analog output signals are digitized to provide a measure of beam intensity incident on each target from a heliostat. The digitized intensity for a particular frame is correlated with absolute irradiance measurements made nearly simultaneously by a calibration procedure utilizing three target mounted radiometers. The targets are flat metal structures painted with a high temperature white paint specifically selected for its near-Lambertian reflectance characteristics to minimize glare and provide uniform reflection over the target surface. Three radiometers are positioned about the center of the target within the area of a centered beam image so as to provide the necessary beam irradiance measurements over some portion of the moderate to high intensity regions of the beam and thus improve the calibration curve accuracy.

Simultaneous measurements of the sun's radiance distribution are made with a specially modified video camera (termed the sunshape camera) which tracks the sun. These data, coupled with the absolute measurements of incident irradiance, are used in computer codes which compare actual and theoretically ideal heliostat irradiance distributions. A video monitor allows the operator to view the sun for cloud detection.

Radiometers located in the field as part of the data acquisition subsystem (DAS) determine incident solar irradiance, which is used to establish heliostat reflective efficiency as measured at the target. Beam centroid data are obtained to establish heliostat tracking errors.

3.2 SUMMARY OF BCS HARDWARE

The BCS is composed of the following major equipment with interfaces to the plant operator and other subsystem equipment of the power plant:

- Four video cameras with mountings, camera housings, sun shade and power/signal interfaces.

- Four camera lenses with remote iris and focus control.
- Camera control unit with electronics to control the iris opening, lens focus, camera power, and video switching unit for the four BCS cameras.
- Video switching unit with electronics to switch the analog video signal line of each camera, under control of software in the BCS computer.
- Video signal digitizer to convert the analog signal amplitude of each pixel in the picture to a digital form and also convert the digital data to analog form for display on a video monitor.
- BCS computer interface with the video signal digitizer, the video control unit, the target shutter control (optional capability not currently in use) and instrumentation system, and the BCS CRT/keyboard terminal.
- The target shutter control and instrumentation system with associated electronics to command the radiometer shutter open/close position and provide signal conditioning and data acquisition capabilities for target radiometer sensor measurements. (Target shutters are not presently used to improve reliability, speed and accuracy as discussed in a subsequent section.)
- The BCS CRT/keyboard terminal to display processed BCS data to the operator and provide the operator interface (keyboard) with which to interact with the BCS software controlling the BCS activities.
- The terminal hardcopy unit to make permanent paper copy of CRT/keyboard terminal displayed information.
- The BCS target and target mountings for radiometers and shutters.
- Radiometers to sense incident light from the heliostat beams and the background ambient light from each of the field quadrants.
- The radiometer shutters that open and close the radiometer sensor opening to the light source (currently maintained fully open).
- The sun shape camera, including an equatorial mount, tracker, environmental housing, and timer circuits for track control.
- The Eppley Normal Incident Pyrheliometer (NIP) located on the roof of the control building.

3.3 BCS HARDWARE ORIENTATION

The BCS hardware is distributed in five major areas of the plant, with communications between equipment derived from land line connections. The equipment orientations are as follows:

- Video cameras, lenses, housings, and sunshields - mounted on foundations installed in the collector field along the four compass points as shown in Figure 3-1. The cameras in the east and west field are 20 feet from the center of the road and the north field camera is 16 feet from the center of the north road. The north, east and west cameras are 856 feet from the center of the tower base. The location of the cameras from the receiver tower center puts the north field camera 1.07° from the normal of the north target and the east and west cameras are 1.34° from their respective target's normal. The south field camera is 60 feet from the south road center and is 850 feet from the tower base. This makes a 4.04° angle off the target normal. The effect due to the camera viewing the target slightly off axis is an intensity decrease determined by $\cos^4$ (4.04°), or 0.015%, for the south field camera and is estimated to be less for the other three cameras.

- The Eppley Normal Incident pyrheliometer located on the roof of the control building.

- Video camera control unit, video signal switch, and BCS computer interface - located as rack mounted equipment in the equipment room of the control building. Figure 3-2 shows the orientation of this equipment in the equipment room.

- CRT terminal and hardcopy unit - HP-9845 located as table mounted equipment in the data evaluation room.

- Video monitor - located as console mounted equipment of the Master Control Console (MCC) in the control building and as portable 9" monitors in the engineering evaluation room.

- Target shutter control and instrumentation system - located as rack mounted equipment on the 13th level of the receiver tower. A plan view of this equipment rack orientation on the 13th level of the receiver tower is shown in Figure 3-3.

- BCS targets - located on the receiver tower with the top of the target oriented twenty-six (26) feet below the bottom of the receiver. A target is located in each of the north, east, south and west quadrants of the collector field. Each target is canted 13° with respect to vertical. Figures 3-4 and 3-5 show the orientation of the BCS target on the receiver tower.

- Radiometers (pyrheliometers) - located on each of the receiver tower targets. Four radiometers are located on each target. Three radiometers have shutter control capability and are oriented in a triangle design about the

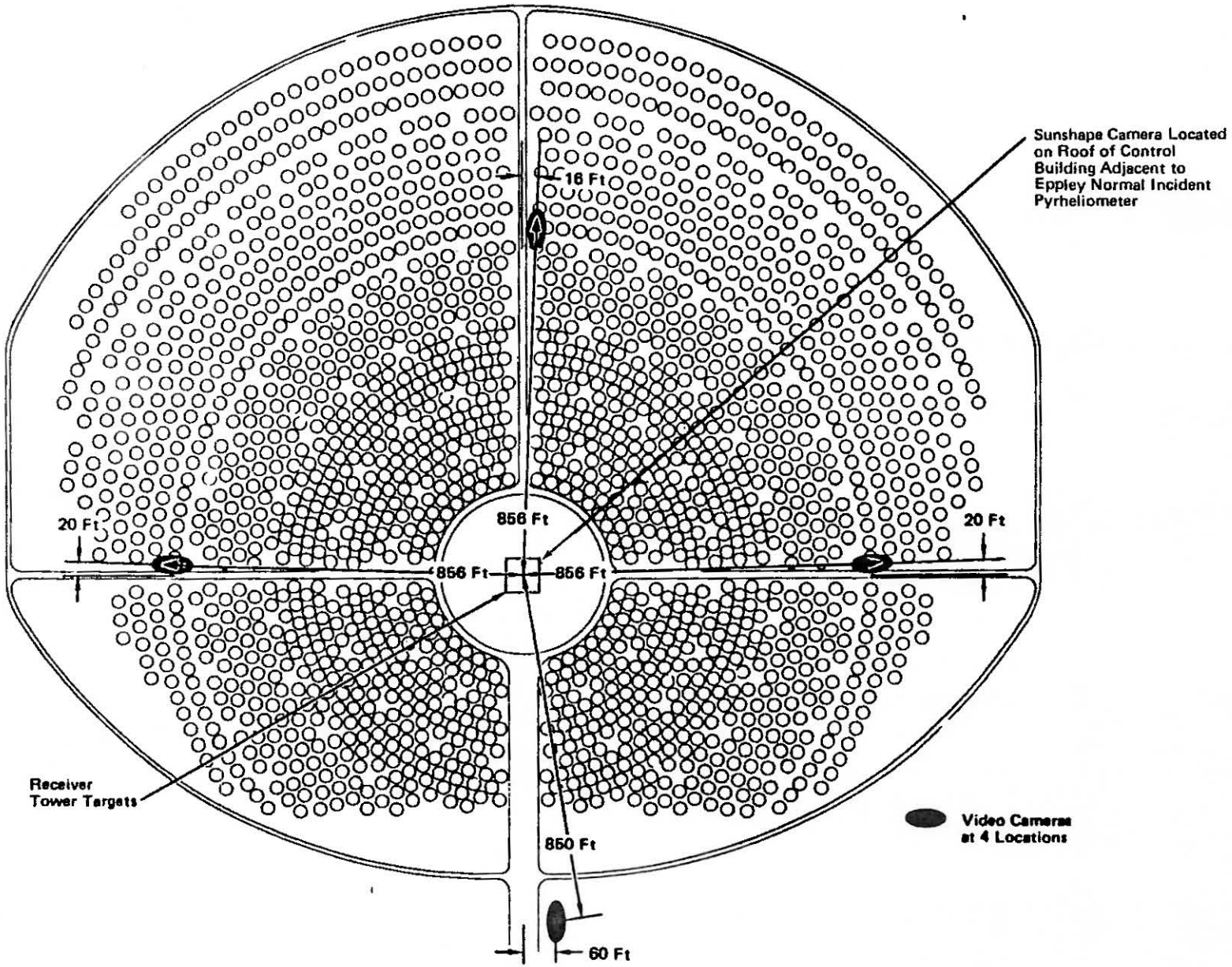

Figure 3-1. BCS Camera Orientation Landscape

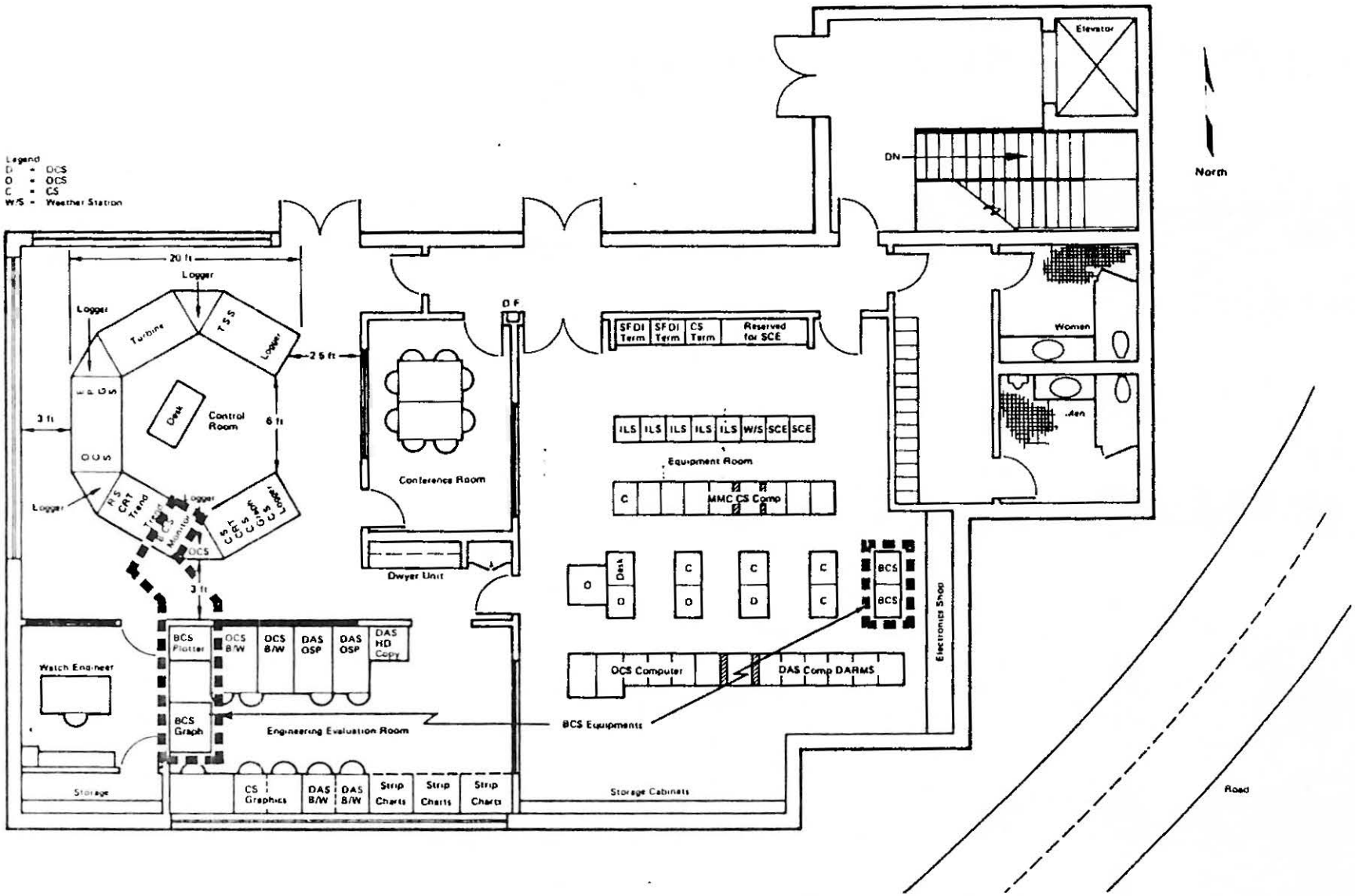

Figure 3-2. Plant Control Building: Second Floor Plan BCS Equipment Layout Landscape

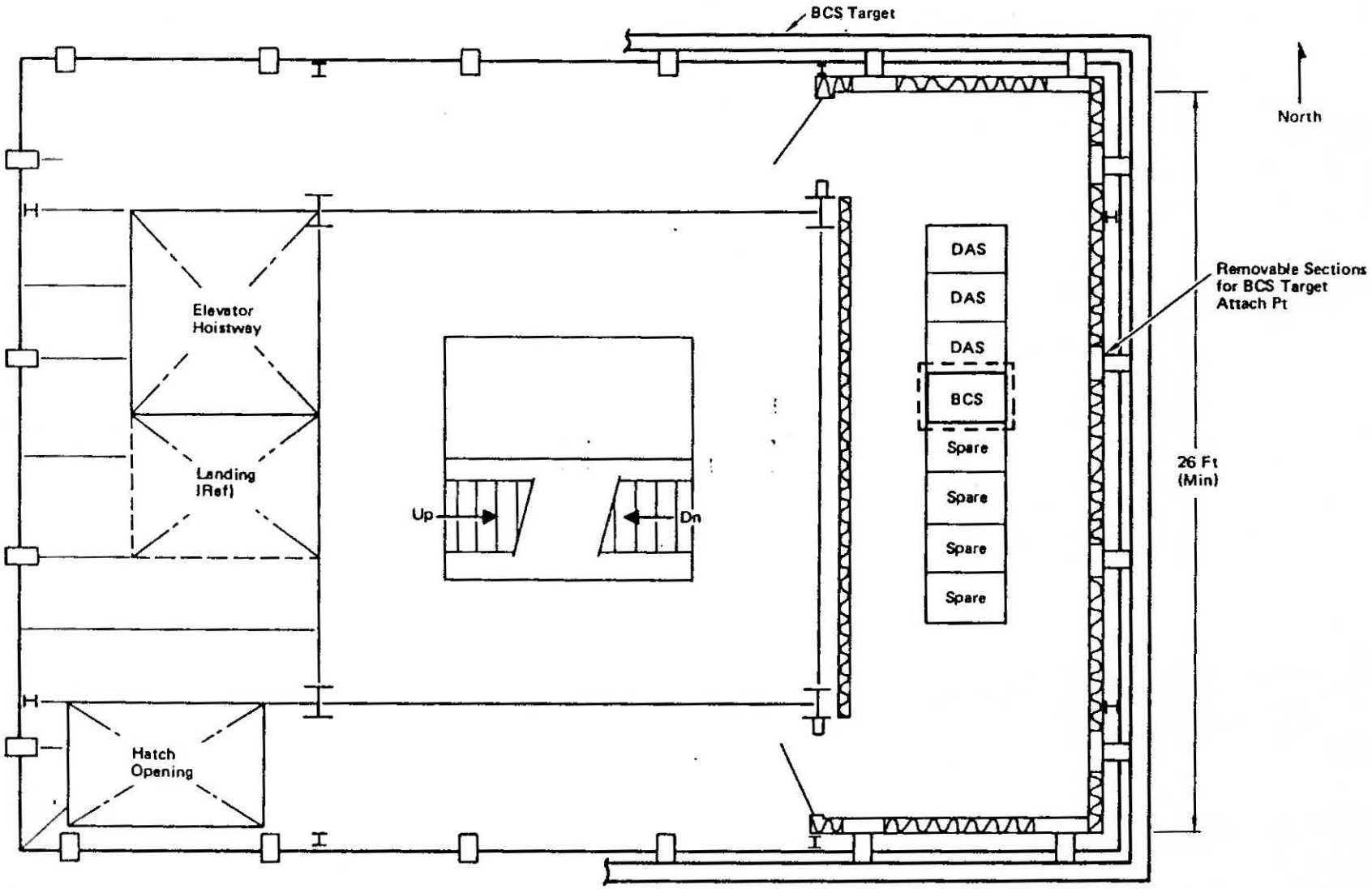

Figure 3-3. Equipment Orientation – Level 13 of Receiver Tower Landscape

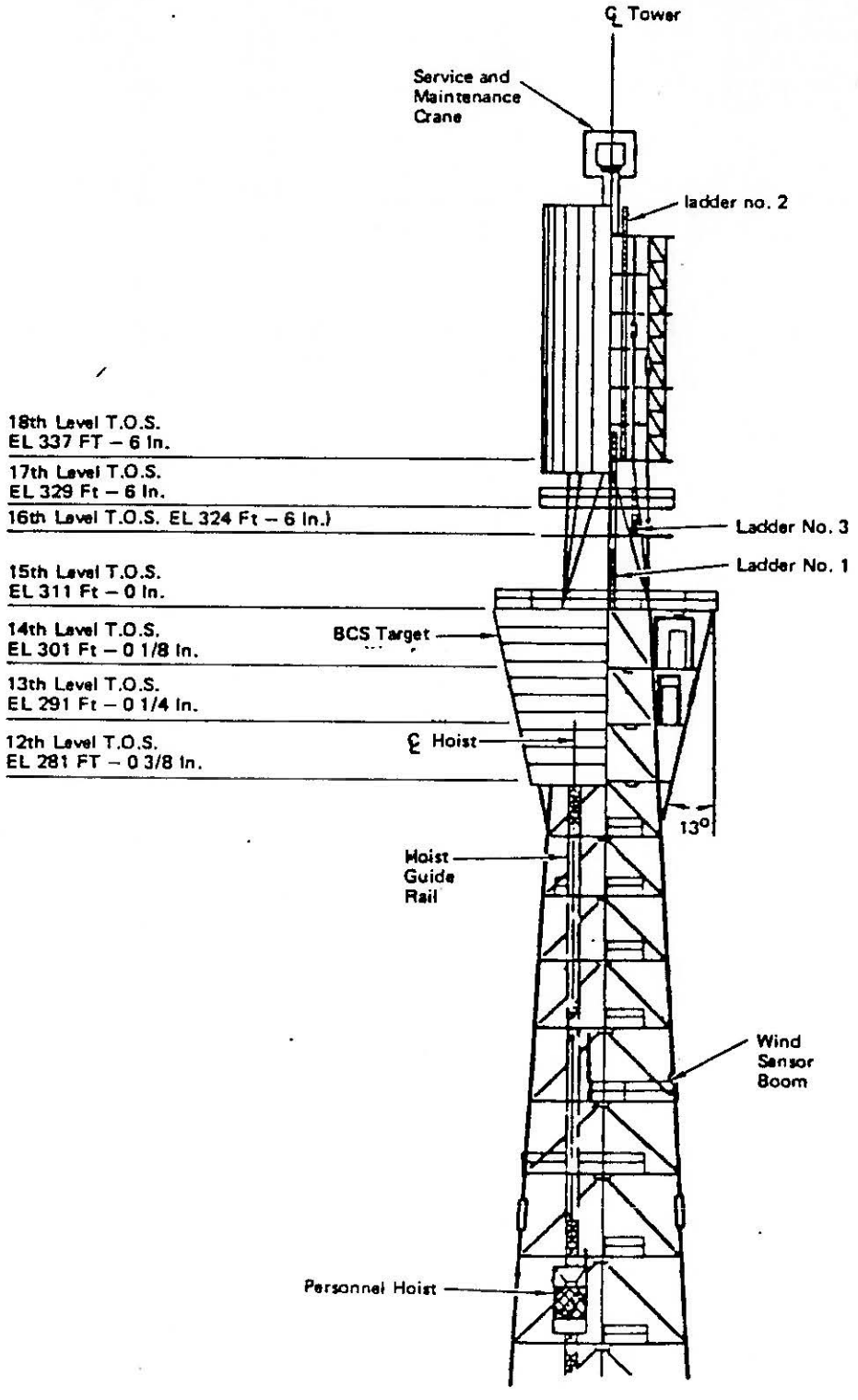

Figure 3-4. BCS Target Orientation

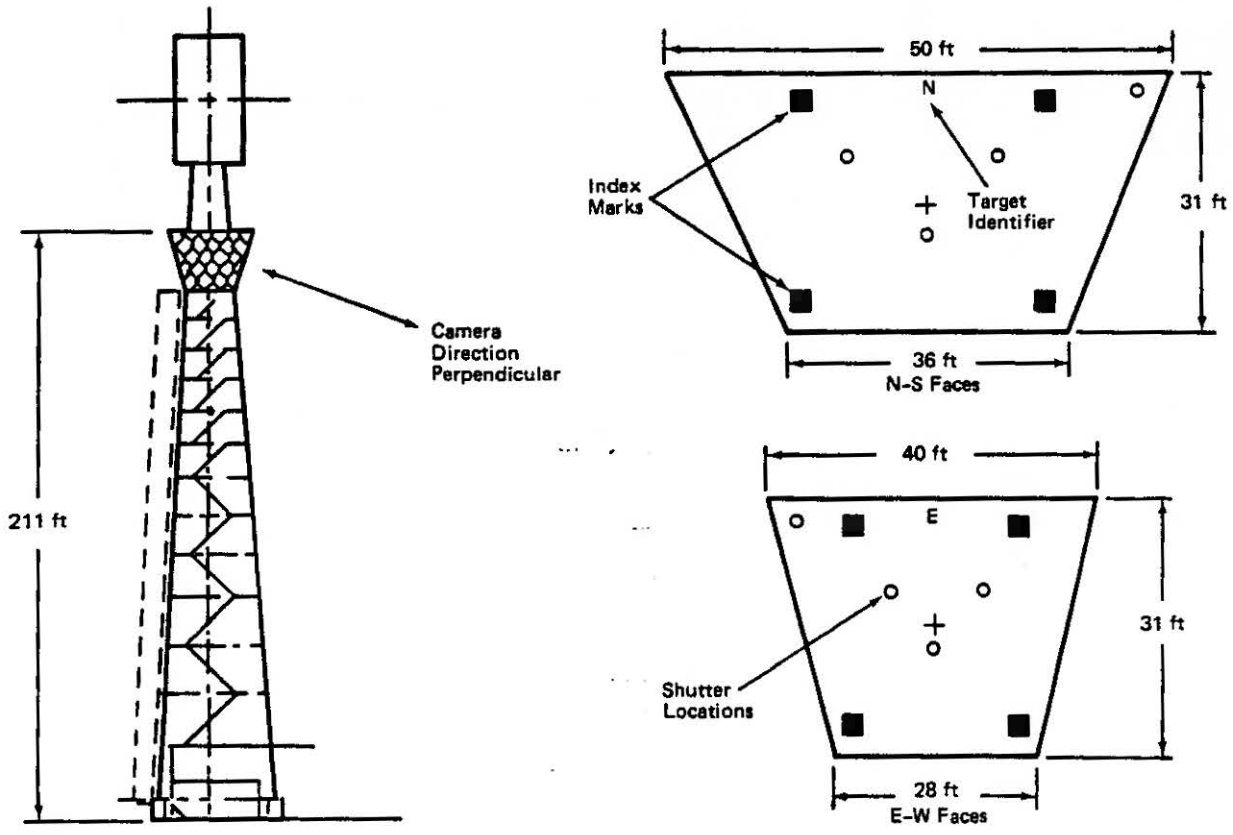

Figure 3-5. BCS Targets

target center. This arrangement permits sensing of the beam incident light for beams positioned off center of the target. The radiometer in the upper corner of each target is not presently used and thus is available as a spare. Figure 3-6 shows the typical radiometer locations on the BCS target.

3.4 COMPONENT DESIGN DESCRIPTION

A summary of the major BCS components is given below.

3.4.1 BCS Video Camera

The video camera is a model 2850C-207 low light television camera manufactured by COHU, Inc. Electronics Division. The camera is equipped with an RCA model 4532 B/H silicon diode array vidicon tube and a COHU model 2820 C-204 10:1 zoom lens with a 2X extender. Features include remote iris and zoom control, antiglare shields, sealed environmental housing, Dual Tone Modulated Frequency (DTMF) control from the BCS computer interface, circuit modifications to remove automatic gain control (AGC) and a stable platform to minimize camera movement and wind induced vibration (see Figure 3-7). Detailed descriptive material is given in Appendix A.

The antiglare tube and shields (see Appendix B) eliminate stray light from clouds, receiver, sun, etc. which could cause erroneous measurements. The shields are formed to match the shape of the target and two or three are used as multiple light baffles.

The camera has a relay lens for the black level mask and space for a variety of filters which may be used to flatten the response of the camera over its spectral response range. These features are described in greater detail in following sections.

3.4.2 BCS Video Camera Foundations and Mounts

The video cameras are mounted in the field on adjustable camera mounts bolted to a reinforced concrete pedestal and mounting plate. Specifications for the camera foundation, pedestal, and camera mount are presented in Appendix C.

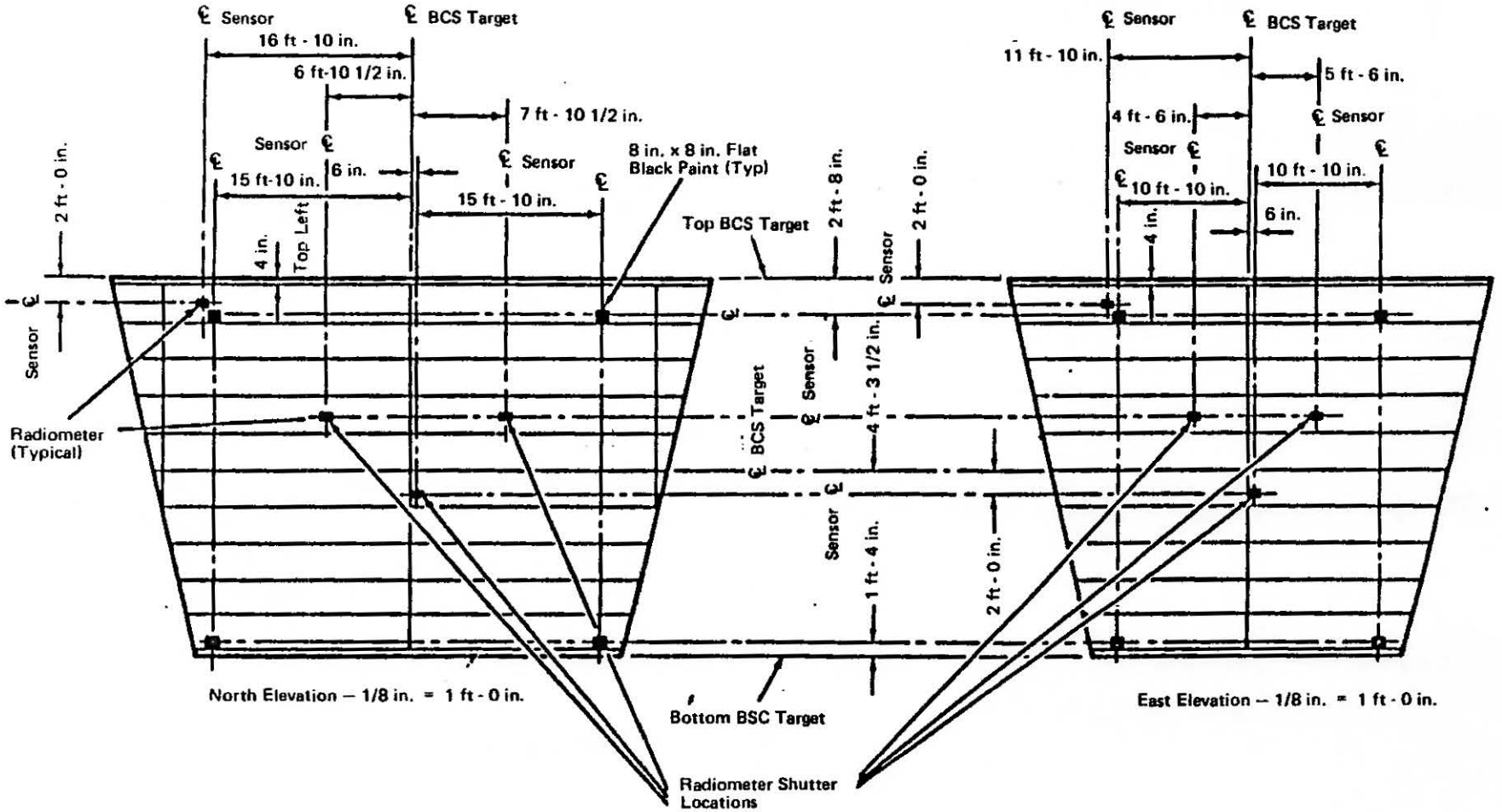

Figure 3-6. Radiometer and Radiometer Shutter Orientation Landscape

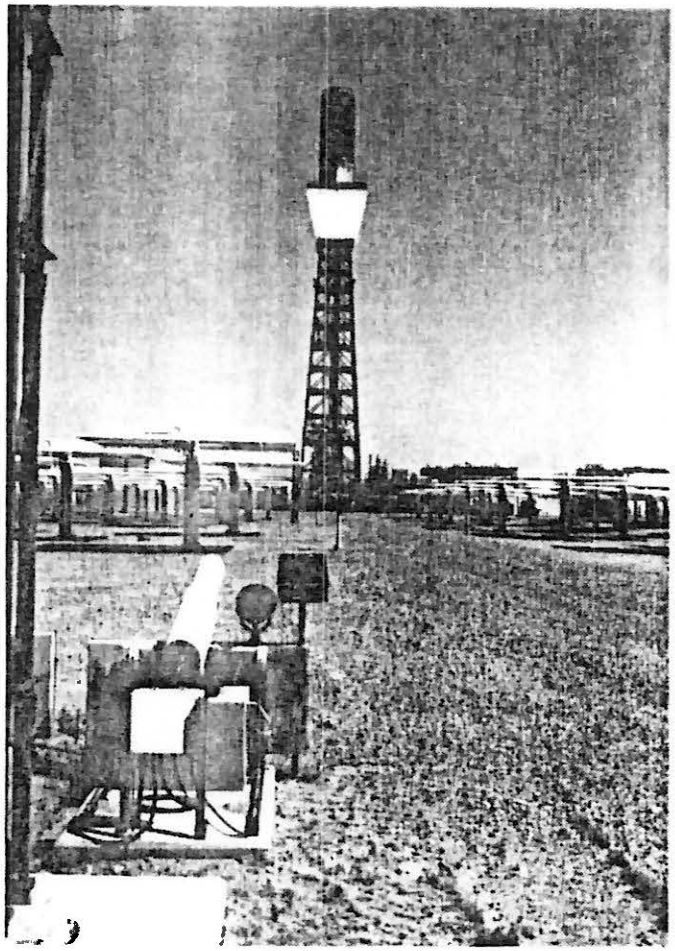

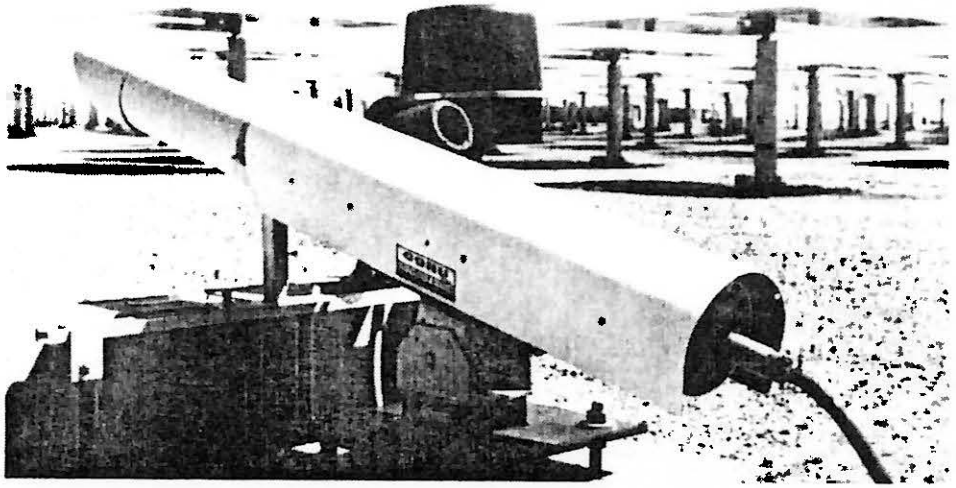

- Cohu Model 2850C Camera
- Modified to Operate as Radiometer
- Silicon Diode Array Vidicon

Figure 3-7. BCS Camera

3.4.3 Remote Camera Control System

Camera selection and iris control are accomplished by a noise resistant Dual Tone Multifrequency (DTMF) command system composed of a transmitter in the camera control rack and a remote receiver near each camera. This system is described in Appendix D.

The transmitter is a COHU model DTMF 100 modified for the Solar I application. Integral manual control switches are provided to select the desired camera, apply power, and control the iris or place it in automatic mode. Reed relay outputs from the MODCOMP model 1136 module in the BCS computer provide programmable camera selection and iris control. Camera control commands are encoded to digital form and transmitted to the selected receiver over standard twisted pair wires using audio tones to represent the digital information. The transmitter also sends camera select commands to route the desired video input through the video switch to the digitizer.

The COHU model DTMF 200 receiver decodes the command data from the transmitter and provides power and iris control commands to its associated video camera.

3.4.4 Video Switch

The video switch is a Pelco Model VS504R switching matrix which routes the selected video input (North, South, East, West or Sunshape camera) to the video digitizer. The video switch is described in Appendix E.

3.4.5 Video Digitizer

The Video Digitizer System is a Quantex Model DS-12 Digital Image Memory/Processor. This system: 1) accepts the video signal from the video camera (conforming to the EIA RS-170 standard); 2) converts the signal to a digital form; 3) stores the digital data; and 4) transmits the data to the BCS computer upon command over an IEEE 488 interface. A block diagram of the video digitizer is shown in Figure 3-8. A description and specification of this equipment is presented in Appendix F.

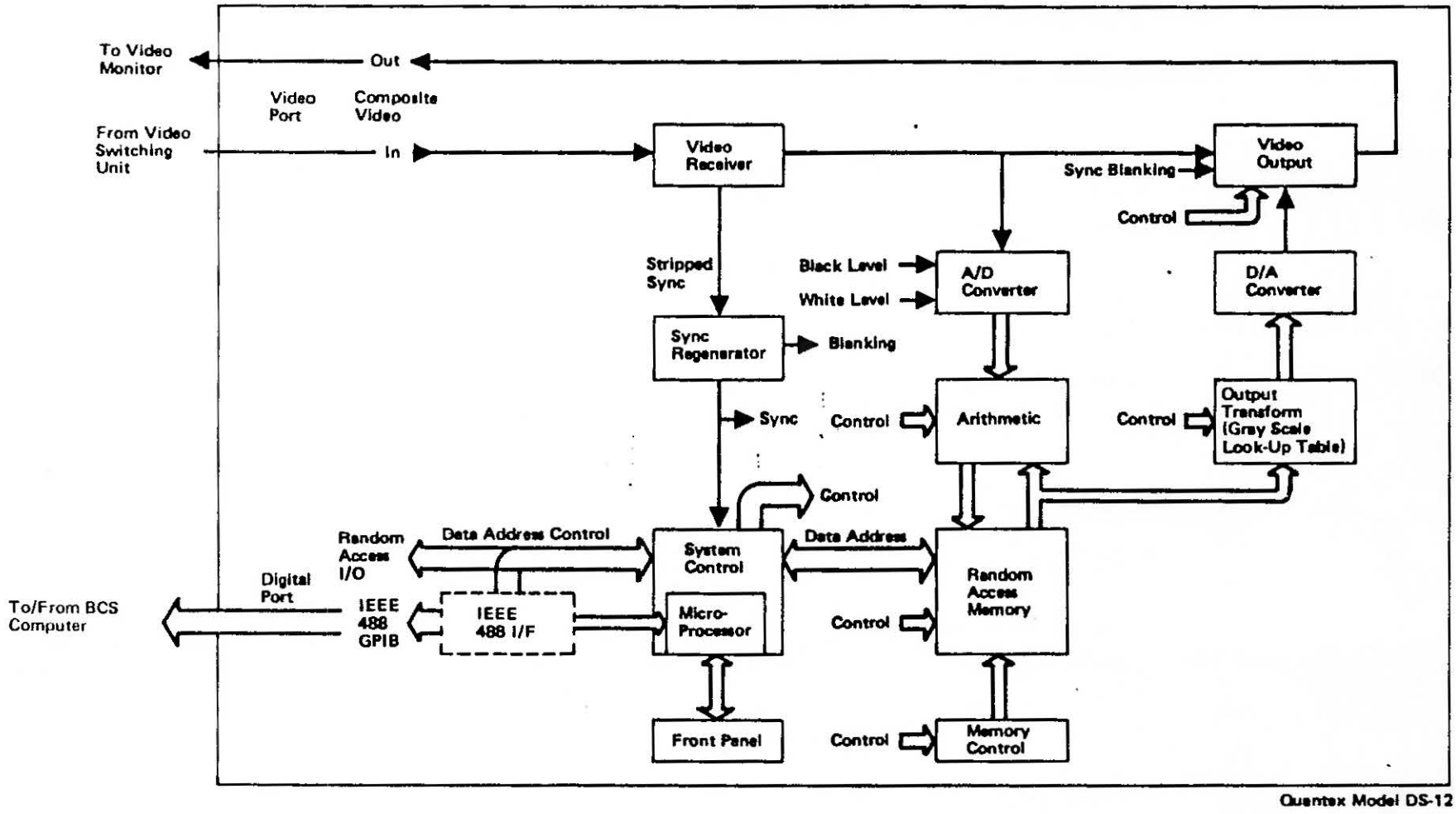

Figure 3-8. Video Digitizer Block Diagram Landscape

Incoming composite video is stripped of sync and applied to a high speed A/D converter. Data from the A/D passes through the arithmetic processor where it may be combined with memory data through hardwired arithmetic processes which include summation with data already in memory, averaging, and subtraction. The resulting data is then stored in memory.

The IEEE Standard 488 interface connects the digital memory port and the system control microprocessor to the MODCOMP Model 5488 controller in the BCS computer. This interface connects the digitizer to a direct memory access channel of the BCS computer and allows block transfer of image data and program control of the digitizer functions.

A standard EIA RS-170 video output is routed to the BCS monitor CRT in the receiver console in the control room. Processed data is routed through a D/A converter to the digitizer or unprocessed data may be selected.

3.4.6 Target

The targets are steel panels painted with a flat-white, near-Lambertian paint. It is not necessary to have a perfect Lambertian surface, with uniform reflected radiance independent of the angle of incidence of the beam from a heliostat, because a separate calibration curve is obtained for each heliostat beam. However, the flat white paint eliminates glare and the reflectivity is reasonably uniform over the angular difference associated with the "out of flatness" or waviness of the target itself, and the geometric variation in incident and reflected angles over the beam itself. Tests of the target uniformity when illuminated by direct sunlight showed the reflectivity values to be uniform and this reflectivity has remained uniform for three years without maintenance.

Each target consists of 20 individual panels hoisted and assembled in place on each side of the tower. Accurately located horizontal frames are permanently attached to the side of the tower. The panels are of 6061-T6 aluminum and 0.125 inches thick. Panel flatness criteria is less than $\pm$1" per 10'. Each panel is attached horizontally and anchored. Panel installation begins at the target bottom and progresses to the top using ten panels

covering 36" each. Ten more panels are installed adjacent to the first ten. The largest panels are 3' x 20'; the rest are shortened to accommodate the shape of the target. An extrusion is riveted to the top edge of each panel and is hooked over a leg of the 3" channel. The bottom edge of each panel has a continuous aluminum angle riveted to it. To the horizontal flange of the angle a clevis and compression spring are tensioned to hold the top edge of the under panel secure. Each of the targets is erected in place with a 1/4" spacing between adjacent targets to accommodate expansion.

The paint used is from Koppers Corp (City of Commerce, California) and is a gloss level 11 flat white high temperature paint. The paint is applied in two cross coats over an appropriate primer.

3.4.7 Target Shutters

Three target shutters are provided on each target. The shutters allow the total blocking of the light source impinging at the radiometer apertures located closest to the target center. The three shutters on each target are pneumatically controlled by a single solenoid operated valve that is activated from the MODACS III digital output circuitry.

A schematic of the target shutter is given in Appendix G.

However, the target shutters are no longer used because the rapid movement of the heliostat beam, even with low wind speeds, made it difficult to obtain accurate correlations of irradiance and observed brightness. The time required to close the shutter and scan the target (~ 0.5 second) was too great, and therefore the shutters were deactivated. Simultaneous irradiance and brightness readings are now made with the shutters open.

3.4.8 Radiometers (Pyrheliometers)

Four radiometers are located on each target in the patterns as shown in Figure 3-6. The radiometers are Medtherm Corp. Model FDTW-2.5-20020. The radiometers measure the light intensity incident on the surface of the sensor and provide an analog signal proportional to the light intensity to the MODCOMP MODAC III Analog Input Circuitry. The measurements are digitized and

subsequently transmitted to the BCS computer where the values are used in beam characterization computations.

The radiometers may be thermally controlled to protect the sensor below and above the temperature range of 45°F to 130°F by flowing a water/ethylene glycol mixture through the radiometer housing. A thermocouple is provided in the sensor; however, this measurement is not used by the BCS.

A description, specification and installation schematic of the Medtherm Model FDTW-2.5-20020 radiometer is presented in Appendix H.

3.4.9 Target Shutter Control and Instrumentation System

The Target Shutter Control and Instrumentation System is a MODCOMP Model MODACS III Subsystem interfaced to the BCS computer, the radiometers and the target shutter control solenoids.

The MODACS III Subsystem is a computer based system located in the Receiver Tower remote from the BCS computer. Communications between the MODACS III Subsystem and the BCS computer is accomplished using asynchronous serial telephonic signal transmission techniques in conjunction with EIA RS232C interface specification. Short haul modems are used to provide the local communications link. The modems are Expander Inc. Model SHM modems.

Descriptions and specifications of the MODCOMP MODACS III Subsystem and the Expander Model SHM Modems is presented in Appendix I and J respectively.

3.4.10 Sunshape Camera

The sunshape camera is a specially modified video camera mounted on a Meade telescope tracker. This camera tracks the sun and provides radial radiance distribution data for engineering evaluation purposes. The sunshape camera is described in Section 5.

Section 4
BEAM CHARACTERIZATION SYSTEM OPERATION AND PRINCIPLES

4.1 OPERATION

Automatic BCS operation normally occurs as required on a daily basis whenever conditions permit. Heliostats are automatically selected from a file, or heliostat candidate list, such that 60 heliostats can be tested each day. To avoid stray beams from heliostats in an adjacent quadrant invalidating a test run, opposite quadrants and targets are tested; i.e., the north and south field heliostats are sequentially moved onto the north and south targets while the east and west field heliostats continue to track on the receiver. Later, the east and west field heliostats are sequentially tested.*

Three runs are taken during the day (morning, noon, afternoon) such that the tracking aimpoint variations can be assessed and a nominal aimpoint selected. This procedure is used since heliostat aimpoints often exhibit a diurnal variation.

At the end of the day, the aimpoint data, based on the measured beam intensity centroids, may be used, in conjunction with associated data, to bias the heliostat tracking data in the heliostat array controller (HAC), and thus correct the aimpoint.

The BCS is operated in a near automatic fashion and interfaces with the heliostat array controller (HAC), data acquisition system (DAS) and the plant operator. Movement of an individual heliostat on to the tower-mounted target and calibration of the heliostat is possible during the normal steady-state operating modes of the total system.

BCS operation is divided into the following phases: Initialization, Measurement, Termination, General, and Off-line. During the initialization

*Although this procedure minimizes stray beams in most cases, conditions still exist for which stray beams pose problems. Data validity algorithms reject these cases.

phase, three lists of heliostats to be measured are created from the off-line phase, and any neighboring heliostats which will cause blocking and shadowing are also identified. These lists are transferred to the HAC while the initialization of the BCS software and hardware is carried out. This initialization also involves the selection of start time, alarm thresholds, and sample rates.

During the measurement phase, the heliostats are brought on target, the background is determined and subtracted from the data, and a calibration curve results. The calibration curve relates digital values of observed video brightness to watts/m^2 as determined by the target radiometers.

Centroids are determined and averaged, and beam powers are calculated and compared to theoretical values.

In the Termination phase, results are sent to the HAC, spillage power is calculated, data reports are printed, and the master file is updated. The Off-line phase involves data plots, creating the candidate lists, and other support functions. The General phase handles such tasks as message communication with the HAC and error message communication with the HP.

The HAC controls the heliostats such that each beam is moved on and off the target as required. As each selected heliostat is trained on the target, the appropriate video camera is switched to view the beam and the video signal is digitized and transmitted to the BCS computer. The BCS computer processes the digitized data, correlates the data with absolute intensity measured by target mounted radiometers, and outputs the processed data on a CRT display terminal that has a hardcopy capability.

A computer program resident in the BCS determines which heliostats could block or shadow the test heliostat. These heliostats are first commanded to a face-up stow position. The test heliostat is moved from the receiver to a standby aimpoint, and when the interferring heliostats are stowed, the test heliostat beam is moved onto the target. The 8-bit video digitizer takes an "image grab" and the computer analyzes the data. If the beam is too bright, i.e., the digitizer shows saturated values (255), or too dim (peak values less

than 150) the camera iris is adjusted automatically to obtain the correct brightness range. Ten image grabs are then taken and stored in rapid succession.

A calibration curve is constructed from the digitized brightness values at the three points on the target where the radiometers are located, and the corresponding radiometer measurements of irradiance (watts/m^2). A total of 30 data points is obtained, from which a curve relating brightness to irradiance is determined. A message is then sent from the BCS to the HAC that the beam scans are complete, the HAC moves the beam off the target, and a background image grab is taken. The background brightness values are subtracted from the previous beam brightness values taken 5 to 25 seconds previously. The calibration curve is then used to obtain the net irradiance corresponding to each pixel. Calculations are then made of beam centroid, beam power, spillage power, etc., as described in the following sections.

Immediately after the last beam scan, an image grab is taken of the sun and the corresponding irradiance as measured by an adjacent Eppley Normal Incident Pyrheliometer. Correlation of the digitized video image of the sun and the measured irradiance gives the radiance (watts/m^2 steradian).

This procedure is followed sequentially at a rate of roughly 30 heliostats per hour with most of this period required for repositioning interfering heliostats.

The detailed operating procedure, operator functions, and BCS prompts and responses are described in Reference 10, Beam Characterization System Operator and Users Manual.

4.2 PRINCIPLE OF OPERATION

The BCS acquires a large number (256 x 256) of relative brightness values (termed DIR numbers) by digitizing the video signal associated with a single video scan of the beam image on the target. These qualitative brightness data can be transformed into quantitative irradiance data using a calibration technique which associates the brightness at several points on the target with

simultaneous, quantitative radiometer measurements taken adjacent to those points. The calibration curve obtained is then applied to all of the brightness values such that the irradiance at each pixel, the net beam power, the centroid of the beam, and isoflux contours can be determined.

In order to achieve reasonable accuracies, however, a number of requirements must be met, as discussed below.

4.2.1 Accuracy Enhancement

4.2.1.1 Alignment

The principal requirement for accurate power measurements is that the beam must cover at least one of the three central radiometers, preferably with the higher irradiance region of the beam. Because the Solar I heliostats have a single mirror module cant angle configuration, beam irradiance for outer row heliostats shows a central maximum and gradual decrease with increasing radius out from the beam center. Close-in heliostats, however, show little overlap, and exhibit a great deal of non-uniformity, with each mirror module, as well as spaces between the modules, being distinguishable. As a result, close in heliostats may cover a radiometer with a rapidly varying irradiance distribution or slope or not cover any radiometer. Any heliostat movement further changes the irradiance on the radiometer. These effects decrease accuracy by increasing the data spread for the calibration curve. Power measurement accuracy is therefore greater for outer field heliostats which normally give good calibration curve results. Because of this close-in heliostat nonuniformity, multiple heliostat scans are taken (usually ten scans) from which up to thirty data points correlating irradiance and brightness may be obtained for the three radiometers. The increase in data improves the curve fit.

Heliostat initial alignment has shown relatively large errors (up to 1 to 3 meters centroid error) and thus some beams barely cover even one radiometer. In this case, power measurement results may not be accurate, but the beam centroid data is in general accurate and a bias update can be achieved. Subsequent tests of this redirected beam give more accurate beam power and centroid results.

4.2.1.2 Shading Corrections

Response over the vidicon tube face normally exhibits a relatively flat maximum near the center and a drop off in the outer region. This non-uniformity decreases the net power reading and causes a centroid error; it is corrected by an algorithm which increases the brightness (or DIR number) in the proper proportion, depending on the pixel position. The correction data are obtained by occassionally (i.e., once every 2-4 months or whenever the tube is replaced) pointing the cameras into an integrating sphere which has uniform illumination. An image grab is taken and stored as a corrective "white file." Similarly, an image grab is taken without any light to obtain a black file.

The integrating sphere, lamp, and power supply are described in Appendix K. The detailed procedure is presented in the Operator and Users Manual, Reference 10.

The correction is then applied as a proportional increase of intensity of the actual image file, pixel by pixel, based on the response to uniform illumination.

In particular, the correction is determined by equating the ratio of net corrected DIR number for the image divided by the actual net DIR number to the ratio of the net corrected DIR number for the uniformly illuminated integrating sphere divided by the actual net DIR number, or

$$\frac{D_{\substack{\text{ACTUAL}\\\text{CORRECTED}}} - D_{BL}}{D_{ACTUAL} - D_{BL}} = \frac{D_{\substack{\text{INTEG SPHERE}\\\text{CORRECTED}}} - D_{BL}}{D_{\text{INTEG SPHERE}} - D_{BL}}$$

The term D_{BL} is the black level reading (i.e., digital value with no light entering camera). The $D_{\substack{\text{INTEG SPHERE}\\\text{CORRECTED}}}$ is the corrected digital brightness

value for the sphere at its maximum value near the center, or, to be more practical, an average of the peak values near the center (say, the average of values for $123 \leq V \leq 133$ and $123 \leq H \leq 133$). The actual range of peak values should be determined from the integrating sphere data, and care should be taken to exclude the first 10-20 columns and 10-20 rows, since these have overshoot values for our system and should not be used in any data.

Assuming that $D_{\substack{\text{CORRECTED} \\ \text{SPHERE}}}$ is the maximum value near the center, or an average maximum value, denoted by $D_{\substack{\text{MAXIMUM} \\ \text{SPHERE}}}$, we now have

$$D_{\substack{\text{CORRECTED} \\ \text{IMAGE}}}\Big|_{V,H} - D_{BL}\Big|_{V,H} = \left[D_{\substack{\text{ACTUAL} \\ \text{IMAGE}}}\Big|_{V,H} - D_{BL}\Big|_{V,H}\right]\left\{\frac{D_{\substack{\text{MAXIMUM} \\ \text{SPHERE}}}\Big|_{\text{CENTER}} - D_{BL}\Big|_{\text{CENTER}}}{D_{\substack{\text{ACTUAL} \\ \text{SPHERE}}}\Big|_{V,H} - D_{BL}\Big|_{V,H}}\right\}$$

The V,H represent the values of the pixel positions, based on rows and columns, respectively.

To summarize, the actual image file is corrected for shading by the above equation so that the corrected DIR values are essentially the same as would be obtained with an ideal vidicon having a uniform response to a uniform light field.

4.2.1.3 Brightness/Irradiance Correlation

Accurate results are dependent on the correlation of a brightness value obtained at a point on the target with the corresponding irradiance measured at that point at nearly the same instant. Either of two methods are used to accomplish this. The first method uses a shutter at each radiometer, coated with the target paint. When the shutter is open, the radiometer measures the irradiance and immediately after the shutter is closed, the video digitizer takes an image grab. The brightness of that particular spot on the beam can then be correlated with the irradiance reading immediately prior to shutter closure. The time between the two measurements is approximately 0.5 to 1 second. This technique is workable for beams having reasonably uniform

irradiance and little rapid beam movement. For beams having an irregular irradiance distribution, and beam movement, the correlations show increased scatter. The second method is to leave the shutters open and obtain data on brightness from the adjacent pixels. This approach was originally used for the NWC tests. (Reference 1). The average brightness is then correlated with the radiometer reading taken at the same instant. This technique has proven to be more accurate and can be further improved by reconfiguring the shutter opening, but to date this has not been done.

In principle, the radiometer as seen by the camera is darker than the immediate surrounding target area, but since the radiometer and target hole can be less than the characteristic dimensions of a pixel (3 to 4 cm/pixel), the camera response to this dark region is slight. In addition, iteration techniques can be used to determine the brightness that would have been observed at the radiometer, if it were negligibly small, and thus corresponded to a uniform reflectivity target. The technique currently in use is a compromise based on two factors. First, the actual position of the radiometer is not known with certainty to better than approximately $\pm$ 1.0 pixel because of tower and camera movement due to wind and temperature. Techniques are available to precisely determine the radiometer location associated with each image scan, but these have not been applied. The second factor is the time and effort involved in applying iteration techniques. As a compromise, the closest adjacent pixel values are averaged and these are used.

An array of either nine or five adjacent pixels may be used, centered on the predetermined location of the radiometer. Currently, the five closest pixel values are used, with the center pixel defined by the radiometer location.

It should be further noted that multiple scans (usually 10) are taken to determine the brightness (DIR numbers) and radiometer readings.

4.2.1.4 Background

The target background irradiance is time and position dependent as a result of incident light variations on the target from the sun, clouds, ground, and especially, wide angle scattering from the heliostats. The time between a power scan and a background scan is approximately 5 to 30 seconds, and slight background changes can occur. Since background area is several times the beam area, a relatively small change in background can introduce a non-negligible error in net beam power. Several techniques are used to minimize this effect. First, if incident solar irradiance is changing rapidly, a flag is set, alerting an evaluator that conditions may be changing rapidly. Second, the background brightness on the target periphery is monitored continuously and the background values adjusted so as to nearly correspond to the values during the time the individual beam scans were taken. This technique is presented in Appendix L. Third, the region outside the beam is examined by an algorithm which adjusts the difference such that it becomes minimal. In effect, the region outside the beam should have a net irradiance of zero when the total irradiance minus the background irradiance is examined.

4.2.1.5 Target Radiometer Response

Ideal Radiometer with Cosine Response

An ideal radiometer has a cosine response to incident irradiance. Thus, from Figure 4-1, it is seen that a beam projected onto a target will be detected as having a decreased irradiance (relative to the normal incidence irradiance) at a given point as the incident beam angle, α increases with respect to the target normal. Thus, the irradiance, I, measured at the radiometer is related to the normal incident irrandiance by:

$$I_{\substack{\text{Measured} \\ \text{Net}}} = I_{\substack{\text{Net Normal} \\ \text{to Line of} \\ \text{Sight} \\ \text{Heliostat}}} \cos \alpha$$

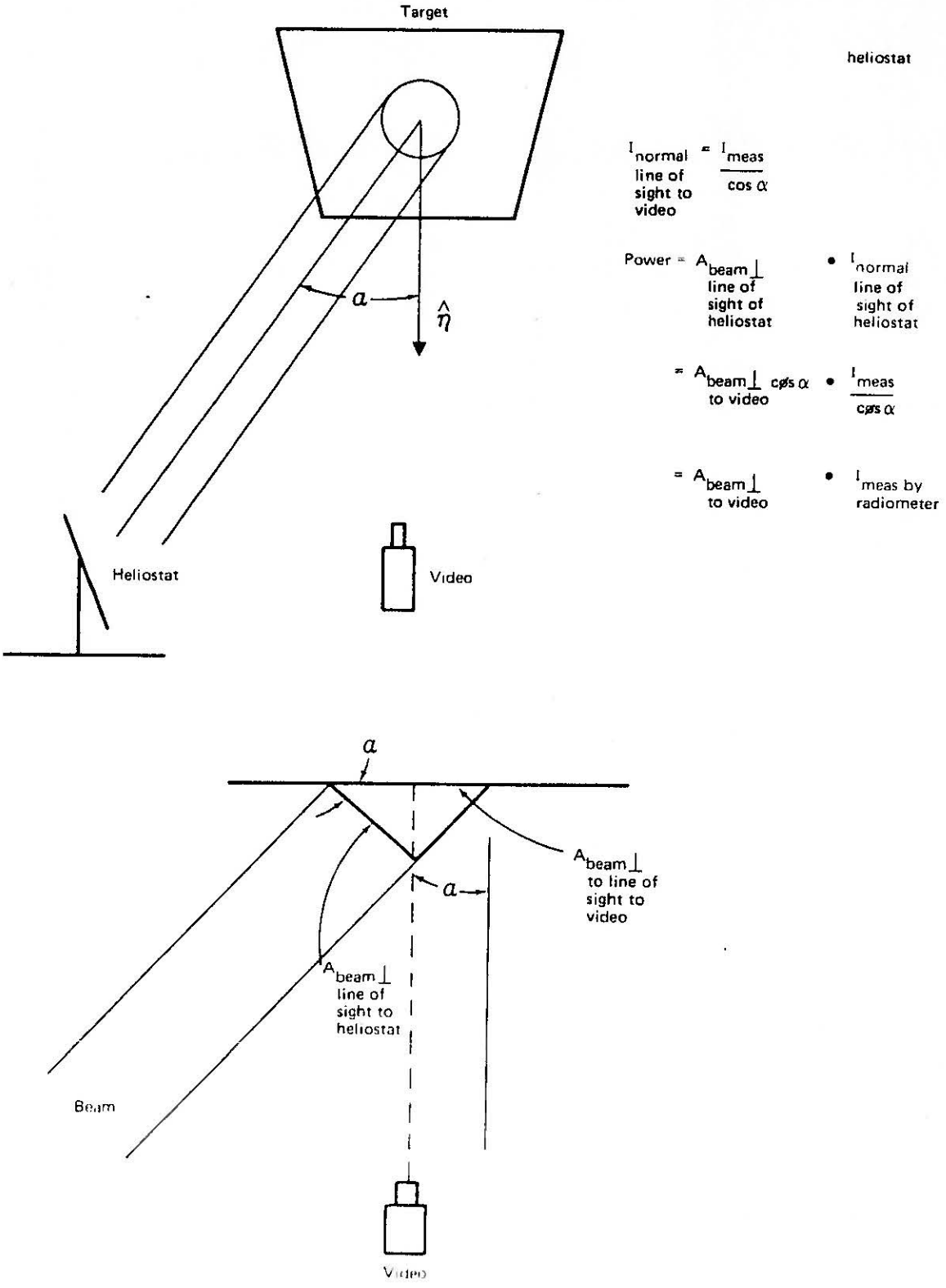

Figure 4-1. Relationships of Irradiance and Area

Conversely, the beam area as seen by the camera, (which is located on the target normal), will increase as the angle α increases. Thus,

$$A_{\substack{\text{Beam} \perp \\ \text{Line of Sight} \\ \text{to Heliostat}}} = A_{\substack{\text{Beam} \perp \\ \text{Video Line of} \\ \text{Sight}}} \cos \alpha$$

The power incident on the target for a given area is $I_{Net}.A$. The total beam power can be determined as

$$\text{Net Power} = A_{\substack{\text{Beam} \mid \\ \text{Line of Sight} \\ \text{to Heliostat}}} \times I_{\substack{\text{Net} \\ \text{Normal to Line of} \\ \text{Sight to Heliostat}}}$$

and

$$w = \frac{\text{Observed Width of Horizontal Line on Target}}{\text{Corresponding Number of x Pixels}}$$

$$h = \frac{\text{Observed Height of Y Direction Line on Target}}{\text{Corresponding Number of Y Pixels}}$$

The number of pixels scanned is n_1 which is less than 256 x 256 for the Solar One BCS.

4.2.1.6 Radiometer Non-Cosine Response

Field tests of several of the radiometers indicated that the response to solar irradiance at various incident angles was not in complete agreement with the expected cosine dependence. Therefore, tests were performed by MDAC at the Solar I site and by Hycal Engineering in the laboratory to determine the radiometer output versus incident angle using both field data and the Hycal calibration facility.

Since

$$I_{\substack{\text{Net}\\ \text{Normal to Line of}\\ \text{Sight to Heliostat}}} = I_{\substack{\text{Measured}\\ \text{Net}}}/\cos\alpha,$$

correcting $I_{\substack{\text{Measured}\\ \text{Net}}}$ by cos α gives values at each pixel of the irradiance and thus printouts of this type would correspond, in effect, to a target normal to the line of sight from that particular heliostat.

However, we may sometimes wish to have irradiance printed out as that incident on the target. In this case, the $I_{\substack{\text{Measured}\\ \text{Net}}}$ values are printed out directly. As long as the proper area is used with the irradiance values, the net power for the entire beam is the same because

$$\text{Net Power}_{\text{Entire Beam}} = \sum_{i=1}^{n} \left(\Delta A_{\substack{\text{Beam}\perp\\ \text{Line of}\\ \text{Sight}}} \right)_i \left(I_{\substack{\text{Net Normal to}\\ \text{Line of Sight}\\ \text{to Heliostat}}} \right)_i$$

$$= \sum_{i=1}^{n} \left(\Delta A_{\substack{\text{Beam}\perp\\ \text{Video Line}\\ \text{of Sight}}} \cos\alpha \right)_i \times \left(\frac{I_{\text{Measured, Net}}}{\cos\alpha} \right)_i$$

$$= \sum_{i=1}^{n} \left(\Delta A_{\substack{\text{Beam}\perp\\ \text{Video Line}\\ \text{of Sight}}} \right)_i \left(I_{\substack{\text{Measured}\\ \text{Net}}} \right)_i$$

Where,

$$\Delta A_{\substack{\text{Beam}\perp\\ \text{Video Line}\\ \text{of Sight}}} = wh$$

Target Pyrheliometer Incident Irradiance Angle Dependence and Correction

The target pyrheliometer (Medtherm S/N 81809, West Target) exhibited an approximate cosine response when calibrated by Hycal Engineering, but the deviation from a true cosine response was 5% at an incident angle of 45°, and thus, a correction has been determined. Hycal data are shown in Table 4-1 and Figure 4-2. These data were curve fit by an HP 9845 plot routine; results are shown in Table 4-2 and Figure 4-3 with the equation for the Medtherm response in terms of the angle of the incident beam with respect to the normal to the aperture face. The corrections obtained from the single Medtherm test are used for all Medtherms since time and budget did not permit testing all Medtherms, and there was no requirement for highly accurate power measurements.

The correction is applied only to the total power, and not to the discreet irradiance values. The correction to the power is:

$$\text{TOTPWR} \times \frac{\cos \phi}{\left([A_0 + A_1\phi + A_2\phi^2 + A_3\phi^3] \div 100 \right)}$$

where the A_i coefficients are shown on Figure 4-3.

The equations for the angle ϕ between the normal to the pyrheliometer, n, and the vector between the point on the target center and a heliostat, L, are given in Appendix M for each target.

Table 4-1. Hycal Data

McDonnell Douglas P. O. # 28128934

Instrument Type: Pyrheliometer I.D. # F1850L

The subject pyrheliometer was calibrated at 0°, 20°, 30°, 40° and 50° angles with respect to the source. The unit was centered 14 1/2 inches from the source for all calibrations with a source diameter of 2 inches. The following results were obtained:

Angle, ϕ	M.V.O.P. @ 1 Solar Constant	% of Full Scale Output	Cosϕ x 100	Error %
0°	4.32 mv	100%	100.00%	0
20° (.349066R)	4.00 mv	92.7%	93.97	1.35
30° (.523599R)	3.66 mv	84.8%	86.6	2.08
40° (.698132R)	3.18 mv	73.6	76.6	3.92
50° (.872665R)	2.07 mv	60.5%	64.28	5.88

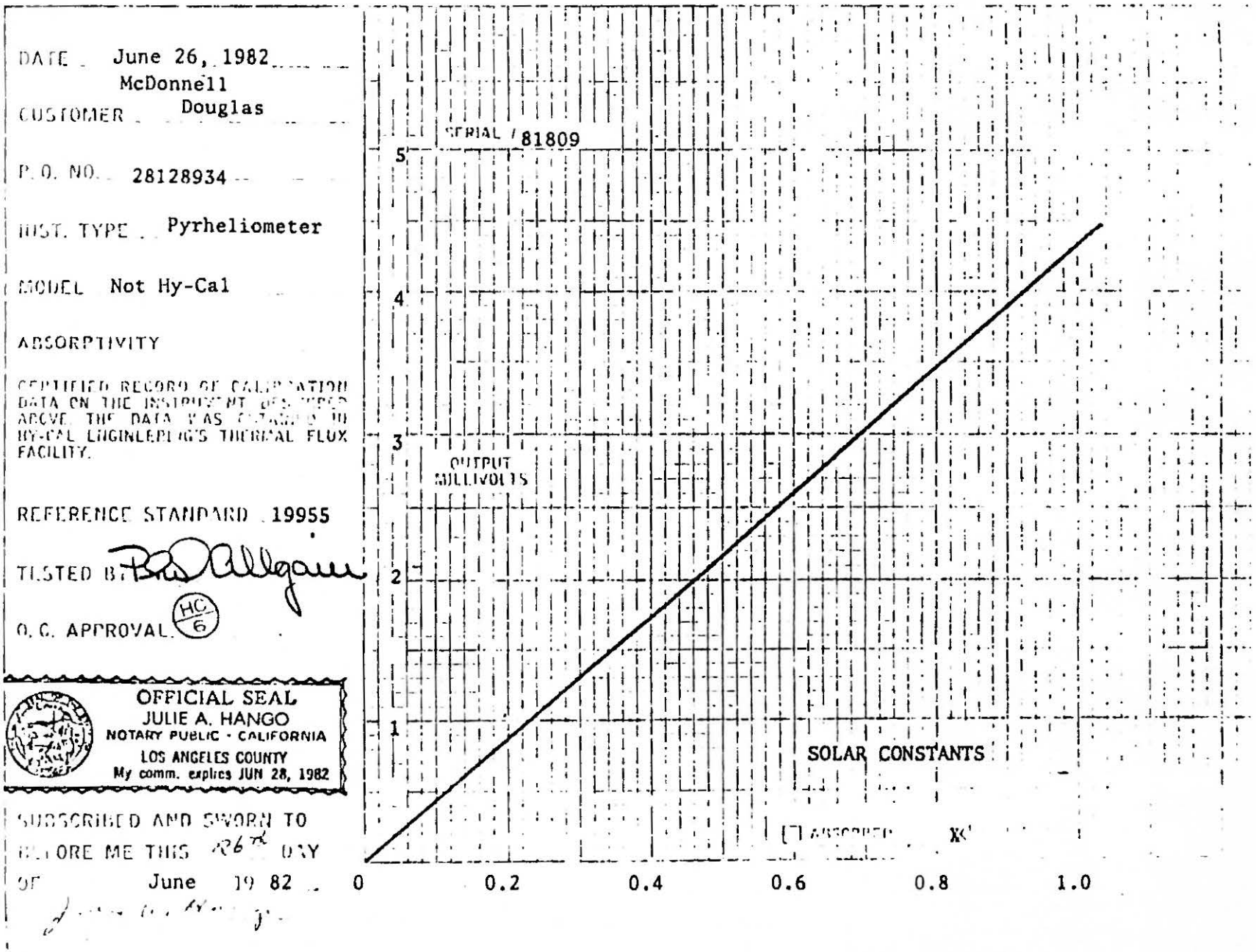

Figure 4-2. Hycal Response Curve

Table 4-2. Curve Fit Results

DATA

Point # 1: X = 0 Y = 100
Point # 2: X = .349066 Y = 92.7
Point # 3: X = .523599 Y = 84.8
Point # 4: X = .698132 Y = 73.6
Point # 5: X = .872665 Y = 60.5

Polynomial Model: Y=A(N)*X^N + A(N-1)*X^(N-1) + ... + A(1)*X +A(0)

Coefficients:

A(0) = 99.990566027
A(1) = -1.5134719
A(2) = -57.7587631
A(3) = 8.6947612

Source	Df	SS	MS	F
Regression	3	978.562	326.187	4939.36669847
Residual	1	.066	.066	
Total	4	978.628		

DATA COMPARISON

Point #	1:	X = 0	Y = 100	EQN	99.99057	Delta:	.00943
Point #	2:	X = .349066	Y = 92.7	EQN	92.79434	Delta:	-.0
Point #	3:	X = .523599	Y = 84.8	EQN	84.61132	Delta:	.1
Point #	4:	X = .698132	Y = 73.6	EQN	73.74151	Delta:	-.1
Point #	5:	X = .872665	Y = 60.5	EQN	60.46226	Delta:	.0

MAXIMUM DELTA: .1886792568

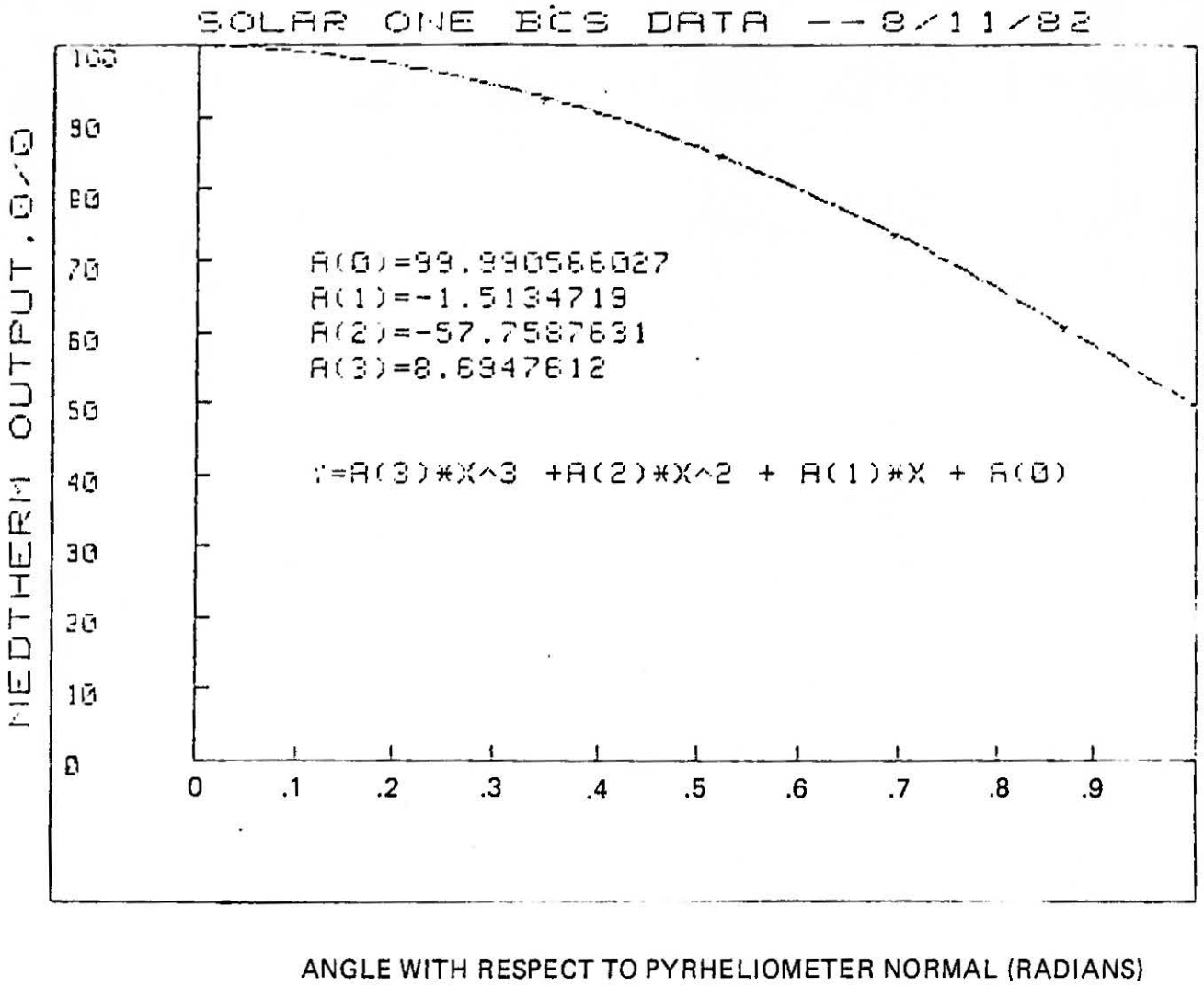

Figure 4-3. Medtherm Output (Percent) vs. Angle, ϕ, in Radians

4.2.1.7 Radiometer Calibration Discrepancy

A discrepancy of about 12.5% was noted between the Hycal and Medtherm calibration coefficients for S/N 81809. Results of our effort to explain this discrepancy are given in Appendix N. It was concluded that the Medtherm values were consistent with Eppley Normal Incidence Pyrheliometer readings to within 1-2%, and tests to verify the calibration coefficients performed at Medtherm were within 1% of the original values. Therefore, the Medtherm values are used. No explanation for the difference in values between the two facilities was found. However, it is important for accurate power and power effectivity values that intercomparison tests be made between the target radiometers and field pyrheliometer.

4.2.2 Development of Calibration Curve

The observed brightness, or DIR numbers, D, corrected for shading, are linearly related to the incident irradiance on the target, I, in w/m^2, by:

$$D_{corrected} = AI + D_{BL} \qquad 4.2.2\text{-}1$$

When the beam is on the target, we have:

$$D_{\substack{total \\ corrected}} = AI_{total} + D_{BL} \qquad 4.2.2\text{-}2$$

When the beam is off the target and the background scan is taken:

$$D_{\substack{background \\ corrected}} = AI_{background} + D_{BL} \qquad 4.2.2\text{-}3$$

and equation 4.2.2-3 must be updated, as discussed in the section 4.2.1.4. These equations are applied at the target radiometer locations, denoted 1, 2, 3. Thus, at each radiometer location:

$$D_{\substack{total \\ corrected}} - D_{\substack{background \\ corrected \\ update}} = A\,(I_{total} - I_{background}) \qquad 4.2.2\text{-}4$$

Three radiometers are used in order to increase the accuracy of the calibration curve in minimum time. Multiple scans are used to decrease error due to beam movement.

The value of the calibration coefficient, A, is determined from a least-squares curve fit to the pairs of net DIR numbers and net irradiance values obtained. Three radiometers are used in order to increase the accuracy of the calibration curve in minimum time. Further, the curve fit must be based on a curve that goes through zero, and thus a slightly different least square curve fit approach is used. In general, the curve should satisfy:

$$\sum_i (y_i - y_i')^2 = 0 \qquad 4.2.2\text{-}5$$

where, for $y_i = 0$ at $x_i = 0$, we use

$$y_i = Ax_i \qquad 4.2.2\text{-}6$$

Thus:

$$\sum_i (Ax_i - y_i')^2 = 0 \qquad 4.2.2\text{-}7$$

Differentiating with respect to A and solving:

$$A = \frac{\sum_{i=1}^{n} y_i' \, x_i}{\sum_{i=1}^{n} x_i^2} \qquad 4.2.2\text{-}8$$

The value of y_i' corresponds to $D_i - D_{BG_i}$ at radiometer i, with x_i given by $I_{total_i} - I_{background_i}$. Again $D_i - D_{BG_i}$ is the corrected value. Thus:

$$D_{corrected}\Big|_i - D_{background}\Big|_i = \left(D_{actual}\Big|_i - D_{background}\Big|_i\right)$$

$$\times \left[\frac{D_{\substack{maximum\\integsph}}\Big|_{center} - D_{\substack{black\\level}}\Big|_{center}}{D_{\substack{actual\\integsph}}\Big|_i - D_{\substack{black\\level}}\Big|_i}\right] \qquad 4.2.2\text{-}9$$

Equation 4.2.2-8 can now be expressed as:

$$A = \frac{\sum_i \left(D_{actual}\Big|_i - D_{\substack{background\\updated}}\Big|_i\right)\left(\frac{D_{\substack{maximum\\integsph}}\Big|_{center} - D_{BL}\Big|_{center}}{D_{\substack{actual\\integsph}}\Big|_i - D_{\substack{black\\level}}\Big|_i}\right)\left(I_{total_i} - I_{\substack{back-\\ground\\updated}}\right)}{\sum_i \left(I_{total}\Big|_i - I_{\substack{background\\updated}}\Big|_i\right)^2} \qquad 4.2.2\text{-}10$$

4.2.3 Beam Irradiance

The digitized response, (i.e., DIR number) of the camera at i,j is proportional to scene brightness (i.e., radiance) corresponding to a particular pixel having row, i, and column, j, location. Thus, the net radiance, $B(i,j) - B(i,j)_{background}$ is proportional to the net corrected DIR numbers, or

$$D(i,j)_{\substack{corrected}} - D_{\substack{background\\corrected\\updated}} = C\left(B(i,j) - B(i,j)\Big|_{background}\right) \qquad 4.2.3\text{-}1$$

The net radiance from the target at i,j is proportional to the net irradiance incident at i,j, divided by the solid angle corresponding to the pixel area. Thus,

$$B(i,j) - B(i,j)\Big|_{background} = I_{net}(i,j)/\Delta\theta_x\Delta\theta_y \qquad 4.2.3\text{-}2$$

where $\Delta\theta_x$ and $\Delta\theta_y$ are the angles subtended by the width and height of a pixel.

Substituting 4.2.3-2 into 4.2.3-1 and incorporating $\Delta\theta_x$ $\Delta\theta_y$ into the new calibration coefficient, we have,

$$D(i,j)_{\text{corrected}} - D(i,j)_{\substack{\text{background}\\\text{corrected}\\\text{updated}}} = AI_{Net}(i,j) \qquad 4.2.3\text{-}3$$

Where

$$A = \frac{C}{\Delta\theta_x \Delta\theta_y}$$

At this point, it can be seen that $\Delta\theta_x$ and $\Delta\theta_y$ need not be determined since they are incorporated in the coefficient A, which is determined by the curve fit to the correlated data. Equation 4.2.3-3 is in the usual form for correlating DIR values with irradiance.

The net irradiance at any point on the target is determined from the net DIR values (corrected and updated), divided by the value of A determined from the least squares curve fit to the pyrheliometer data and corresponding DIR values. Thus, the net irradiance for each pixel at points other than the pyrheliometer locations is expressed as:

$$I_{NET}(i,j) = \frac{1}{A}\left(D(i,j)_{\text{corrected}} - D(i,j)_{\substack{\text{background}\\\text{corrected}\\\text{updated}}}\right) \qquad 4.2.3\text{-}4$$

or

$$I_{NET}(i,j) = \frac{1}{A}\left[\left(D(i,j)_{\text{actual}} - D_{BL}(i,j)\right) - \left(D_{BG}(i,j)_{\text{actual}} - D_{BL}(i,j)\right)\right] \cdot \left(\frac{D_{TTR_{t_i}} - D_{BL_{TTR}}}{D_{TTR_{t_{BG}}} - D_{BL_{TTR}}}\right)\left[\frac{D_{MAX_{\substack{\text{integsph}\\\text{center}}}} - D_{BL_{\text{center}}}}{D(i,j)_{\substack{\text{actual}\\\text{integsph}}} - D_{BL}(i,j)}\right] \qquad 4.2.3\text{-}5$$

Note that the $D_{TTR_{t_i}}$, etc. terms are included to update, and thus correct for, background variations as discussed in Appendix L.

The net irradiance as expressed above, Equation 4.2.3-5, is the irradiance incident on the actual target. Later, the irradiance will be determined for a target normal to the line-of-sight from the heliostat to the target.

4.2.4 Beam Power

The net beam power is the sum of the net irradiance value at each pixel times the pixel area. Net irradiance is determined for each pixel location given the digitized brightness value (DIR number) and the slope, A, of the calibration curve. Thus, the net beam power, with shading correction and background update, is

$$P_{beam} = \int_{surface} I_B(x,y)\, dS = \frac{\Delta S}{A} \sum_{i,j} \left\{ \left[D_{actual}(i,j) - D_{BL}(i,j) - \left(D_{\substack{BG \\ actual}}(i,j) - D_{BL}(i,j) \right) - \left(\frac{D_{TTR_{t_j}} - D_{BL_{TTR}}}{D_{TTR_{T_{BG}}} - D_{BL_{TTR}}} \right) \right] \times \frac{D_{max_{integsph}}\Big|_{center} - D_{BL}\Big|_{center}}{D_{\substack{actual \\ integsph}}(i,j) - D_{BL}(i,j)} \right\}, \qquad 4.2.4\text{-}1$$

where ΔS is the area of a pixel, and A is given by equation 4.2.2-10.

The pixel width and height as seen by the TV camera is determined from the known registration points on the target, and thus the characteristic pixel area can be determined.

The three registration marks at the corners of the target are located as a part of BCS initialization.

From these data it is possible to calculate the pixel distance in units of distance (cm).

The general algorithm is:

$$\text{Pixel Dist.}(x) = \frac{Dpx}{\text{Pixel Count }(x)} \qquad (4.2.4\text{-}2)$$

$$\text{Pixel Dist.}(y) = \frac{Dpx}{\text{Pixel Count}(y)} \qquad (4.2.4\text{-}3)$$

where

Dpx	= Distance between registration marks in x direction.
Dpy	= Distance between registration marks in y direction.
Pixel count (x)	= Number of x-pixels between registration marks.
Pixel count (y)	= Number of y-pixels between registration marks.
Pixel Dist. (x)	= Pixel width (x-direction) centimeters.
Pixel Dist. cy	= Pixel height (y direction).

Once the pixel distances are calculated, the surface area that each pixel represents can be calculated by multiplying the x and y distances together:

Δ S = Area (pixel) = Pixel Dist.(x) * Pixel Dist.(y).

4.2.5 Centroid

The centroid of the beam is determined in the x and y directions. The X centroid value corresponds to the position of a vertical line (as seen by the camera) for which the reflected beam power is the same to the left and right of the line. The y centroid value corresponds to the position of a horizontal line in the x direction for which the the reflected power is the same above and below the line. The method of calculation is as shown below:

$$\text{x centroid} = \sum_{i=1}^{N} \frac{\left(\begin{array}{l}\text{Total Net}\\ \text{Power in}\\ \underline{\text{i}}\text{th column}\end{array}\right) * \left(\text{lever arm}_{(x)i}\right)}{\text{Total Net power (whole target)}} \qquad (4.2.5\text{-}1)$$

$$y\ \text{centroid} = \sum_{i=1}^{N} \frac{\left(\begin{matrix}\text{Total Net}\\ \text{Power in}\\ \underline{\text{ith}}\ \text{row}\end{matrix}\right) * \left(\text{lever arm}_{(y)i}\right)}{\text{Total Net power (whole target)}} \qquad (4.2.5\text{-}2)$$

where:

Total Net power in ith column (or row) is the total power obtained by adding all pixel area net powers in a particular column or row. Net power is the total power minus the background power.

The lever arm is the distance of the row or column being calculated away from a reference point.

The calculated centroids as obtained in the above equations are in terms of distance across the target as viewed by the camera. These values must be translated to the target aim point.

For the x direction, the calculated centroid is in terms of distance but starting at the first column of the TV frame.

The pyrheliometer reference points must be correlated to the pixel columns and then the centroid deviation away from the target aim point can be calculated.

4.2.6 Power Measurement Accuracy

Accurate determinations of beam power are important for primarily two reasons. First, beam power is needed to assess heliostat performance, determine spillage power, assess need for cleaning the heliostats, and evaluate plant performance. Second, power measurements are needed in assessing data validity for aimpoint bias updates. The latter reason is more applicable to normal plant operation. Generally, if the power measurement is accurate, centroid measurements are accurate. However, inaccurate power measurements do not necessarily invalidate centroid measurements because the major reason for inaccurate power is that the slope of calibration curve is in error. Since this effect increases or decreases each irradiance value proportionately, centroid is not affected. Therefore, the initial primary purpose of the power measurement was to assist in establishing data validity. Later, it was determined that accurate power measurements would be useful in determining heliostat and plant performance, and therefore modifications were made to the system to improve power data accuracy. These modifications included:

(1) Deactivating the target radiometer shutters, which caused an excessive time delay relative to wind induced motion.

(2) Painting the target radiometer shutter area white so that more accurate brightness correlations could be obtained.

(3) Modifying the software to incorporate analytical improvements such as background updates and corrections to vignetting.

The most practical method of determining power measurement accuracy is to determine power effectively (ratio of measured to theoretical power) for particular heliostats over a day. The standard deviation is an indication of the measurement repeatability. However, this method does not determine the actual error, even if the heliostat reflectively is known, because of uncertainties in the amount of reflected beam power lost due to atmospheric attenuation and scattering at the heliostat. Both of these effects can be minimized by testing heliostats close to the receiver. However, since all the heliostats have the same mirror module cant angles, corresponding to superposition of individual mirror modules for a far field location, the mirror module beams have very little overlap for the heliostats in the inner rows. As a result, beam irradiance is low, significant irradiance value variations can occur over a few inches, and the overall effect is to reduce power measurement accuracy for close-in heliostats.

Other errors include the effects of wind and tracking motion on beam movement at the target and the limitation of having a single pyrheliometer for solar irradiance measurement which, although located in the center of the field, is relatively far from most of the heliostats, and thus can not necessarily determine heliostat incident irradiance accurately. However, tests with low winds and clear sky conditions have been performed frequently, and typical results are shown in Figure 4-4. Measurement repeatability (for 5-10 runs over approximately 1 minute) is shown by the power effectivity standard deviation, which is usually less than $\pm$ 2%. The mean value for a series of heliostats is usually within $\pm$ 5 to 10% of the field average reflectivity, for clear sky, low wind conditions. Sequential power effectivity measurements on the same heliostat, over the course of the day, is typically within $\pm$ 5%.

Summary of BCS Data 9/13/83												
HEL No.	Centroid Average Time	Normalized Centroid and Standard Deviation (in.) (Horizontal)	(Vertical)	Theo Power (W)	Power Effectivity (%)	Std Dev Power (%)	Ave Spill Power (%)	Std Dev Spill Pwr (%)	Invalid Data Flags	INSOL (W/SQM)	Wind Speed (MPH)	Ambient Temp (Deg F)
2903	12:13:41	19.9 ± 9.6	-9.0 ± 6.2	31125	86.0 ± 1.8	2.1	0.4	0.0	0000000000	886.2	6.8	98.2
2917	12:19:42	33.0 ± 5.4	29.1 ± 1.3	30603	83.4 ± 1.5	1.9	2.0	0.0	0000000000	884.3	7.2	98.5
2904	12:25:24	44.6 ± 4.2	68.5 ± 1.8	31363	72.0 ± 0.9	1.3	11.9	0.0	0000000000	887.0	9.7	99.1
2918	12:31:25	21.1 ± 4.2	-39.1 ± 9.5	31411	89.6 ± 1.2	1.3	1.1	0.0	0000000000	892.4	7.2	99.1
2803	12:37: 6	10.0 ± 6.1	-15.0 ± 1.2	31495	87.6 ± 1.1	1.3	2.0	0.0	0000000000	891.1	11.5	99.3
2817	12:43:50	7.5 ± 5.4	-13.7 ± 2.3	31132	84.7 ± 0.9	1.1	0.0	0.0	0000000000	886.9	5.7	99.3
					83.88 ± 6.2							

Invalid Data Flags Definition	
Position	Definition
1	The Horizontal or Vertical Centroid is Greater Than 150 In.
2	The Standard Deviation of the Centroid is Greater Than 2 Ft.
3	The Power Effectivity is Greater Than 140 or Less Than 60%
4	The Percent Std. Dev. of Effectivity is Greater Than 8.0%
5	Percent Std. Dev. of Measured Power is > 5.0%
6	Wind Speed is Above 25 mph
7	Irradiance Defaulted to 1000.0 Watts Per Meter Sq.
8	Default Cal Curve Used and Effectivity Set to 80 if Bit 3 Set
9	Background Update Factor Not Used. Default = 1.0
10	Sunshape Data Not Acquired

Figure 4-4. Summary of BCS Data

Further increases in accuracy require

(1) Modification of the DAS solar insolation sampling rate to acquire data more frequently and simultaneous with each power scan.

(2) Addition of at least one more target radiometer to assure that relatively high irradiance regions of the beam strike at least one radiometer.

(3) Data acquisition under conditions of low wind, clear sky conditions.

(4) Measurement of heliostat reflectance on the same day or at least within a few days of the test.

(5) Incorporation of software to assess calibration curve data scatter so that conditions leading to inaccurate results can be identified.

4.2.7 Centroid Measurement Accuracy

Three methods were used to establish that the BCS centroid accuracy is of the order of $\pm$ 1 pixel for nominal test conditions, which corresponds to a centroid location uncertainty on the target of approximately $\pm$ 2 inches.

The first method involved use of 1" x 2" visually uniform white targets on a uniformly black background, placed approximately 10 feet in front of a BCS camera. Calculated centroids were compared with the geometric centroid and found to be within $\pm$ 1 pixel. This test eliminated errors due to beam and tower movement.

The second method involved use of a 5" x 5" mirror reflecting sunlight onto a small, temporary target placed approximately 30 feet in front of a BCS camera. In this case, the actual centroid could not be determined but repeated measurements over a period of less than 1 minute gave a centroid standard deviation. This test eliminated uncertainties in the BCS target nonuniformity and beam movement (sun induced beam movement was less than 0.1"), but used a simulated beam. A series of 10 tests showed that the equivalent centroid standard deviation on the BCS target corresponded to $\pm$ 1.8" in x and $\pm$ 2.46" in y. Since some of this error was attributable to test conditions (primarily wind-induced movement of the temporary target), the BCS intrinsic error is less.

The third method involved monitoring the standard deviation for a series of close in heliostats tested under moderately low wind conditions of

approximately 8.5 mph. Results are summarized in Table 4.2.7-1 which show standard deviations in x and y of ± 1.6" and ± 1.7", respectively. Testing close-in heliostats minimized error due to beam movement, and results would be conservative because of the beam shape. A similar test was run on heliostat 2063, one of the outer heliostats for a wind speed of 14.8 ± 2.4 mph; the x,y centroids were ± 1.4 and ± 3.5", respectively even for these relatively severe conditions.

The angular error associated with these centroid position uncertainties is of the order of ± .15 mr for heliostats at 1000 ft. Again, part of the uncertainty is due to wind or control system induced movement of the beam, tower movement, etc., and thus the BCS can be seen to provide accurate centroid measurements. Multiple centroid measurements are made for each heliostat (usually ten), so that beam movement affects can be assessed. If the standard deviation is relatively low, then centroid data is applicable to bias updating, assuming it is valid in all other respects. The details of these data validity algorithms are discussed further in subsequent sections.

Table 4.2.7-1

Date: 4/21/84

Centroid Standard Deviation for Relatively Low Wind Speed Conditions

Heliostat #	Standard Deviation X	Standard Deviation Y	Wind Speed
115	1.06	1.61	11.9
117	1.04	.94	8.1
121	.61	1.87	12.2
123	.75	1.2	10.1
125	.85	1.81	10.2
128	1.46	1.1	7.2
104	4.15	2.78	8.9
129	.78	2.1	5.7
130	.72	.92	6.4
106	2.98	1.75	6.1
131	.68	1.15	2.5
107	2.6	2.1	3.6
132	1.16	1.09	5.5
108	4.48	3.53	10.8
115	1.7	.93	5.5
117	1.04	1.61	3.8
119	.68	1.69	4.8
121	.3	1.19	5.6
123	1.35	1.39	9.9
125	.37	1.83	11.8
104	1.23	2.49	12.7
130	1.45	2.02	5.8
108	3.55	3.09	9.1
131	0.63	1.71	11.4
132	1.45	1.86	10.9
117	4.84	2.2	9.9
119	1.66	1.54	17.1
121	1.75	2.07	9.8
	1.6" average	1.71" average	8.5 mph average

Section 5
SUNSHAPE CAMERA DESIGN

The sunshape camera shown in Figure 5-1 is located on the Control Building roof adjacent to an Eppley Normal Incident Pyrheliometer (see Appendix P). The sunshape camera tracks the sun during BCS data acquisition and measures the solar radiance distribution an instant after the beam data is obtained for each heliostat. All of these data are stored on tape for engineering evaluation purposes, such as comparisons of the actual and ideal beam irradiance distributions, determination of effects of atmospheric scattering and clouds on solar radiance, and calculations of the solar irradiance which could be redirected to the receiver by an ideal heliostat. These evaluations are needed to determine the nature and magnitude of energy losses.

The basic video camera is identical to the BCS field cameras except for the optics, vidicon tube, environmental enclosure, and filters. Camera modifications for elimination of AGC and black level control are identical, and shading corrections are made in the same manner.

A Hamamatsu IR vidicon (N214) is used, having a spectral response from 400 to 2000 nm, with good sensitivity in the far red range.

The spectral response characteristics of the Hamamatsu N214 tube shows a high peak in the visible and a decrease out to about 2000 nm. However, the sun's radiance has a spectral dependence that depends on radius from the sun's center. Therefore, to obtain a valid radiance distribution for the total sun's radiance over all wavelengths, the tube's spectral response must be corrected by filters to obtain at least a reasonably constant output over its spectral range. A wide variety of off-the-shelf filters were investigated to obtain a set which provided reasonable flatness to the spectral response curve. The filters selected and the response are shown in Figure 5-2. Presently, shading corrections must be made with the filters removed since the decreased radiance at the vidicon with the filters makes the integrating sphere too dim to be seen.

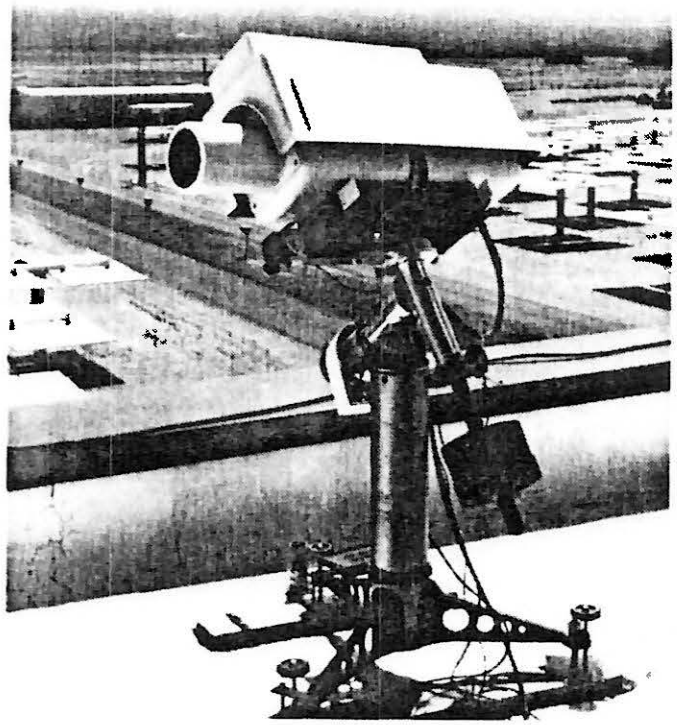

- 2850C Cohu Camera with Lenzar Optics 200 to 1400 MM Lens
- Lenzar Optics Envirogard Housing (Peltier Effect Cooling)
- Meade Corp Equatorial Tracker with Dual Axis Corrector System
- Mounted on Roof of Control Building, Adjacent to Eppley Normal Incident Pyrheliometer
- Hamamatsu N214 Tube (400 to 2000 MM)
- Filter to Flatten Vidicon Response
- Computer Controlled "Image Grab" for Digitizer Correlated with Heliostat Beam "Image Grab"

Figure 5-1. Sun Shape Camera

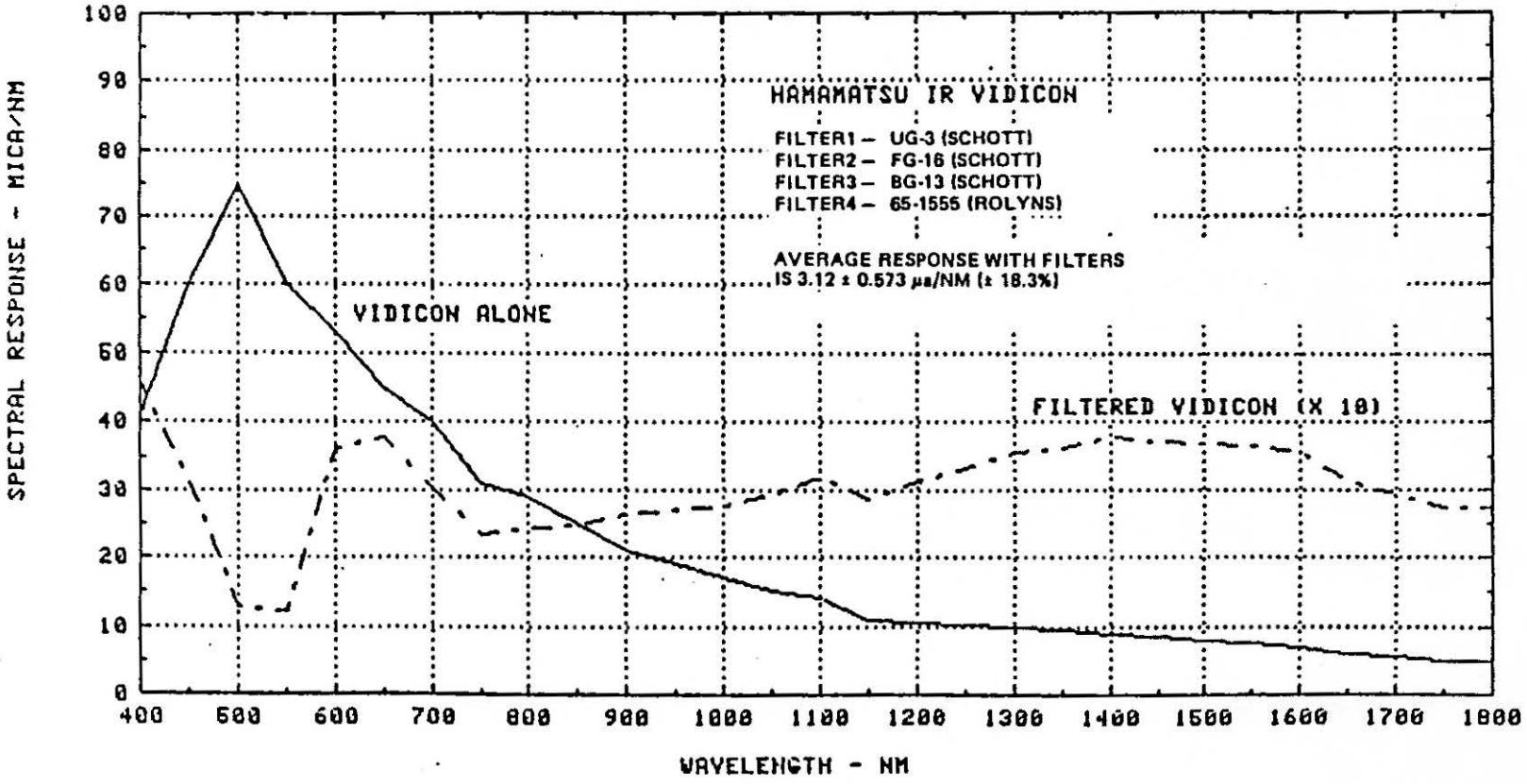

Figure 5-2. Corrected Camera Response with Selected Filters Landscape

The camera and optics are enclosed in a Lenzar Optics Envirogard housing which uses solid state (Peltier effect) cooling to maintain the enclosure temperature at approximately 10°C (50°F) (see Appendix Q). A Lenzar Optics 200 to 1400 mm zoom lens is used so that a wide range of magnifications can be obtained.

The camera is mounted on a Meade tracker (see Appendix R). Dual-axis corrector controls located at the BCS console allow the operator to position the camera as required for continuous sun tracking. Initial alignment is required each morning of the test day. This simply involves swinging the camera to point at the sun and turning on the tracker. A timer shuts off the tracker late in the afternoon.

Sunshape camera calibration is obtained by comparing the sum of the net DIR values to the irradiance, over the solid angle corresponding to the Eppley Normal Incident Pyrheliometer. Thus, knowing the solid angle of each pixel, (which is determined by viewing any object of known angle or height and width a given distance from the camera), the calibration coefficient used to transform 8-bit DIR values into absolute radiance units (w/m^2 steradian) is found from

$$K = \frac{I_{NIP}}{\left\{ \sum_{i=10}^{256} \sum_{j=17}^{256} \left[D(i,j) \Big|_{\text{Corrected}} - D(i,j) \Big|_{\text{Black}} \right] \right\} \Delta\theta_x \Delta\theta_y}$$

where

I_{NIP} = Eppley N.I.P reading (w/m^2)

$D(i,j) \Big|_{\text{Corrected}}$ = Digital image radiometer intensity (0-255 bits) as digitized video signal, corrected for shading and vignetting

$D(i,j) \Big|_{\text{Black}}$ = Black level of camera

$\Delta\theta_x$ = Characteristic angle per pixel in the x-direction (horizontal), radians per pixel

$\Delta\theta_y$ = Characteristic angle per pixel in the y-direction (vertical), radians per pixel

The radiance, B(i,j), in w/m2 steradian at i,j is thus,

$$B(i,j) = \frac{I_{NIP}\left[D(i,j)\big|_{\text{Corrected}} - (D(i,j)\big|_{\text{Black}}\right]}{\left\{\sum_{i=10}^{256}\sum_{j-17}^{256}\left[D(i,j)\big|_{\text{Corrected}} - D(i,j)\big|_{\text{Black}}\right]\right\}\Delta\theta_x\Delta\theta_y}$$

These results over the entire face of the sun involve as many as 65,000 radiance values. Rather than use these in the computer analysis of the ideal beam shape, a radial distribution is developed and stored on magnetic tape with each heliostat beam scan. Tests of the four radial distributions (right, left, top, and bottom) are conducted to assure the sun shape is symmetric and not distorted by clouds. Details of this technique are given in Appendix O.

Section 6
BCS SOFTWARE TOP LEVEL DESCRIPTION

BCS software is organized into five phases, consisting of:

1. Initialization. This phase involves tasks which set up global common, check BCS hardware status, test MODACS hardware, and set up the BCS-HAC input executive.

2. Measurement. This phase involves tasks which acquire flux and irradiance data from the targets, calculate calibration curves, control image grabs based on interrupt signals, and read the pyrheliometer values provided by the MODACS.

3. Termination. This phase terminates the measurements, calculates spillage power, updates the master file (by determining which heliostats were measured on a given day) and prints the test data reports.

4. General. This phase performs tasks involved with sending current time, error, and outstanding messages to the HP, and communication messages to the HAC.

5. Off-Line. This phase includes tasks for archiving BCS data, plotting BCS and sunshape data, retrieving historical BCS data, creating the candidate list of heliostats, establishing white and black files, locating target registration marks, and determining characteristic pixel angles for the sunshape camera.

There are 32 tasks and 61 subroutines, with 5424 lines of executable FORTRAN, 7060 total lines of FORTRAN (including common, equivalence, data, variable definition, and format statements, but excluding comments), and 641 lines of assembly code.

The BCS computer communicates with the HAC computer and receives data as required from the DAS. Heliostat centroid data which have passed validity checks are communicated to the HAC which then calculates the heliostat bias offsets required to correct the beam pointing error.

The BCS top level task activation schematic is shown in Figure 6-1. Details of task activation are given in the BCS Operator/User's Manual and in the BCS Top Level Unit Development Folder (UDF). BCS measurements are initiated by the operator at the HP terminal, with data acquisition under the control of the HAC, which sends heliostat status messages to the BCS computer. The BCS responds to each status message by performing the appropriate task (e.g., acquiring video data from a target, etc.) and sends a status message to the HAC.

The BCS can measure up to 60 heliostats per day, each heliostat being measured up to three times daily. The multiple measurements help to pinpoint the centroid more accurately since the sun movement and heliostat position can change the beam centroid as the day progresses, due to the pedestal tilt and drive unit nonorthogonality errors. Beam power is measured to verify centroid validity and determine heliostat performance.

The centroid information calculated by the BCS is used by the HAC to calculate bias offset for each individual heliostat. Through the use of this offset, the HAC will be able to maintain tracking accuracy for each heliostat over the life of the field.

The general sequence of operation is as follows. The HAC moves a heliostat beam to track on a BCS target (North, South, East, or West). The BCS commands the digitizer to take an image grab of the BCS target with the heliostat beam tracking a specified aimpoint. The digitized image is stored in the memory of the digitizer as a 256 X 256 array with each pixel having a resolution of 8 bits. The 8 bit resolution gives the system the capability of distinguishing up to 256 gray levels. The gray levels give the relative intensity distributions of the image including background light on the target. The software then reads the target radiometers and field pyrheliometer. The beam is then moved off the target and an image grab taken to obtain the background irradiance distribution on the target.

Camera shading and background updates are applied to the data, background data is updated, subtracted from the total beam data to determine the net beam irradiance distribution, and centroid and net beam power are calculated. Upon completion of the measurement phase, plot data and a summary of the BCS data are printed. BCS output and a discussion of typical test data is presented in Section 7.0.

Section 7
OPERATOR INTERFACE

Operator interface with the BCS has been minimized by (1) providing automatic data validity algorithms to verify that bias update data can be used by the HAC and (2) providing automatic responses of the BCS to message status inputs and commands from the HAC. The operator is required to initialize the BCS whenever measurements are required, and, as necessary, to review data acquired.

Procedures for operating the BCS are detailed in the BCS Operator and User's Manual, Reference 10, and are not covered here.

Operator data review is discussed below.

Since BCS data are required for both tracking aimpoint bias updates and detailed engineering evaluations, the types of data display vary from data summary sheets which are scanned by the operator prior to bias updating, to detailed results of beam irradiance distribution over a field of 65,000 pixels with attendant sun shape data, and a complete set of environmental conditions.

The first level results are given as a "Summary of BCS Data," such as shown in Figure 4-4. The summary gives for each heliostat and time:

(1) The beam centroid error as a mean and standard deviation

(2) Theoretical power from that heliostat, at that time, assuming 100% reflectivity, no atmospheric attenuation, and using the projected area of the tracking heliostat with respect to the plane normal to the ray from the target center to that heliostat (see Appendix S).

(3) The so-called "power effectivity" which is in principle the same as heliostat reflectivity except for additional losses due to atmospheric attentuation and various scattering losses contributed by soiling, mirror waviness, solar radiance distribution in the circumsolar region, etc.

(4) Invalid data flags, if warranted, to caution the operator to examine the results prior to bias update.

(5) Environmental conditions (solar insolation as measured by the Eppley Normal Incident Pyrheliometer), wind speed, and temperature.

Generally, for bias update purposes, any power effectivity result which is reasonably close to the expected heliostat reflectivity (which may vary from 70 to 90% depending on degree of mirror cleanliness) is sufficient evidence that the centroid values are valid. Large errors indicate off- nominal occurrences such as no beam on target, multiple beams, etc.

Whether or not bias updating will be applied requires that several additional conditions be met. For example, if the centroid error is small (say, less than 2-3 cm) bias update is not necessary. If the standard deviation of centroid is large compared to the error and wind speed is high, it is evident that the heliostat wind induced oscillations are too large to justify a bias update. Low insolation values, especially values that change significantly from one run to another, imply cloud coverage, and thus bias updates would not be applied until further checks were made.

Trained operators are able to make evaluations rapidly using data such as shown in Figure 4-4. In addition, plots of the beam shape can be generated if additional data are needed to evaluate individual runs. A sample test run is shown in Figure 7-1. This run was made shortly after heliostat 2404 was cleaned and its reflectivity measured. The BCS value of 89.9% compares well with the measured value of 91.8%. The beam shape corresponds to the isoflux contour which contains 90% of the net beam power. This is a transformed beam shape (i.e., normalized) as it would appear projected onto a plane normal to the ray from the heliostat to the target. Overlayed on this beam is the view of the cylindrical receiver as seen from the heliostat; that is, in the normal plane. The normalized plot is required since heliostat beams are incident on a given target over the entire quandrant ($\pm$ 45°), and these oblique views of the beam do not correspond to the beam distribution on the receiver. Receiver panels are also designated as viewed from the heliostat. The derivation of the receiver panel display equations is given in Appendix T.

The derivation of equations for normalizing the beam flux distribution is given in Appendix U.

Normalized Plot

HCNUM	2404
Date	9/13/83
Time of Day	12:08
Centroid Error +/- Std. Dev. (Horiz.)	-6.73 +/- 2.82 In.
Centroid Error +/- Std. Dev. (Vert.)	-22.26 +/- 7.67 In.
Theoretical Power	31727.8 Watts
Power Effectivity +/- Std. Dev.	89.9 +/- 0.9%
Spillage Power	0.0 +/- 0.0%
Insolation Level	888.4 W/M**2
Wind Velocity	3.85 mph
Temperature	97.64 degf
Invalid Data Flags	0000000010

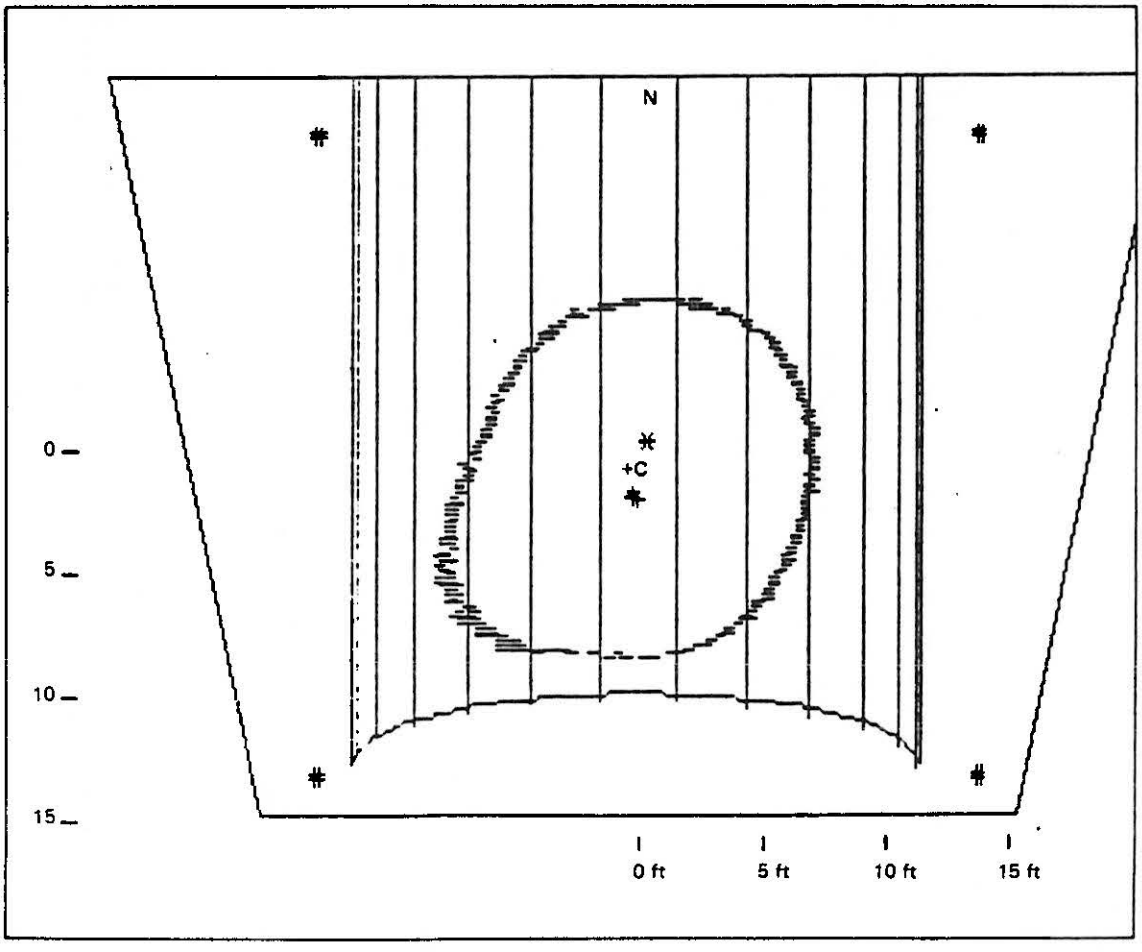

Figure 7-1. Typical Plot of Normalized Beam Relative to Receiver

Only the last beam is normally plotted, and "C" designates the centroid. The other four centroids are shown as crosses. The aimpoint on the receiver is shown as the figure "}{". This aimpoint is changed by the HAC depending on receiver flux distribution requirements. The aimpoint shown corresponds to the aimpoint required at the time the beam is scanned. The trapezoidal figure is the target size and shape a viewed by the camera. This is not transformed to appear as if viewed from the heliostat.

Figure 7-2 shows a beam for heliostat 2904 which has large aimpoint errors and consequently spillage power is significant at 11.9%.

Figure 7-3 shows an abnormal condition in which two heliostats are reflecting light onto the target during a measurement phase. Annotations on the figure point out that the shape and power effectivity indicate inadvertent movement of a close-in heliostat across the target from left to right. This is an example of a condition which would render centroid data invalid automatically, and thus prevent an error in bias update.

A typical sun shape radial radiance distribution curve is shown in Figure 7-4. These radial radiance distributions, with the corresponding characteristic angle associated with the pixel, and the calibration coefficient which transforms the DIR number (0 to 255) into radiance (w/m^2 steradian) are recorded on tape. Results are then used in the heliostat analysis codes (HELIOS, Reference 4 and CONCEN, References 8 and 9).

Normalized Plot

HCNUM	2904
Date	9/13/83
Time of Day	12:25
Centroid Error +/- Std. Dev. (Horiz.)	44.61 +/- 4.16 In.
Centroid Error +/- Std. Dev. (Vert.)	68.53 +/- 1.79 In.
Theoretical Power	31363.1 Watts
Power Effectivity +/- Std. Dev.	72.0 +/- 0.9%
Spillage Power	11.9 +/- 0.0%
Insolation Level	887.0 W/M**2
Wind Velocity	9.69 mph
Temperature	99.14 degf
Invalid Data Flags	0000000000

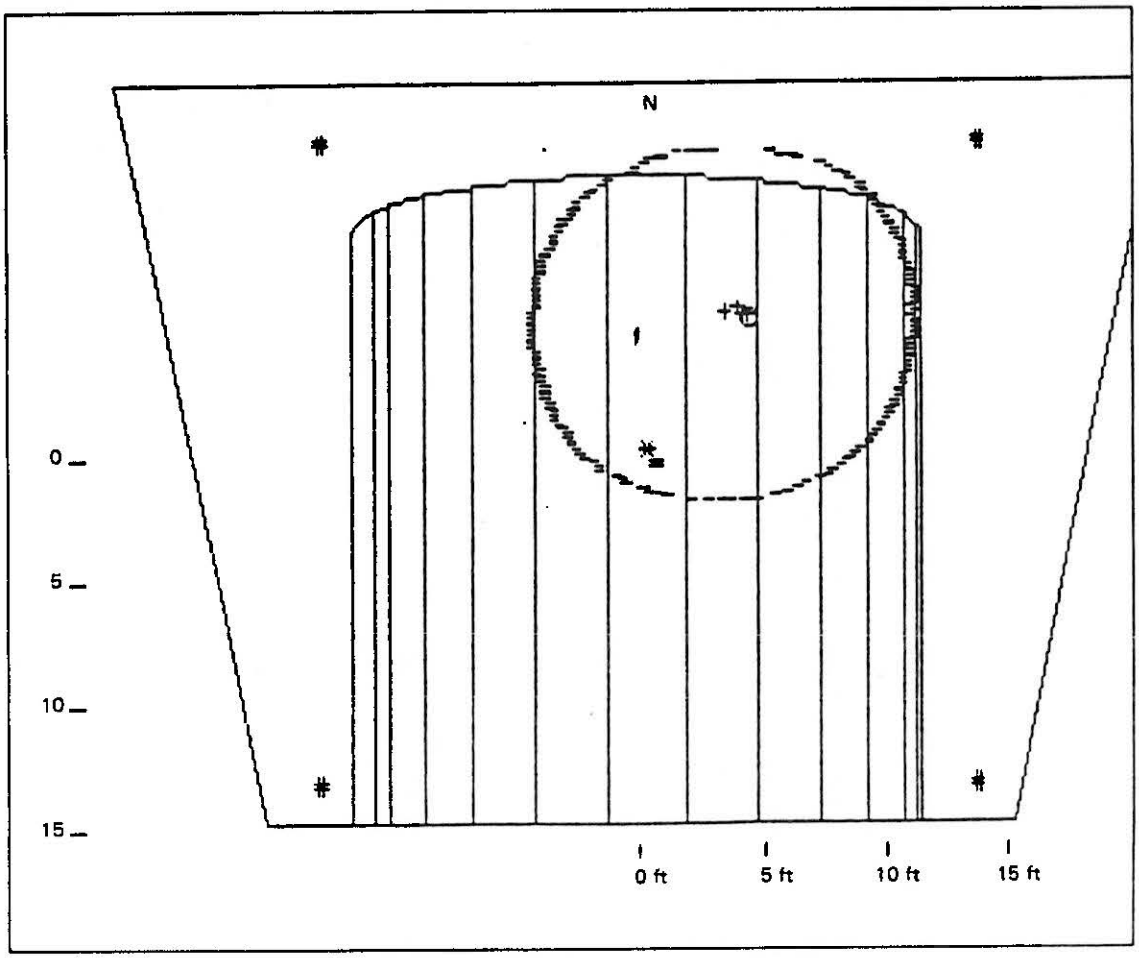

Figure 7-2. Typical Beam with Spillage

HCNUM	2650
Date	7/8/83
Time of Day	13:7
Centroid Error +/- Std. Dev. (Horiz.)	3.67 +/- 12.83 In.
Centroid Error +/- Std. Dev. (Vert.)	-30.19 +/- 1.29 In
Theoretical Power	23882.3 Watts
Power Effectivity +/- Std. Dev.	199.9 +/- 31.9%
Spillage Power	6.0 +/- 3.6%
Insolation Level	868.8 W/M**2
Wind Velocity	5.59 mph
Temperature	92.07 degf
Invalid Data Flags	0011100110

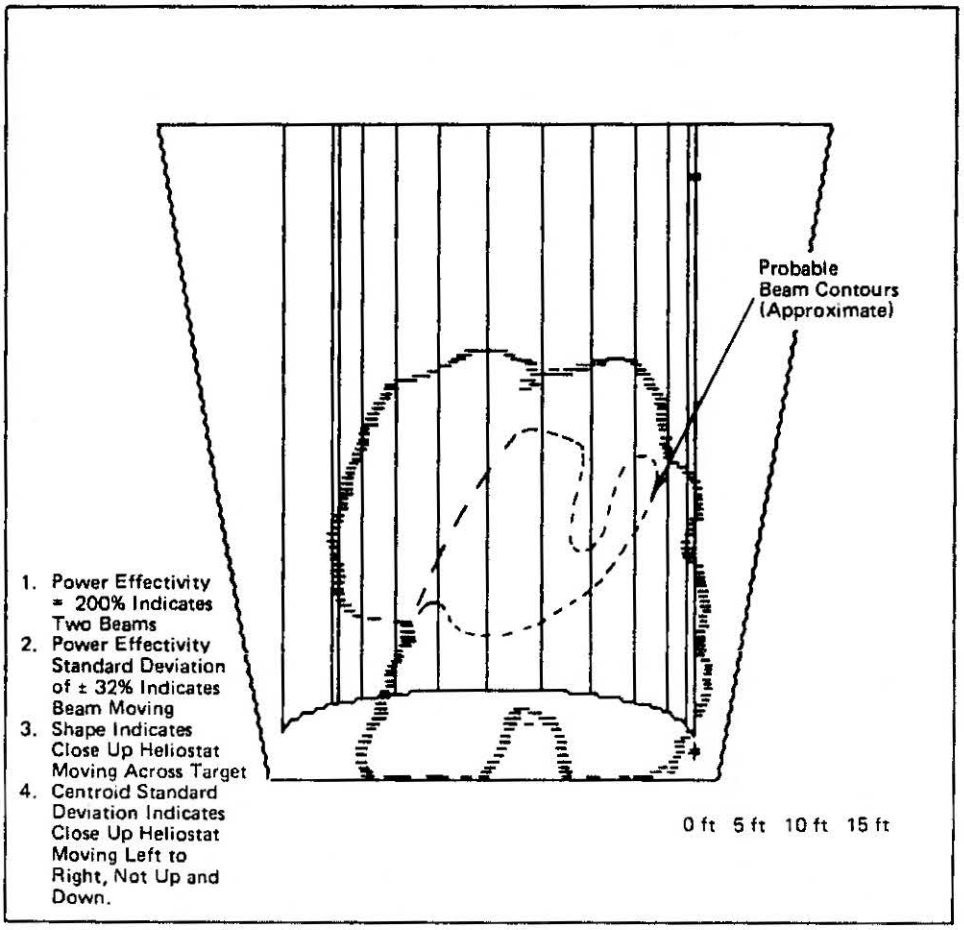

Figure 7-4. Second Heliostat on Target During Measurement Phase

Sunshape Radial Distribution Data

HCNM	134
Date	10/2/83
Time of Day	11:46
Sun Angle in Milli-Radians/Pixel	.092
Brightness in W/M**2 - Steradian-Dir No.	84265.4

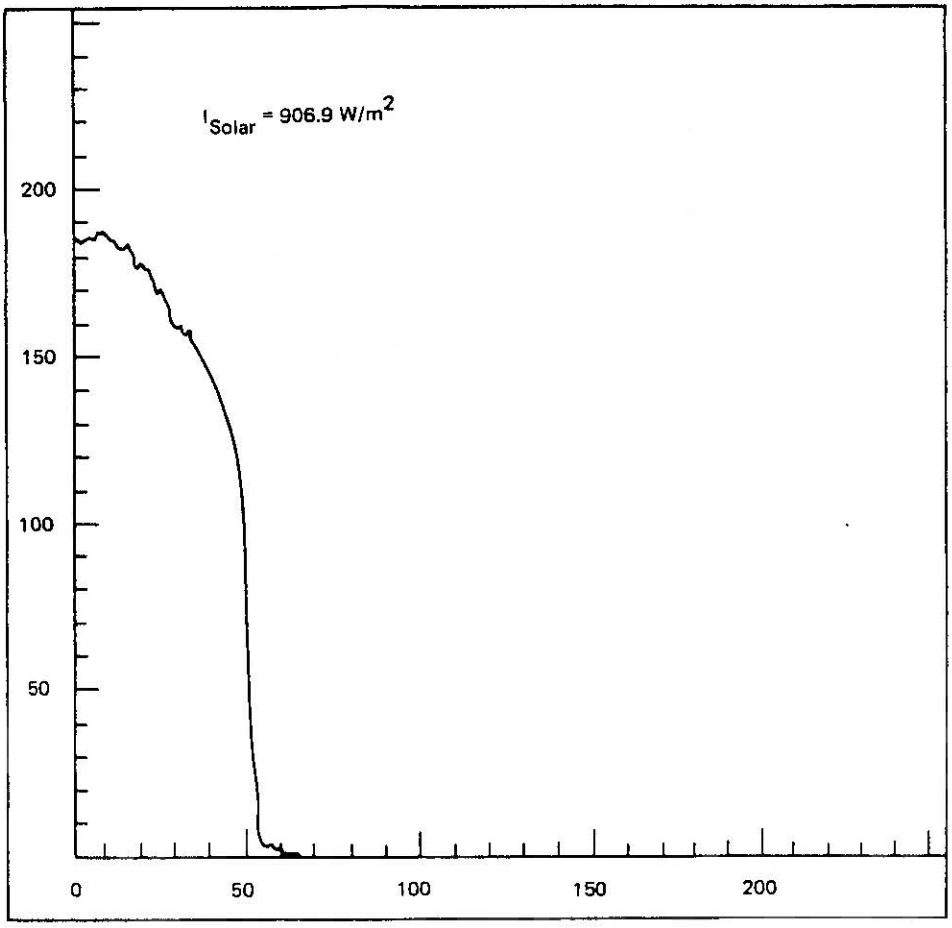

Figure 7.5. Typical Radial Distribution of Radiance

REFERENCES

1. Hallet, R. W., and Gervais, R. L., "Central Receiver Solar Thermal Power System," Volume III--Book 2, SAN-1108-76-8, MDC G6776, McDonnell Douglas Corporation, October 1977.

2. Thalhammer, E. D., "Heliostat Beam Characterization System--Update," ISA/79 Conference Proceedings, Chicago, IL, October 1979.

3. Phipps, G. S., "Heliostat Beam Characterization System--Calibration Technique," ISA/79 Conference Proceedings, Chicago, IL, October 1979.

4. Biggs, F., Vittitoe, C. N., and King, D. L., "Modeling the Beam Characterization System," ISA/79 Conference Proceedings, Chicago, IL, October 1979.

5. King, D. L., and Arvizu, D. E., "Heliostat Characterization at the Central Receiver Test Facility," Trans of ASME, Journal of Solar Energy Engineering, Volume 103, May 1981.

6. King, K. L., "Beam Quality and Tracking Accuracy Evaluation of Second Generation and Barstow Production Heliostats," Sandia Report SAND 82-0181, August 1982.

7. "Pilot Plant Station Manual, 10 MWe Solar Thermal Central Receiver Pilot Plant," RADL Item 2-1, Volume 1, System Description, SAN/0499-57, MDC G8544, McDonnell Douglas Corporation, December 1980, revised September 1982.

8. McFee, R. H., "Power Collection Reduction by Mirror Surface Non-Flatness and Tracking Error for a Central Receiver Solar Power System," Applied Optics, 14, 1493, July 1975.

9. McFee, R. H., "Computer Program CONCEN for Calculation of Irradiation of Solar Power Central Receiver," Proceedings ERDA Solar Workshop on Methods for Optical Analysis of Central Receiver Systems, August 1977.

10. Blackmon, J. B., et al., "Beam Characterization System Operator and Users Manual."

APPENDICES

Appendix A

Cohu 2800C Series TV Cameras

COHU 2800C SERIES

MODEL 2850C
Low Light, Self Contained ENVIRONMENTAL TV CAMERAS

Features

Fully Automatic Operation —
Automatic 640,000 to 1 Light Range, Beam Control, Black Level, Gain Control with 20 dB Range and Bandwidth Reduction, plus Remote Control Capability

Gamma Correction —
Selectable 0.35, 0.5, 0.7, or 1.0

700 TV Lines Horizontal Center Resolution

Resolves 10-Shade Gray Scale with 0.05 Lumens/ft^2 Highlight Illumination on Image Tube Faceplate

Underscan and Overscan Capability . . . White Peak Clipping . . . Internal EIA RS-170 or CCIR Sync, Jumper Selectable

Peak to Average Detector for Automatic Light Control

Dual 75-Ohm Selectable 1 or 1.4 Volt Video Outputs

Environment-Resistant, Sealed Housing with Purge Fitting, Operates under Adverse Conditions and Down to –40°C

Genlock

Bright Light Limiter to Prevent Camera Being "Blinded"

Options —
Screensplitter for Multiple Camera Display
Cable Pre-Equalizer for Output No. 1 Gives 4.5 dB of Signal Increase

Description

The Cohu Model 2850C Low-Light Television Camera is designed for reliable, unattended, continuous-duty operation in a wide variety of day and night monitoring or surveillance applications such as encountered in airports, factories, parking lots, gates, tunnels, bridges, and traffic areas. The cameras will operate automatically in light levels ranging from bright sunlight to moonlight. A camera can be aimed at direct sunlight, without damage to the tube target, and then aimed at a low-light level area and produce a clear, crisp picture.

A Bright Light Limiter circuit allows full camera performance under conditions where blooming from intense scene highlights would otherwise make the picture unsatisfactory. The level and amount of scene highlights affected are adjustable. Highlight level can be set from black to maximum white for best contrast and resolution. This feature makes the 2850C well suited for nighttime applications where automobile headlights, a bright light being turned on, or a flashlight or spotlight can cause accidental or deliberate "blinding" of the camera. (Note: See lens chart on back page for models without this feature.)

Adverse environments (wet or dry, and hot or cold) do not effect the operation of the cameras; they are self-contained and enclosed in environment-resistant housings. The housings are machined of sturdy, highly corrosion-resistant aluminum alloy that is finished with a heat-reflecting, weather-resistant enamel. All camera housings are equipped with a purge fitting to permit purging with dry nitrogen or other moisture eliminators. The 2850C can be operated underwater in depths up to 60 feet

COHU MODEL 2850C-207 LOW LIGHT, SELF-CONTAINED ENVIRONMENTAL TV CAMERA

General Description for Camera Without Modifications Required for BCS

The COHU Model 2850C Low Light Television Camera is designed for reliable, unattended, continuous-duty operation in day and night monitoring or surveillance applications. The cameras will operate automatically in light levels ranging from bright sunlight to moonlight. A camera can be aimed at direct sunlight, without damage to the tube target, and then aimed at a low light level area and produce a clear, crisp picture.

A Bright Light Limiter circuit* allows full camera performance under conditions where blooming from intense scene highlights would otherwise make the picture unsatisfactory. The level and amount of scene highlights affected are adjustable. Highlight level can be set from black to maximum white for best contrast and resolution.

Adverse environments (wet or dry and hot or cold) do not effect the operation of the cameras; they are self-contained and enclosed in environment-resistant housings. The housings are machined of sturdy, highly corrosion-resistant aluminum alloy that is finished with a heat-reflecting, weather-resistant enamel. All camera housings are equipped with a purge fitting to permit purging with dry nitrogen or other moisture eliminators.

The camera has a fully automatic black level compensation system to provide high contrast video over the light level range. Maximum accuracy of picture black level and white level is maintained with a keyed clamp that compensates for image tube dark current variations as a function of the ambient temperature. An adjustable white peak clipper limits video amplitude. Gamma correction of either 1.0, 0.7, 0.5 or 0.35 (selectable by internal jumper) is provided, and automatic beam control stabilizes beam current eliminating the need for initial setup and periodic beam readjustment. An adjustable lens adapter ring provides focus tracking. The camera has two isolated, 75-ohm video outputs with either 1.0 or 1.4V p-p out selectable by jumper. An optional built-in cable pre-equalizer is available for output

*This circuit is disabled for BCS operation.

No. 1 that increases the signal 4.5 dB at 10 MHz. This allows driving up to 2000 feet of RG-11 foam cable.

Protective circuits prevent image tube damage in the event of horizontal or vertical sweep failure. Horizontal and vertical deflection amplifiers are adjustable from 10% underscan to 10% overscan. Internal sync generators provide the built-in, standard 2:1 interlace that meets EIA Standard RS-170. A genlock, which will lock the internal camera sync in phase with an external EIA RS-170. In the case of external sync failure when operating in genlock mode, the camera is automatically switched to internal sync, but the master oscillator will be free running.

Model 2850C camera housings, in addition to being environment-resistant, are tamper-proof; they have no exposed controls. The cameras are suitable for use outdoors in adverse environments as well as indoors. The housings are cylindrical and permit mounting the camera in any position without reversing scans or rotating the yoke. Controls are provided to enter the scanned area on the image tube. Modular construction is used throughout. All modules are of the plug-in type, with no hard wiring, to make servicing simple and easy. Test points and adjustments and test point circuit symbols are silk-screened on the circuit boards for easy identification.

Automatic operation and remote control capability are standard features. An automatic sensitivity control* adjusts a motorized iris on the lens and adjusts the video gain for an optimum picture over a wide range of scene illuminations. The iris can also be remotely controlled for manual operation in specific applications. A peak-to-average detector* allows the automatic sensitivity circuitry to be set at full peak detection or full scene average detection, or any point in between. A remote control is used for variable focal length (zoom) lenses.

All dc voltage supplies and the filament voltage are regulated. Grid and target voltages are adjustable to allow use of several image tube types. The video preamplifier has an operational amplifier feedback circuit using field effect transistors in the first stage, and can handle input signals of up to one microampere without overloading. This provides clear and crisp pictures

*This circuit is disabled for BCS operation.

with maximum detail information and low noise. Total silicon solid-state circuitry, with the exception of the image tube, plus state-of-the-art integrated and transistor circuit design and the use of modular, etched-glass epoxy circuit boards, ensure long and trouble-free operation.

Specifications

Electrical.

	Image Tube Types		Silicon-Target
*Sensitivity: Highlight illumination, in lumens/ft^2, necessary on the image tube faceplate to maintain full p-p video			0.005
Highlight illumination, in lumens/ft^2, necessary on the image tube faceplate to produce a usable picture			0.001
Resolution: With 0.05 footcandle of highlight illumination on the image tube faceplate	Horizontal	Center	700
		Corners	500
	Vertical		350
*Automatic Light Range, with AGC and using specified f/1.4 (T/1.4-T/360) lens with auto iris and ND spot: Scene brightness range over which video output is maintained, ±3 dB (video bandwidth will automatically reduce to approx. 1 MHz by AGC action)			0.05 to 32,000 footlamberts
*Gray Scale Rendition: Highlight illumination, in lumens/ft^2, necessary on the image tube faceplate to resolve all 10 shades of gray on EIA TV Resolution Chart, 1956			0.05

Input Voltage	105 to 130V, 60 Hz; 210 to 260V jumper selectable (with CCIR option 50 Hz)
Input Power	25W camera, 125W max w/heaters
Vertical Sweep Rate	50 or 60 Hz (same as power line freq.)
Horizontal Sweep Rate	15,750 Hz for 60 fields, 15,625 for 50 fields
Scanning	2:1 interlace at 525 lines 30 frames (625 lines 25 frames w/CCIR option)

*All specifications with 2854°K (incandescent illumination)

Sync	RS-170 Specification.
Image Pickup Tube Type	1" diameter, 6" length, magnetic deflection and focus, separate mesh, see Image Tube Type Table
Signal-to-Noise	55 dB, (visual equivalent)
Automatic Black Level	Maintains setup level at 75 ±5 IRE units if picture contains at least 10% black with a horizontal dimension of at least 1% of picture height
Resolution Stability vs Temperature	Meets resolution specifications over temperature range of -40 to 50°C (-40 to 122°F)
Resolution Stability vs Voltage Variation	Meets resolution specifications over input voltage range
Gamma Correction	1.0, 0.7, 0.5, or 0.35, jumper selectable
Signal Transmission Distance (w/RG-11 foam cable)	>1000 feet
W/Genlock Option	>1000 feet from genlock source
W/Pre-Equalizer Option	>2000 feet
Output Video	1.0V or 1.4V p-p composite video, jumper selectable
Video Outputs	Two
Geometric Distortion	Maximum 2%
Scan Failure Protection	Automatic protection for both horizontal or vertical failure
Horizontal Scan Freq.	Master oscillator, phase locked to power line. In genlock mode, with no external drive, master oscillator is free running. Crystal option available.
Vertical Scan Freq.	Derived from master oscillator
Underscan/Overscan Capability	10%

Environmental.

Ambient Temperature Limits	
Operating	-40 to 60°C (-40 to 140°F)
Storage	-62 to 85°C (-79.6 to 185°F), MIL-E-5400R, para. 3.2.24.1

Altitude	Two atmospheres to 100,000 feet (30,480 m), MIL-E-5400R, para. 3.2.24.2, Class 3. Leakage rate $<10^{-4}$ cu. in./hr. at 20 psi
Humidity	100%, MIL-E-5400R, para. 3.2.24.4
Purge Fitting	Standard Schrader tank valve is provided on camera housing to allow camera to be purged with dry nitrogen and to maintain housing interior at atmospheric pressure
Vibration	5 to 30 Hz with 0.03" total excursion, from 30 to 1000 Hz with peak random vibrations of 5 g's without damage or degradation
Shock	15 g's in any axis under nonoperating conditions, MIL-E-5400R, para. 3.2.24.6
Sand and Dust	MIL-E-5400R, para. 3.2.24.7
Fungus	MIL-E-5400R, para. 3.2.24.8
Salt Atmosphere	MIL-E-5400R, para. 3.2.24.9
Explosion	MIL-E-5400R, para. 3.2.24.10
Acoustic Noise	Operates in extremely high acoustic noise environment (150 dB), e.g., close proximity to high-thrust rocket engines

Mechanical.

Dimensions	See dimensional drawings and table
Weight	See table
Type of Lens Mount	16-millimeter "C" mount
Remote Control Provisions	Bright light limiter on/off, bright/dark detection, auto/manual sensitivity, lens iris aperture, lens focus, zoom lens focal length, lens speed operation, and camera power (refer to COHU data sheet 6-684)
Camera Mount	Three 1/4-20 tapped holes, see dimensional drawings
Type of Connector	Bendix PT-07C-20-39P, mating connector supplied. All functions, video, power, and remote controls through single connector

Dimension Table

Model No.	"A" Dimension In.	cm.	Lens*	Weight Lbs.	Kg.
2850C-207	25	63.50	10:1 Zoom w/2X Extender f/2.8	25	11.36

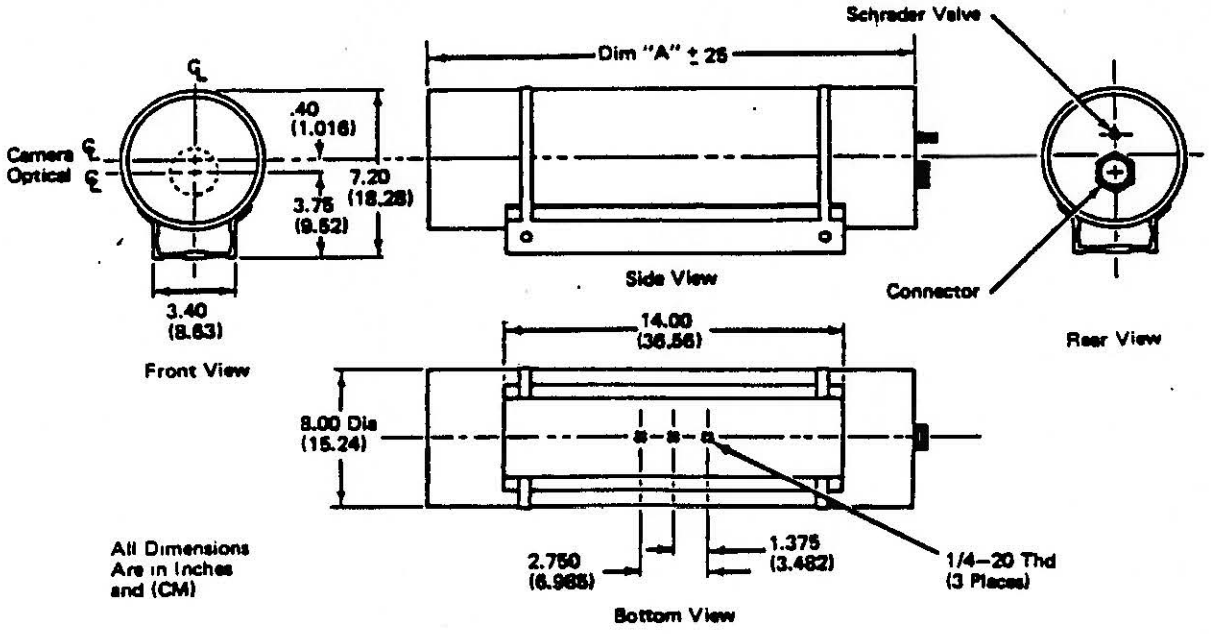

Camer Dimensional Drawing

CAMERA VIDICON TUBE RCA MODEL 4532 B/H

General Data

Electrical:	
Heater Voltage:	
Operational	6.3 V
For standby with no other electrode voltages applied	3.0 V
AC or DC Heater Current at 6.3 Volts (Nominal value)	0.10 A
Focusing Method	Magnetic
Deflection Method	Magnetic
Direct Interelectrode Capacitance:[a]	
Target to all other electrodes	5.7 pF
Optical:	
Optical Distance (See Figure 12)	2.8 ± 0.51 mm (0.113 ± 0.020 in)
Spectral Response	RCA Type V, See Figure 9
Target:	
Maximum useful diagonal or rectangular image	16 mm (0.63 in)

Important - Performance obtainable from the vidicon is directly proportional to the image format size. If at all possible, the camera design should be such as to use the full 16 mm (0.63 in) image diagonal.

Mechanical:	
Base	Small-Button Ditetrar 8-Pin, (JEDEC No. E8-11)
Socket	Cinch[b] No. 8VT (133-98-11-015), or equivalent
Deflecting Yoke - Focusing Coil - Alignment Coil - Assembly (See Figure 2)	Solar Systems Inc., [c,d] No. VYLFA-959, Penn Tran, [c,d] No. 1465, or equivalent
Operation Position	Any
Weight (Approx.)	57 g (2 oz)

Absolute-Maximum Ratings*

	Limiting Values	
Heater-Voltage Tolerance (Operational)	± 5	%
Grid-No. 4 Voltage[f]	500	V
Grid-No. 3 Voltage[f]	500	V
Grid-No. 2 Voltage	350	V
Grid-No. 1 Voltage (Positive value)	0	V
Grid-No. 1 Voltage (Negative value)	-150	V
Heater-Cathode Voltage (Positive value)	10	V
Heater-Cathode Voltage (Negative value)	-125	V
Target Voltage (Briefly during special cycling)[g]	300	V
Target Voltage (During operation)	20	V
Peak Target Current	750	nA
Faceplate:		
Illuminance[h]	$\begin{cases} 6\times10^{7} \\ 6\times10^{8} \end{cases}$	lm/ft^2 (fc) lux
Temperature:		
Operating and storage	-54 to +70	°C

Typical Operation

With tube operated in a Solar Systems Inc. Assembly Type VYLFA-959, or equivalent; scanned area of 12.8 mm x 9.6 mm (0.50 in x 0.38 in); faceplate temperature of 30° C; and standard CCIR "M", or EIA, TV scanning rate (525 lines, interlaced 2:1, frame time 1/30 second).

Grid-No. 4 (Decelerator) Voltage[f]	480 V
Grid-No. 3 (Beam-focus electrode) Voltage[f]	410 V
Grid-No. 2 (Accelerator) Voltage	300 V
Peak-to-Peak Blanking Voltage:	
When applied to grid No. 1	75 V
When applied to cathode	20 V
Target Voltage	8 to 10 V
Focusing-Coil Current[k]	40 mA
Peak-to-Peak Deflecting-Coil Current:	
Horizontal	200 mA
Vertical	20 mA
Field Strength of Each Adjustable Alignment Coil[m]	0 to 4 G (0 to 4x10-⁴T)

Typical Performance Data

Under the conditions shown under Typical Operation

Peak Radiant Responsivity (At 710 nanometers)	330	mA/W
Grid-No. 1 Voltage for Picture Cutoff[n]	-50 to -100	V
Dark Current	3.5	nA
Average "Gamma" of Transfer Characteristic for a Signal-Output Current Between 4 nA and 400 nA	1	
Lag-Per Cent of Initial Value of Signal-Output Current 1/20 Second After Illumination is Removed[p] (See Figure 6)	8	%
Limiting Resolution:		
At center of picture	700	TV lines
At corner of picture (See Figure 7)	500	TV lines
Amplitude Response to a 400 TV Line Square-Wave Test Pattern at Center of Picture[q] (See Figure 7)	35	%
Sensitivity to Tungsten Light Source[r]		
CONDITIONS		
Faceplate Illumination (Highlight)	0.1	lm/ft^2 (fc)
PERFORMANCE		
Sensitivity	4350	μA/lm
Typical Signal-Output Current[s,t]	565	nA
Sensitivity to Visible Light[u]		
CONDITIONS		
Illumination from 2856 K Light Source Incident on Infrared Absorbing Filter (Highlight)	0.1	lm/ft^2 (fc)
PERFORMANCE		
Sensitivity	845	μA/lm
Typical Signal-Output Current[s,t]	110	nA

Spurious Signal Test

This test is performed with the tube carefully focused on a uniformly illuminated test pattern which identifies the zones as pictured in Figure 1. The tube is operated in accordance with "Typical Operating Values" and illumination is adjusted to provide a highlight reference signal current of 300 nanoamperes. After completion of the setup adjustments, light is excluded and the picture examined to locate and measure bright spots. Thereafter, reference

level illumination is applied and the picture examined for additional spots and blemishes other than bright spots.

Spots. Spots are defined as blemishes whose contrast exceeds 10% of the 300 nanoampere reference signal. The size of the spots (diameter, or length plus width divided by two) is measured in terms of the pitch of the raster lines in a 525-line system.

The allowable spots for the 4532/H tube type are shown in Table I. The table defines the acceptable distribution by zones, size and polarity of spots.

Other Blemishes. Smudges, streaks, mottled or grainy background are acceptable only if their video signal current amplitude does not exceed:

3% of the reference signal current for type 4532B/H,

5% of the reference signal current for type 4532A/H and 4532/H.

Table I. Blemish Criteria for Type 4532/H

Blemish Size (Equivalent TV Lines)	Zone 1 Allowed Spots		Zone 1 & 2 Allowed Spots		Zone 1, 2 & 3 Allowed Spots	
	Bright	Total	Bright	Total	Bright	Total
Over 6	0	0	0	0	0	0
Over 4	0	0	0	0	0	0
Over 1	0	0	0	0	0	2
1 or smaller	—	—	—	—	—	—

Minimum separation between any 2 spots greater than 1 raster line is limited to 16 raster lines.

— Spots of this size are allowed unless concentration causes a smudged appearance.

It should be noted that in using narrow band illumination in the near IR region some undesirable spurious signal effects may be evident.

NOTES:

a. This capacitance, which effectively is the output impedance of the tube, is increased when the tube is mounted in the deflecting-yoke and focusing-coil assembly. The resistive component of the output impedance is in the order of 100 megohms.

b. Made by Cinch Manufacturing Company, 1501 Morse Avenue, Elk Grove Village, IL 60007.

c. The magnetic component No. VYLFA-959 is made by Solar Systems, Inc., 37520 Colorado Ave., Avon, OH 44011; the magnetic component No. 1465, by Penn Tran Corp., 1155 Zion Rd., Box 508, Bellefonte, PA 16823.

d. These components, when mounted along the tube axis as shown in Figure 2, will provide minimum beam landing error (maximum signal uniformity) at the recommended grid No. 3/grid No. 4 operating voltage ratio of 0.85. This ratio is determined by the electro-optical characteristics of the target-mesh region which are significantly different from those of the typical vidicon configuration.

e. In accordance with the Absolute Maximum rating system as defined by the Electronic Industries Association Standard RS-239A, formulated by the JEDEC Electron Tube Council.

f. Grid-No. 4 voltage must always be greater than grid-No. 3 voltage. The grid-No. 3/grid-No. 4 ratio of 0.85 provides optimum performance with regard to dark current uniformity, signal discharge uniformity and geometrical accuracy with the recommended deflection-coil assemblies. When using a deflection Assembly other than the recommended type, the ratio of G4 to G3 voltage should be adjusted for optimum performance.

g. If operation is attempted using target voltages typical of conventional vidicons (30 to 50 V), the surface of the silicon target will store a negative (unwanted) charge. This condition may be corrected by briefly overscanning the target with approximately 200 volts on the target and with the beam turned fully on. The beam must then be cut off completely before reducing the target voltage to its normal 8-10 volt value.

h. The tube can withstand the illuminance contained in a focused image of the sun without permanent damage.

i. This target voltage provides an optimum operating point consistent with maximum target discharge capability and optimizes other performance characteristics such as dark current uniformity, lag, and blemish content.

It is highly recommended that the operating target voltage be set to and maintained at 8-10 volts.

k. The polarity of the focusing coil should be such that a north-seeking pole is attracted to the image end of the focusing coil, with the indicator located outside of and at the image end of the focusing coil.

m. The alignment coil should be located on the tube so that its center is at a distance of 93.7 mm (3.69 inches) from the face of the tube, and be positioned so that its axis is coincident with the axis of the tube, the deflecting yoke, and the focusing coil.

n. With no blanking voltage on grid No. 1.

p. For an initial signal-output current of 200 nanoamperes and at recommended target voltage.

q. Amplitude response is the signal amplitude from a given TV line number expressed as a per cent of the signal amplitude from a very-low-frequency (large-area) picture element. In practice, the large-detail reference is usually 15 TV lines with signal amplitude set equal to 100 per cent. The TV line numbers are determined by the number of equal-width black and white lines that will fit into the physical height of the image focused on the camera-tube faceplate.

r. Light source is a tungsten-filament lamp having a lime-glass envelope. The lamp is operated at a color temperature of 2856 K.

s. The deflecting circuits must provide extremely linear scanning for good signal reproduction. Signal current is dependent upon the scanning velocity. Any change in scanning velocity produces a signal error in proportion to the change in scanning velocity.

t. Defined as the component of the highlight target current after the dark-current component has been subtracted.

u. With the same light source specified in footnote (r) except an infrared absorbing filter (Schott Jenaer KG-3, 5.5 mm thick available from Fish-Schurman Corporation, 70 Portland Road, New Rochelle, NY 10802) is interposed between the light source and the faceplate of the tube.

For sharper infrared cutoff, the Kodak Series 305 Infrared Rejection Filter may be used. This series is available from Eastman Kodak Co., Special Products Sales, Rochester, NY 14650.

WARNING – PERSONAL SAFETY HAZARD
Electrical Shock – Operating voltages applied to this device present a shock hazard.

Warning

Failure to observe tne maximum dc electrode voltage ratings can reduce the life expectancy of these tubes. When operated with ratings with the recommended deflection-focusing coil assemblies, the full performance capabilities of the silicon-diode array target will be easily realized. A tube life of many thousands of hours of useful service may be obtained when the tube is operated within the specified maximum ratings.

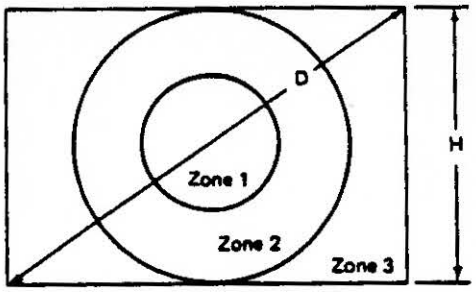

D — Active Target Diameter
H — Raster Height (4 X 3 Aspect Ratio)
Zone 1 — Diameter = H/2, Area ≈ 15%
Zone 2 — Diameter = H, Area ≈ 45%
Zone 3 — Peripheral Area ≈ 40%

Figure 1. Spurious Signal Zones

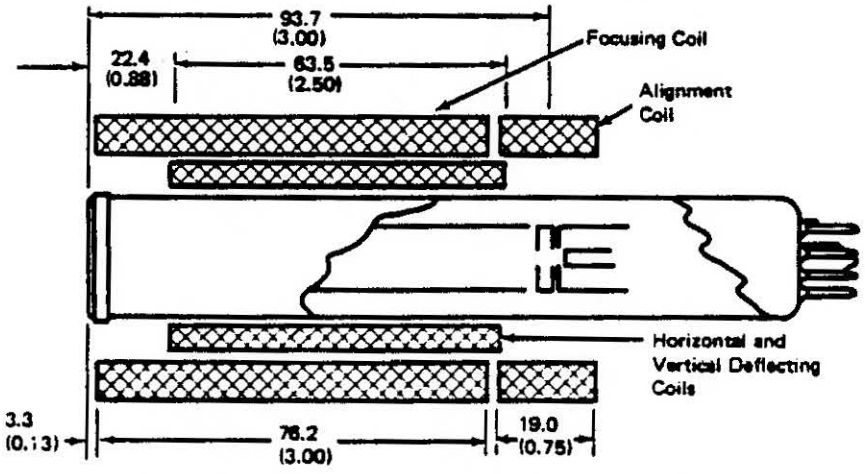

Dimensions in parentheses are in inches.

Figure 2. Recommended Location and Length of Deflecting, Focusing, and Alignment Components to Obtain Minimum Beamlanding Error

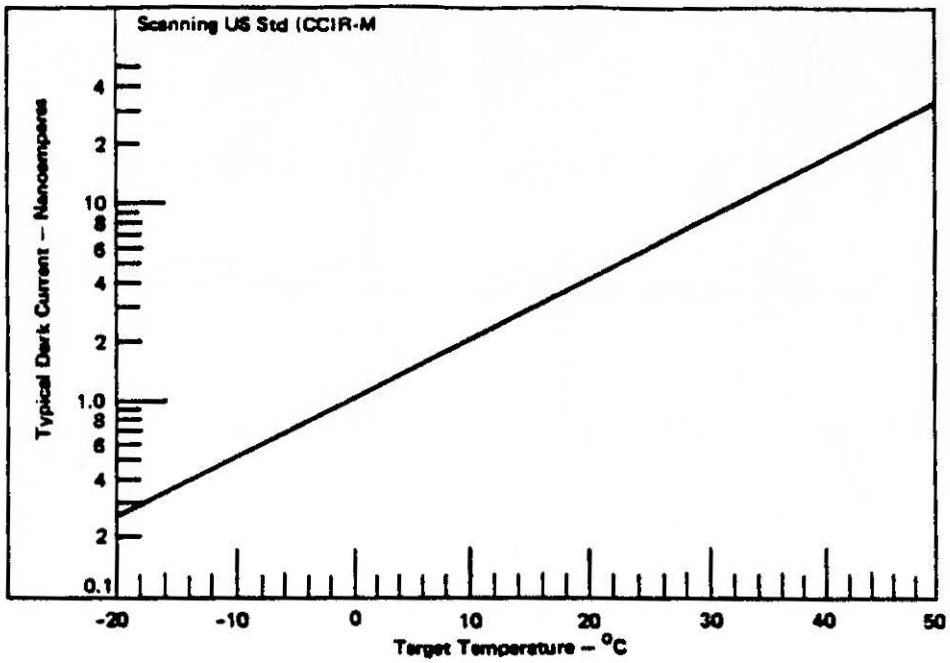

Figure 3. Typical Dark Current vs Temperature

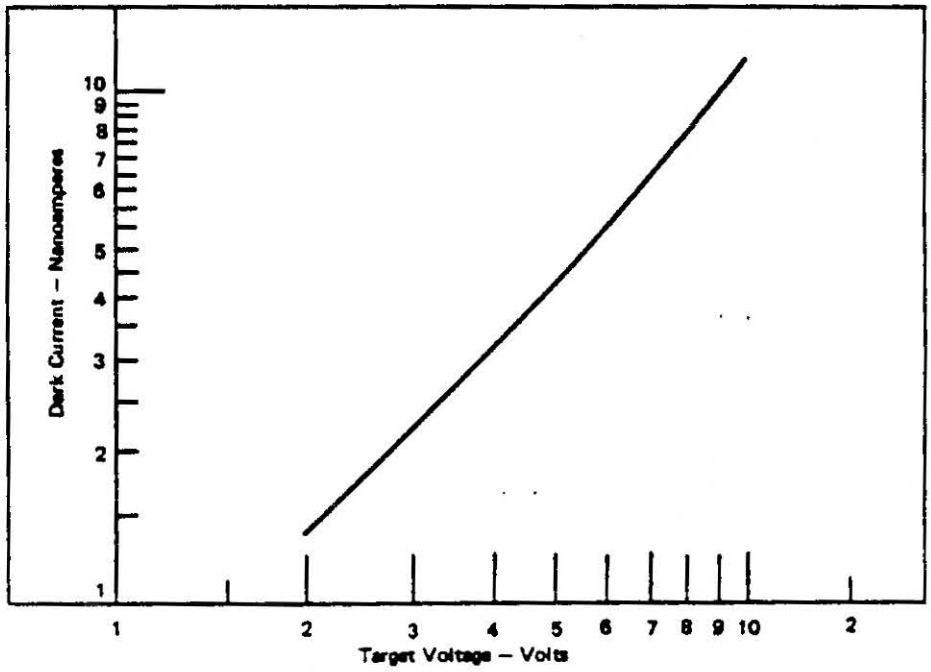

Figure 4. Typical Dark Current Characteristic

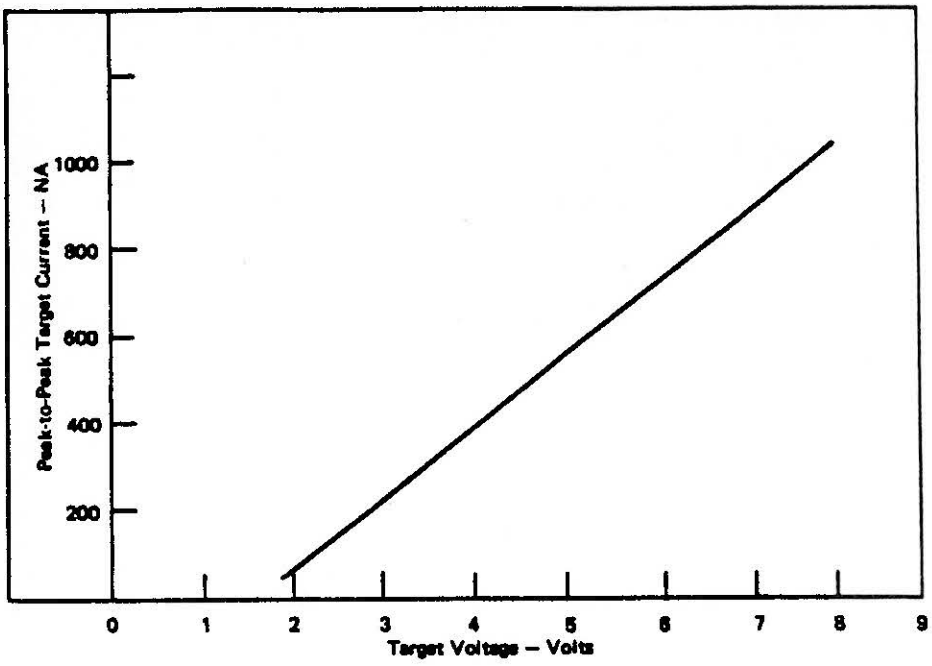

Figure 5. Typical Saturation Target Current Characteristic

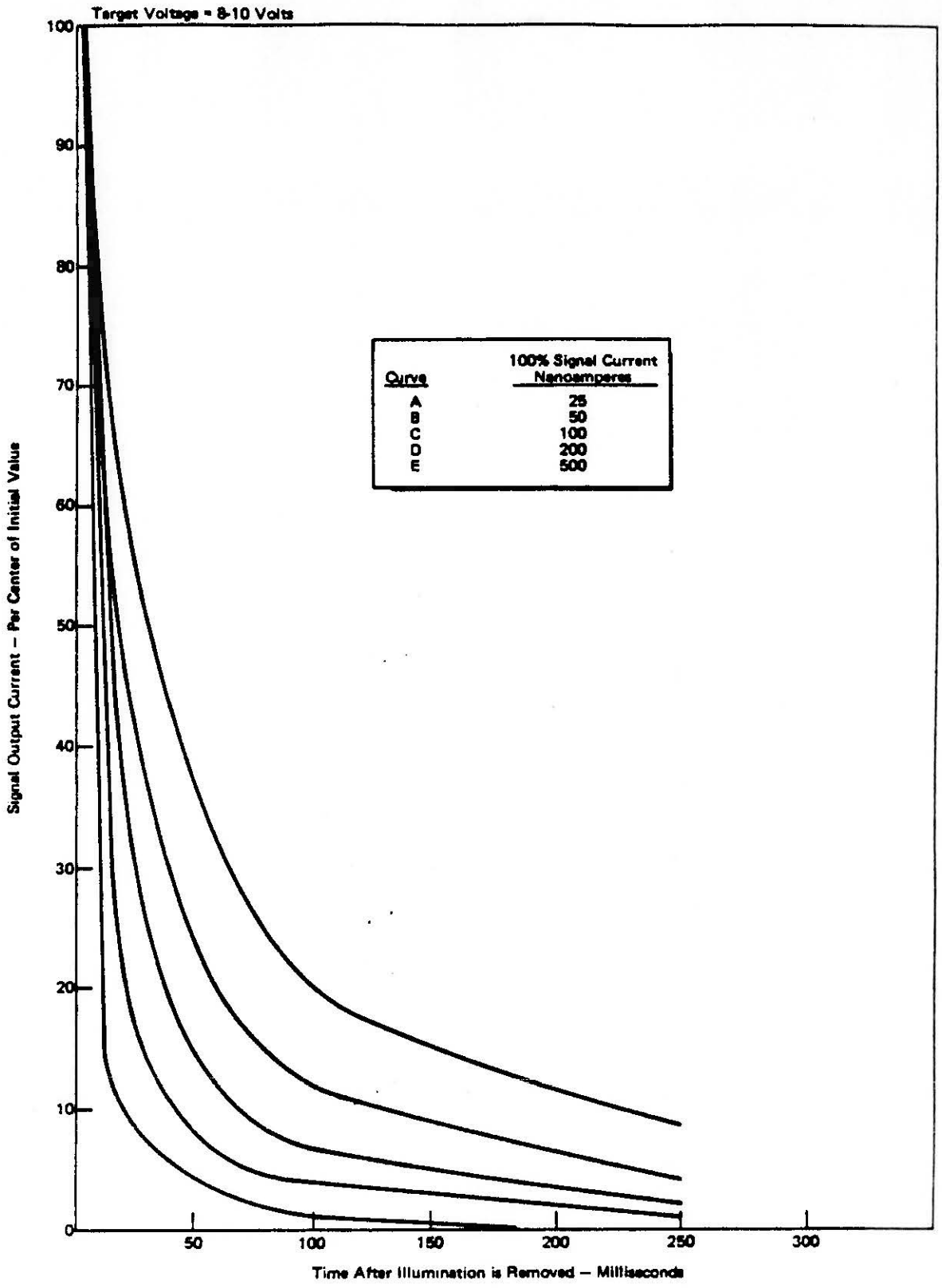

Figure 6. Typical Persistence (Lag) Characteristics

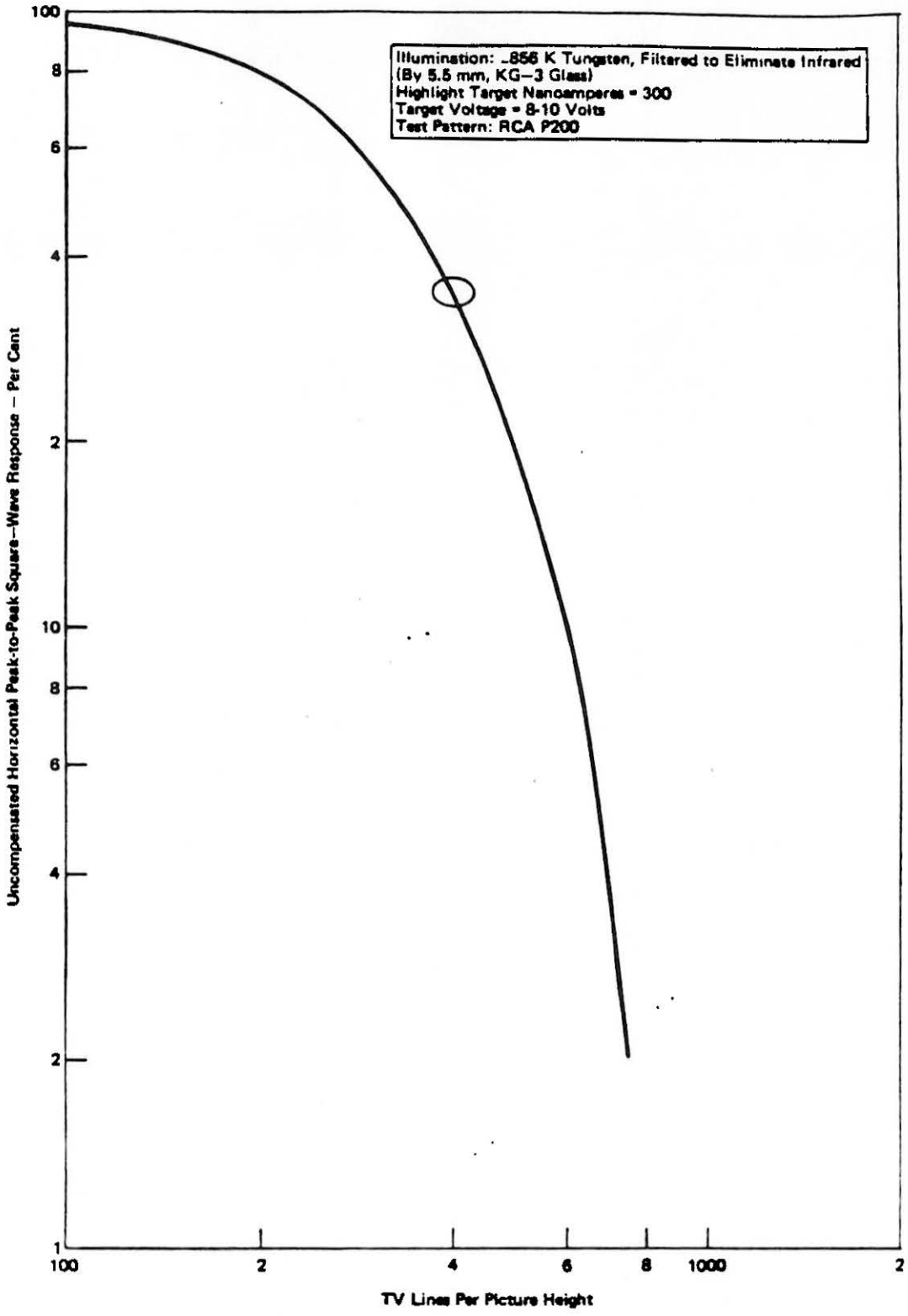

Figure 7. Typical Amplitude Response (CTF) Characteristic

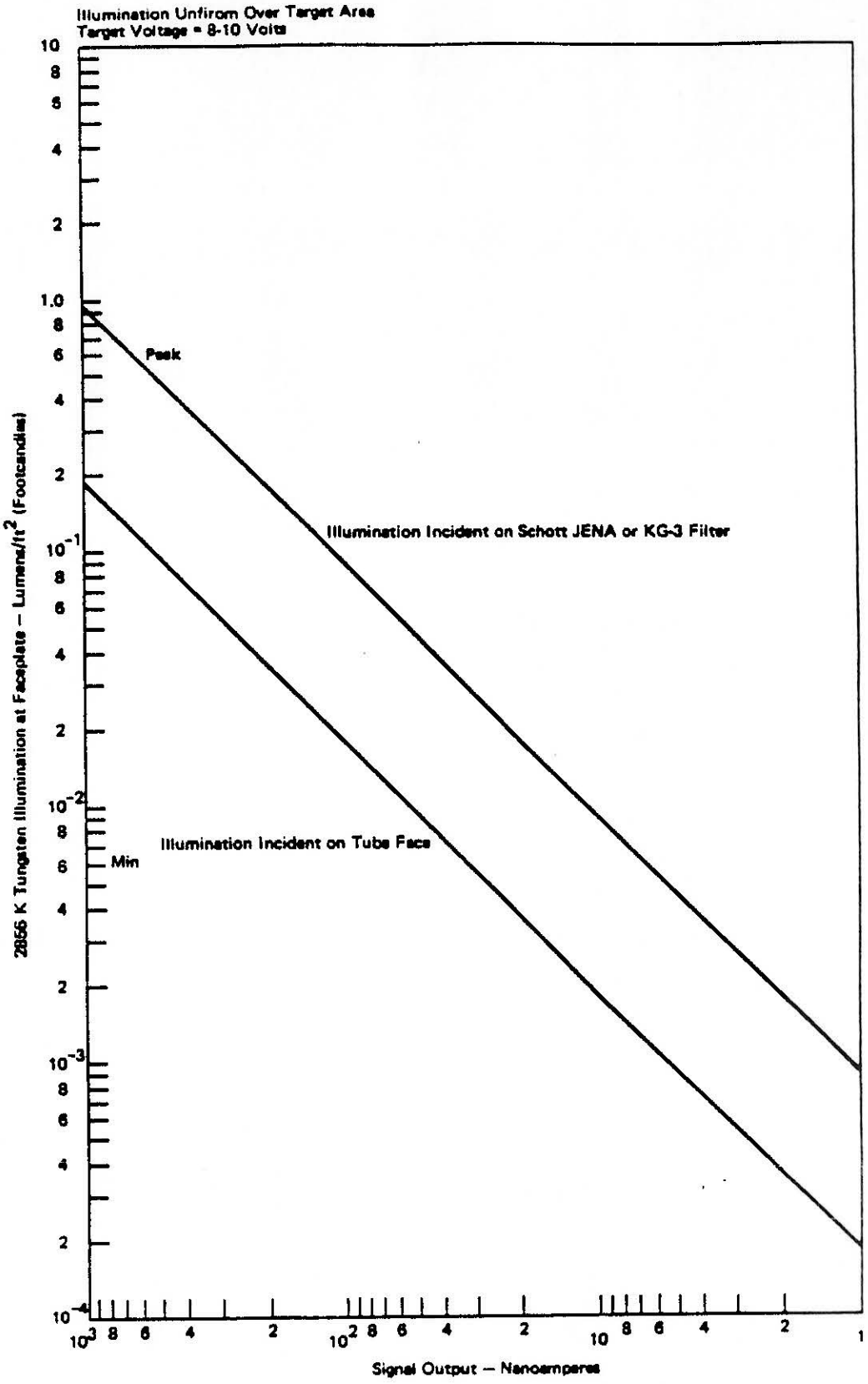

Figure 8. Typical Light Transfer Characteristics

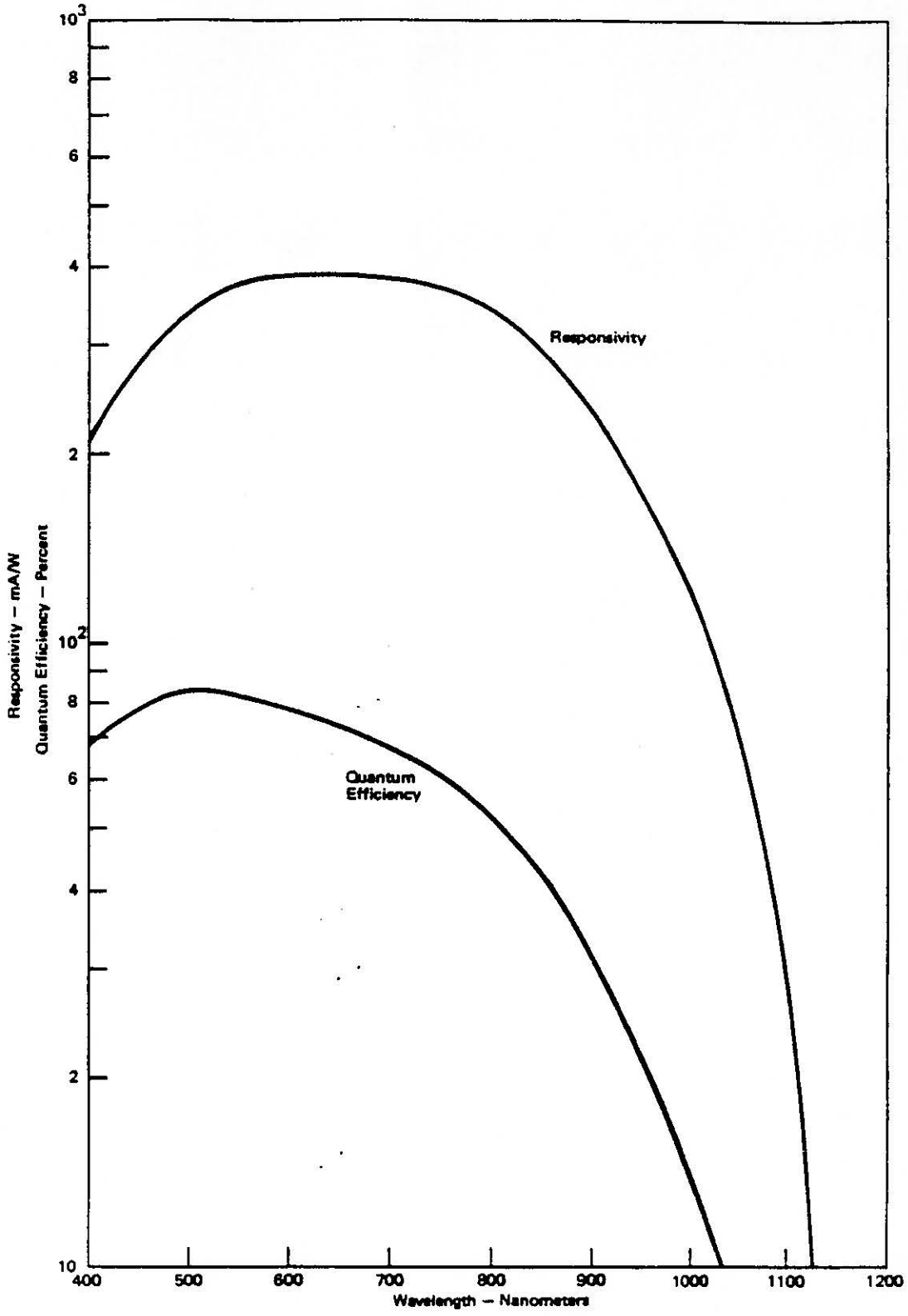

Figure 9. Typical RCA Type V Spectral Response

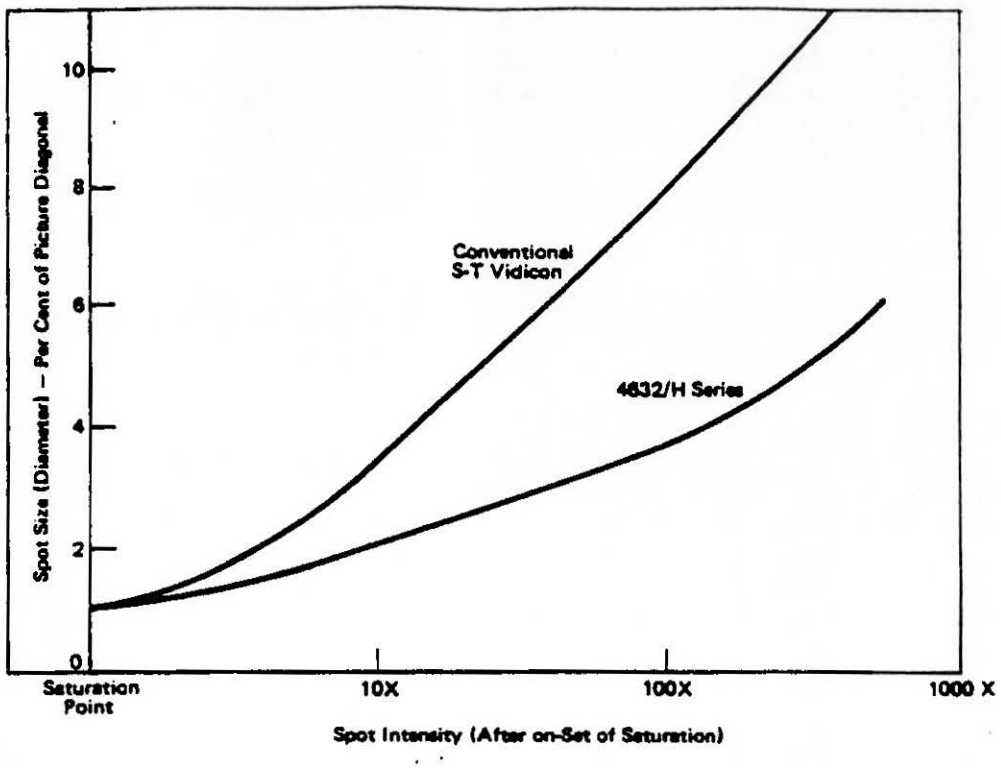

Figure 10. Comparison Between Low-Blooming S-T Vidicon Types 4532/H Series and Conventional S-T Vidicons

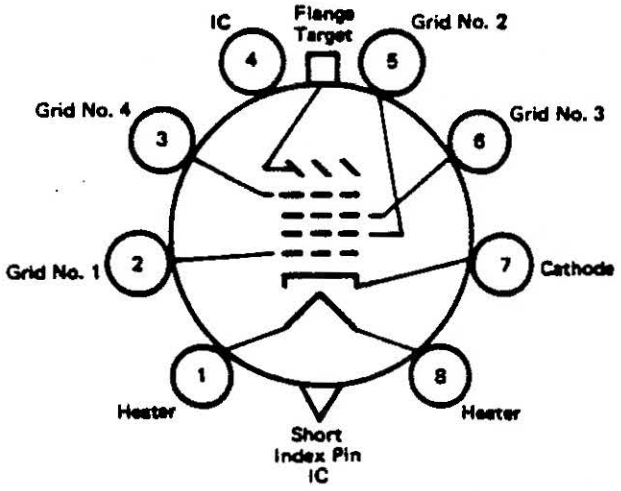

IC = Internal Connection, Do Not Use

Figure 11. Basing Diagram, Bottom View

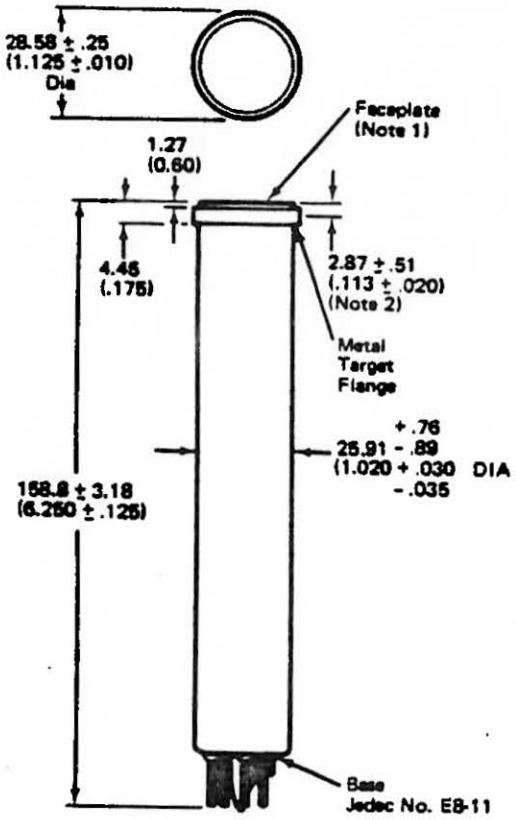

Dimensions in millimeters, dimensions in parentheses are in inches
Note 1 — Faceplate glass is Corning No.7056, or equivalent. Its index of refraction at 589.3 nm is 1.49
Note 2 — Optical distance (front of faceplate to target)

Figure 12. Dimensional Outline

VIDICON DARK CURRENT CLAMP

Dark current, or vidicon output signal without light incident on the vidicon face, increases with temperature. It is necessary to keep this constant in order for absolute irradiance measurements to be made with the BCS.

The COHU cameras used for BCS evaluation have a circuit modification to keep the dark current constant. The sunshape camera also has this circuit modification but in addition is maintained at a constant temperature of approximately $50^{o}F$.

The dark current clamp circuit is shown in the following circuit diagrams. In principle, a black mask located at the focal plane of the relay lens is imaged on the vidicon such that the upper portion of the vidicon has no light incident upon it. This portion of the output signal is compared against a constant voltage and controlled so as to remain constant over a wide temperature range.

Camera output as a function of input light intensity was tested over a range of temperatures from $40^{o}F$ to $140^{o}F$. Up to $120^{o}F$, the output is linear and the peak response is within $\pm$ 2% for the minimum constant light level.

However, the signal-to-noise ratio is decreased and shading is increased. Shading is corrected by use of the white file/black file data in the BCS software. The decrease in signal-to-noise ratio of about a factor of 2 is acceptable.

Video output signal vs light intensity data are presented in the following figures (C-1 to C-7). Light intensity was varied by a calibrated cross-polarizing filter and uniform light source with an opal glass aperture.

GAMMA - TEMPERATURE CURVE

COHU Model 2850C Vidicon (modified)
Tested at MDAC-HB 8-24-81
Temperature: 40 Degrees Fahrenheit
Peak Video to Back Porch Blanking

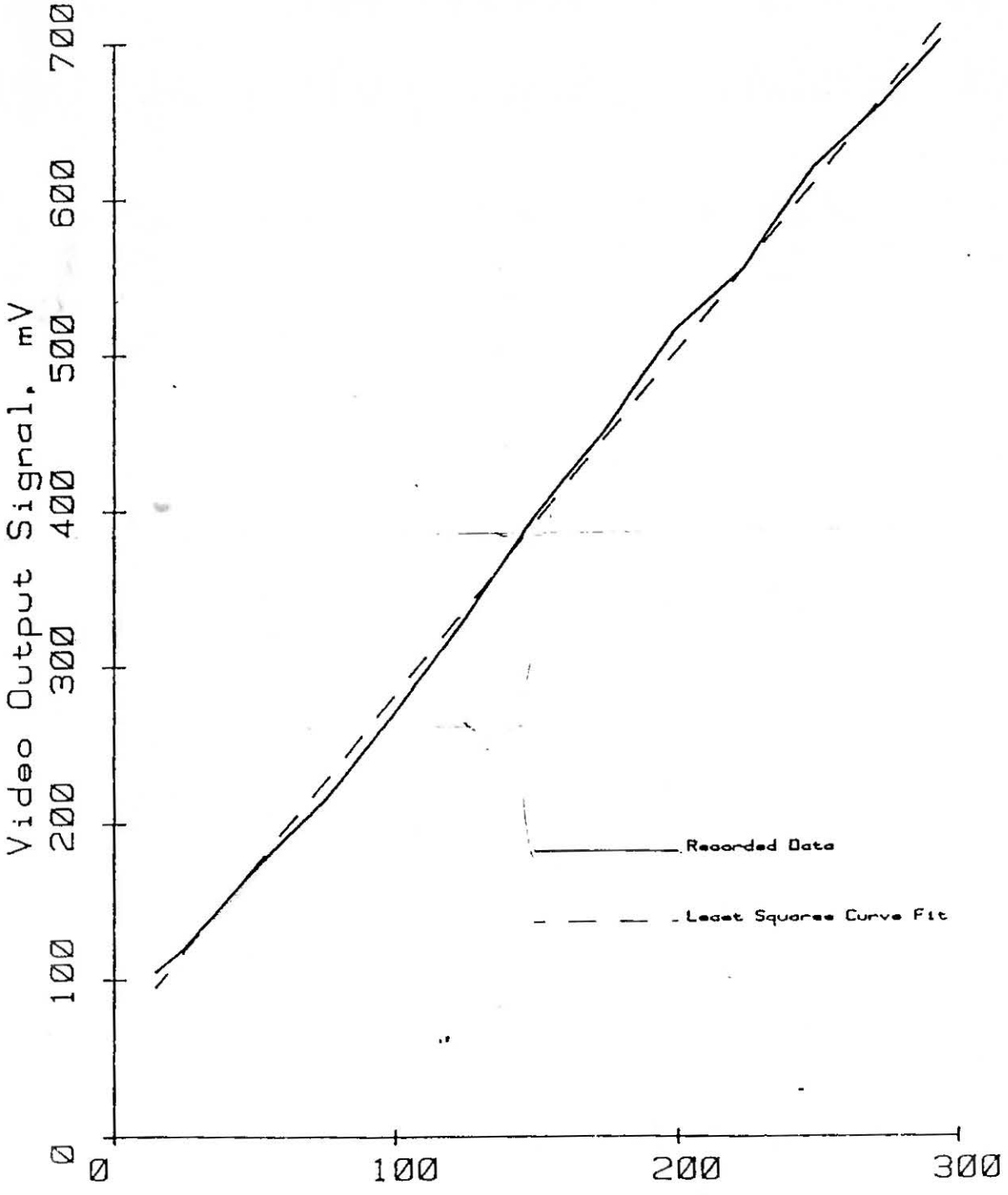

Figure 1

GAMMA - TEMPERATURE CURVE

COHU Model 2850C Vidicon (modified)
Tested at MDAC-HB 8-24-81
Temperature: 60 Degrees Fahrenheit
Peak Video to Back Porch Blanking

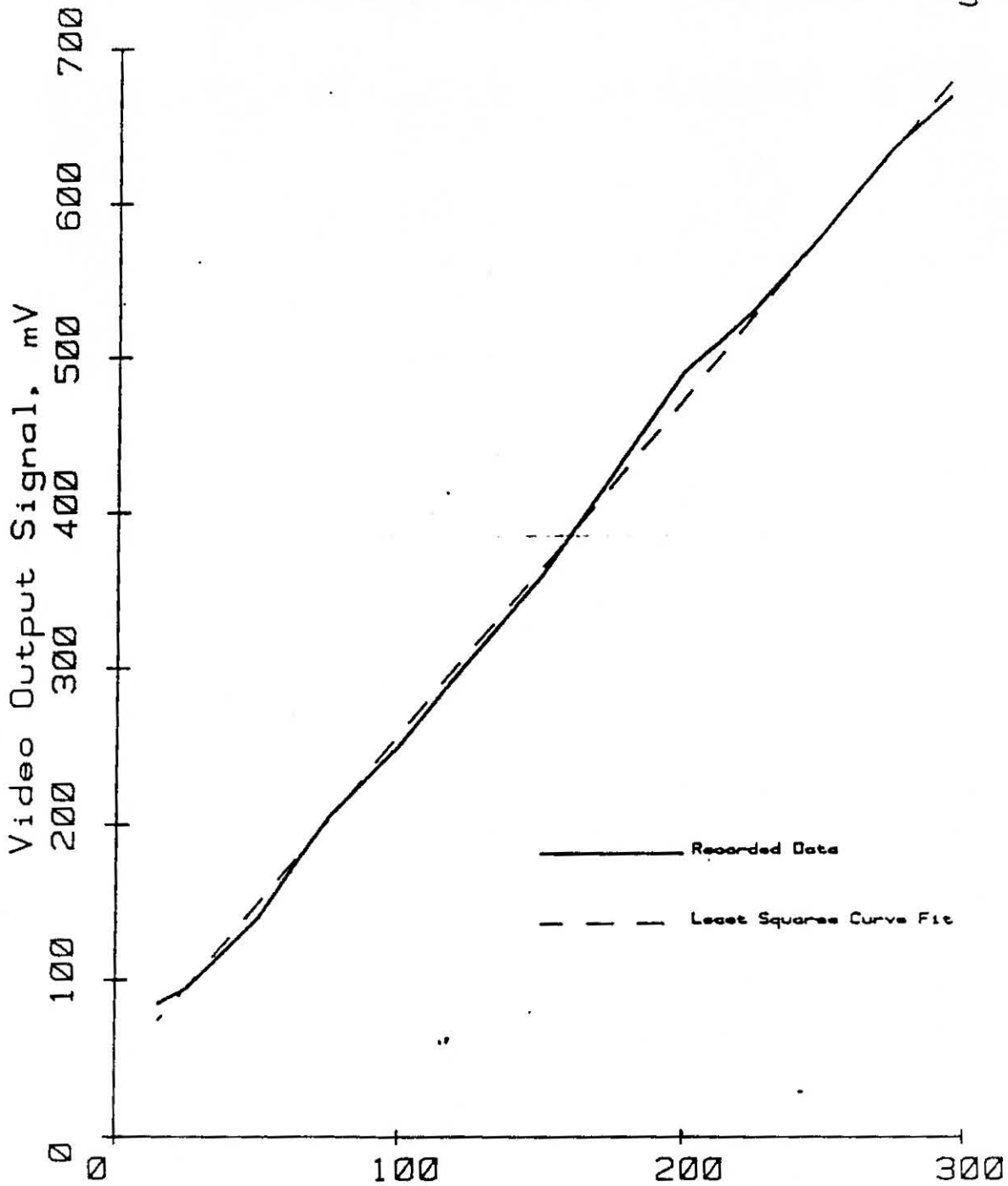

Figure 2

GAMMA - TEMPERATURE CURVE

COHU Model 2850C Vidicon (modified)
Tested at MDAC-HB 8-24-81
Temperature: 80 Degrees Fahrenheit
Peak Video to Back Porch Blanking

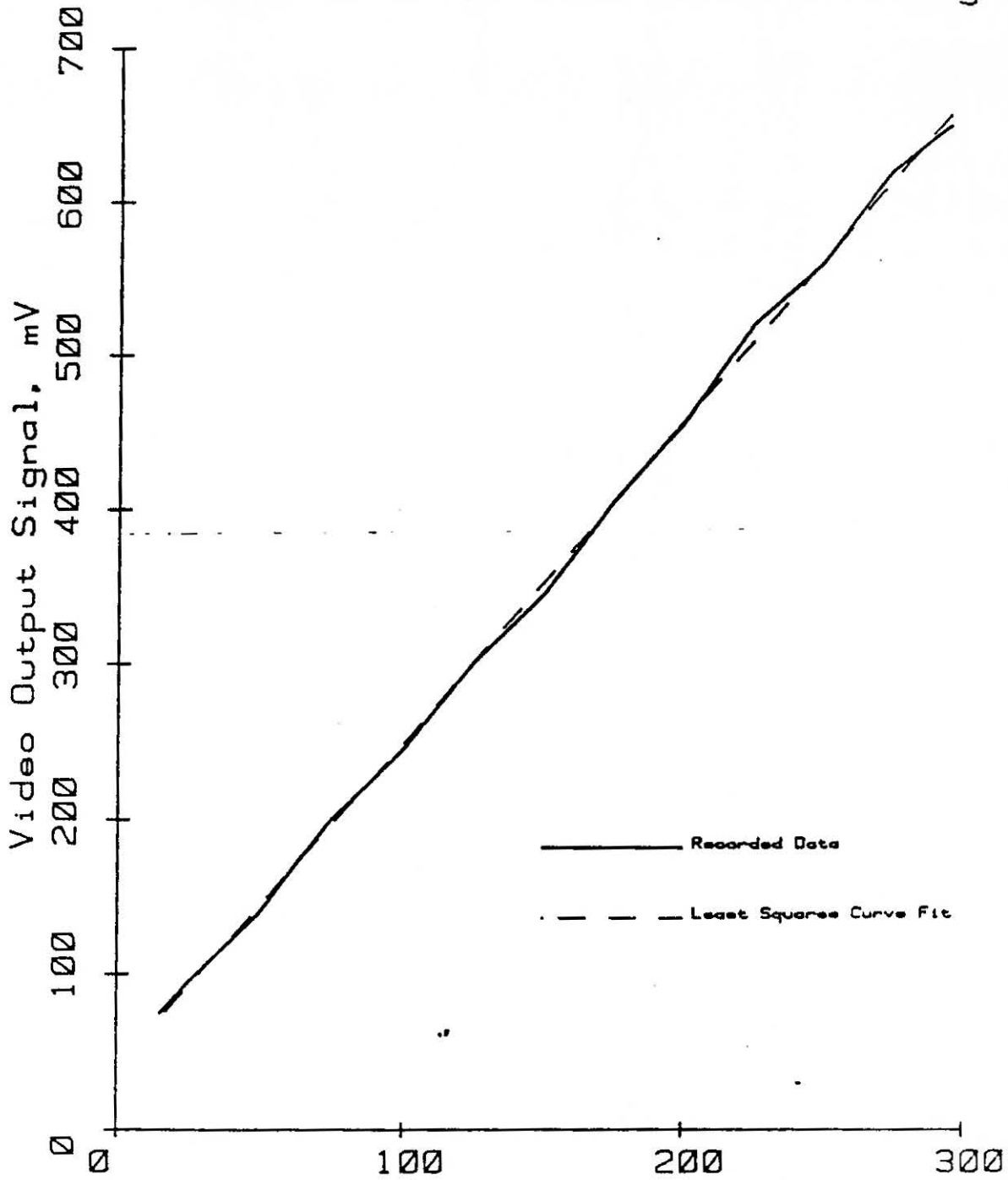

Figure 3

GAMMA - TEMPERATURE CURVE

COHU Model 2850C Vidicon (modified)
Tested at MDAC-HB 8-24-81
Temperature: 100 Degrees Fahrenheit
Peak Video to Back Porch Blanking

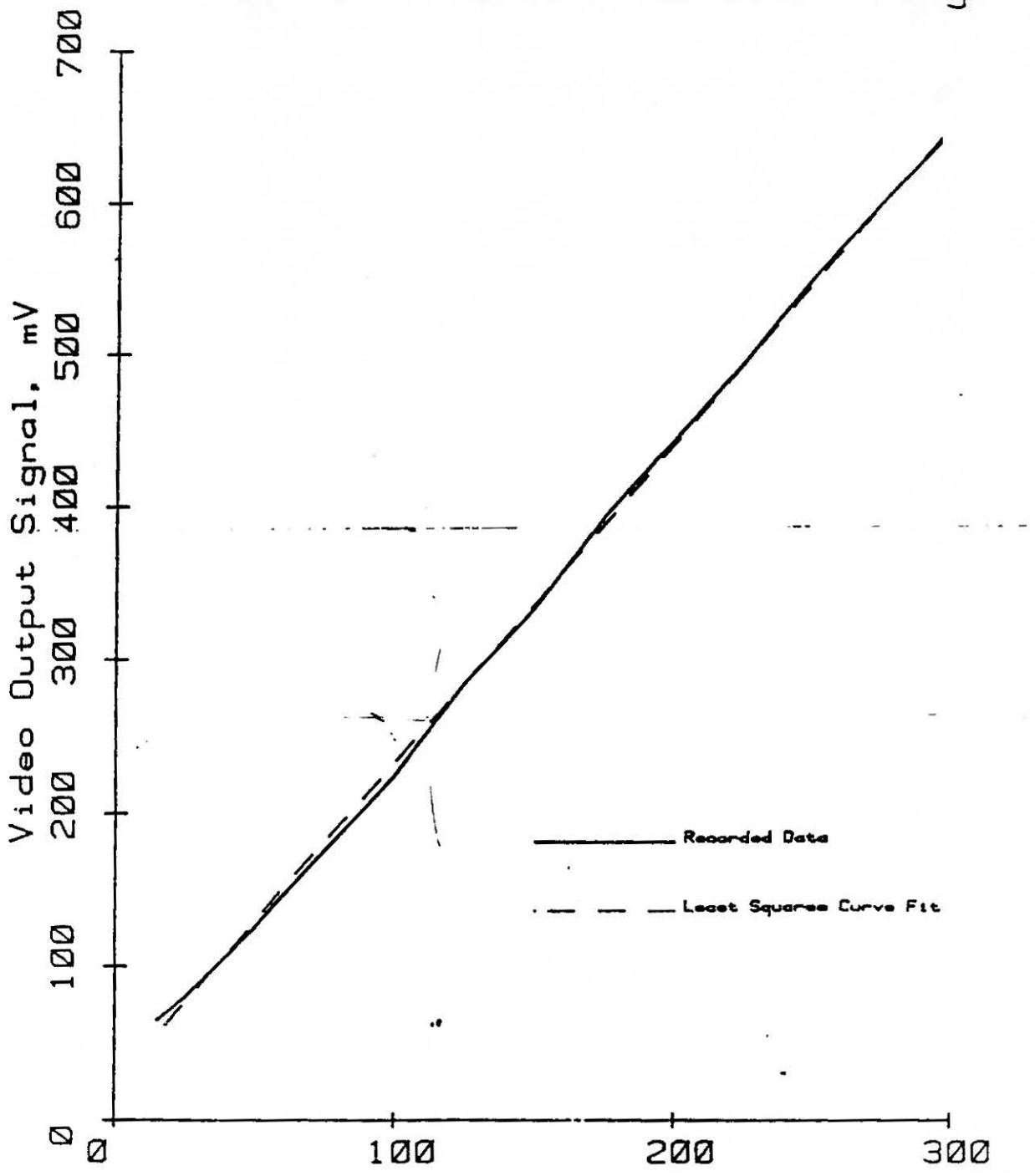

Figure 4

GAMMA - TEMPERATURE CURVE

COHU Model 2850C Vidicon (modified)
Tested at MDAC-HB 8-24-81
Temperature: 120 Degrees Fahrenheit
Peak Video to Back Porch Blanking

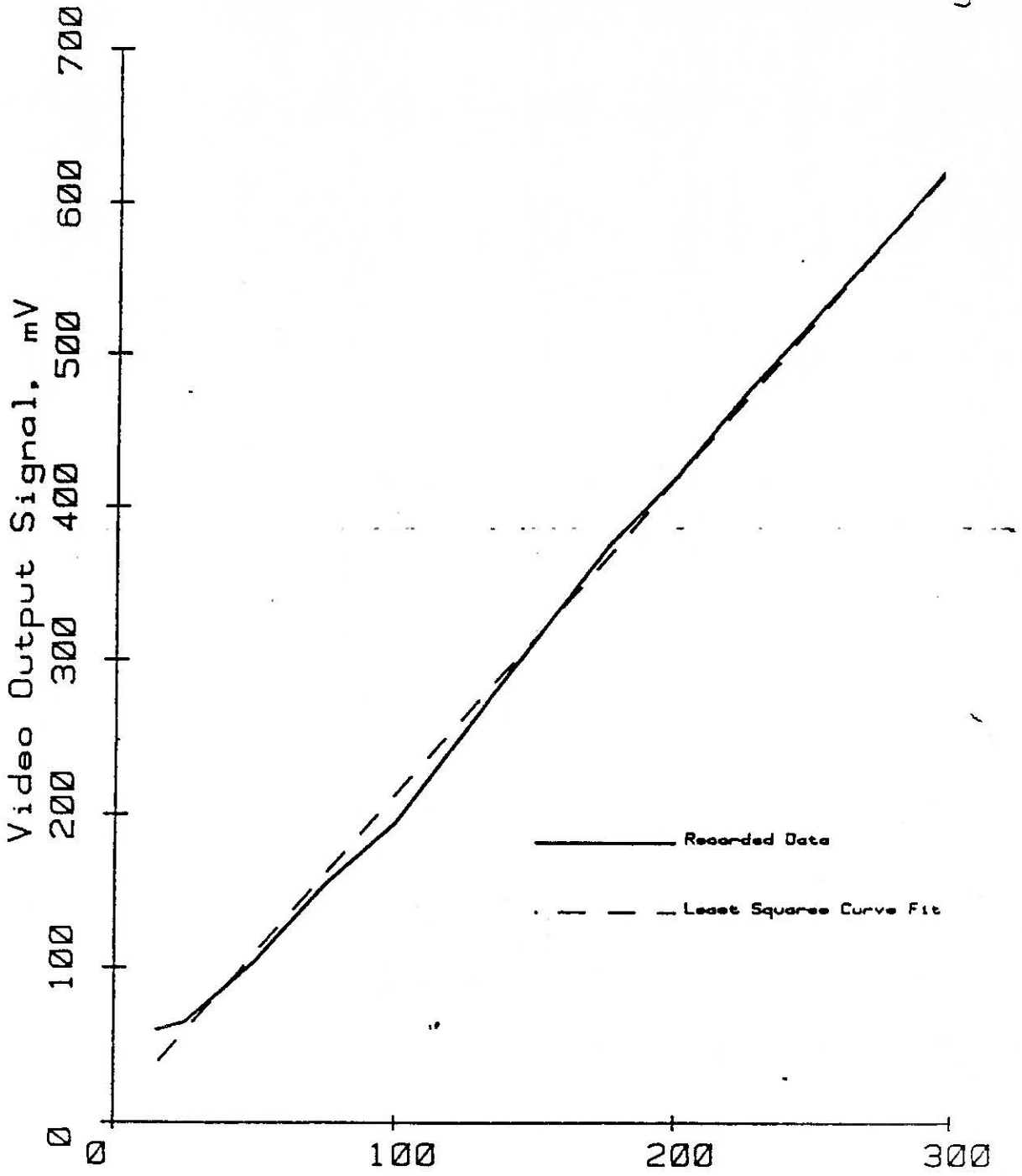

Figure 5

GAMMA - TEMPERATURE CURVE

COHU Model 2850C Vidicon (modified)
Tested at MDAC-HB 8-24-81
Temperature: 140 Degrees Fahrenheit
Peak Video to Back Porch Blanking

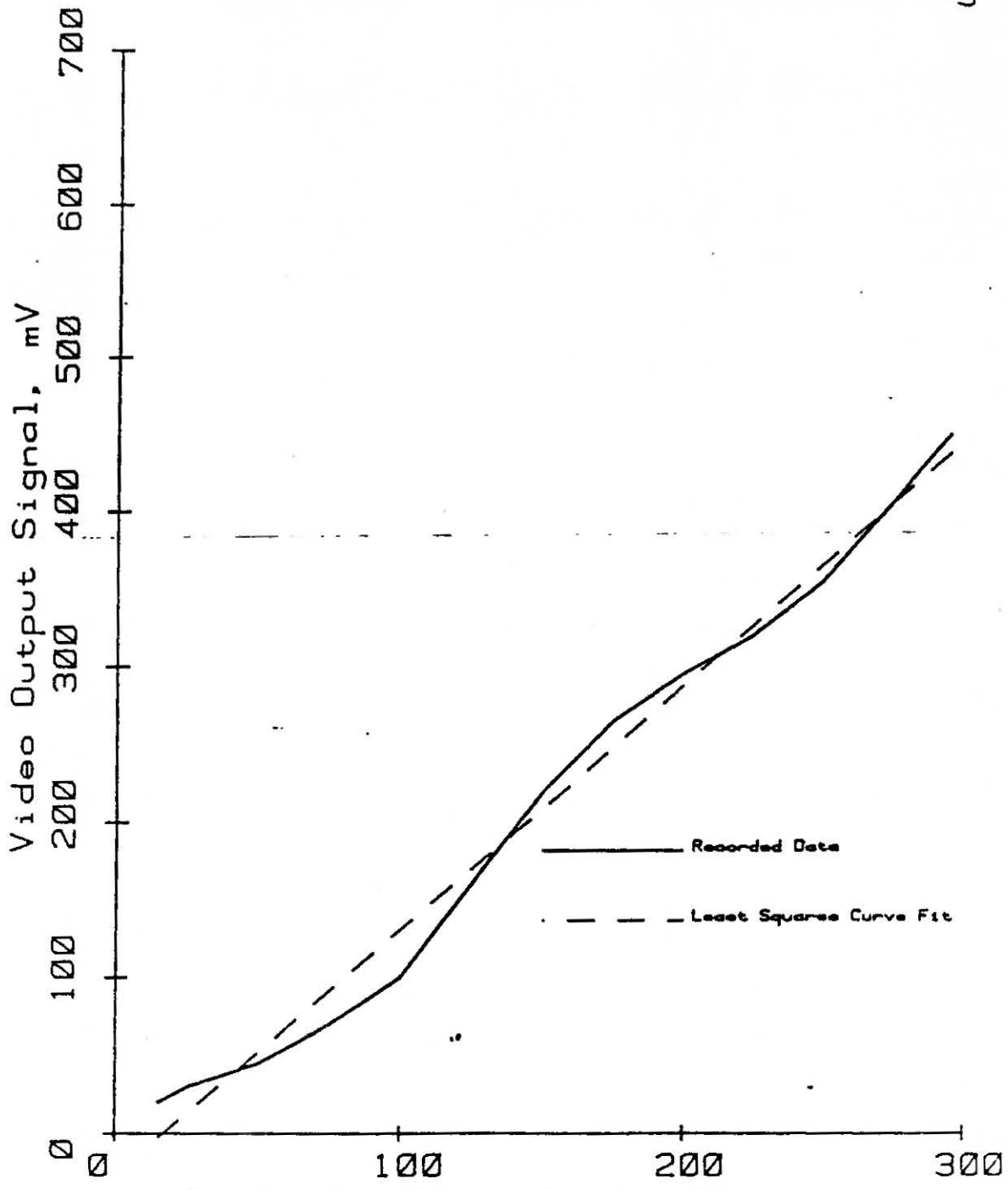

Figure 6

GAMMA -- TEMPERATURE CURVE

COHU Model 2850C Vidicon (modified)
Tested at MDAC-HB 8-24-81
Temperature: 40 (re-test)
Peak Video to Back Porch Blanking

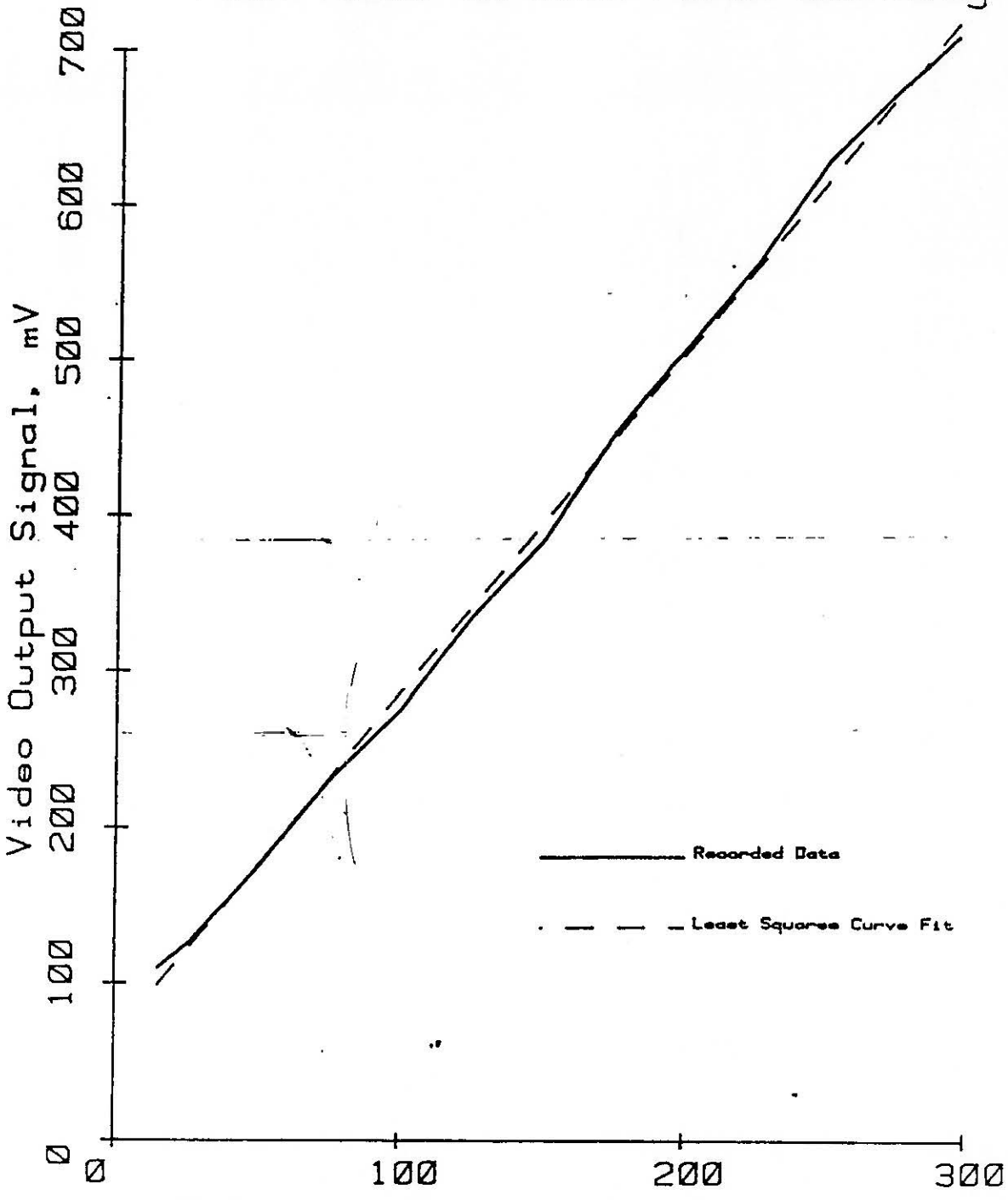

Figure 7

APPENDIX B

ANTI GLARE TUBE AND SHIELDS

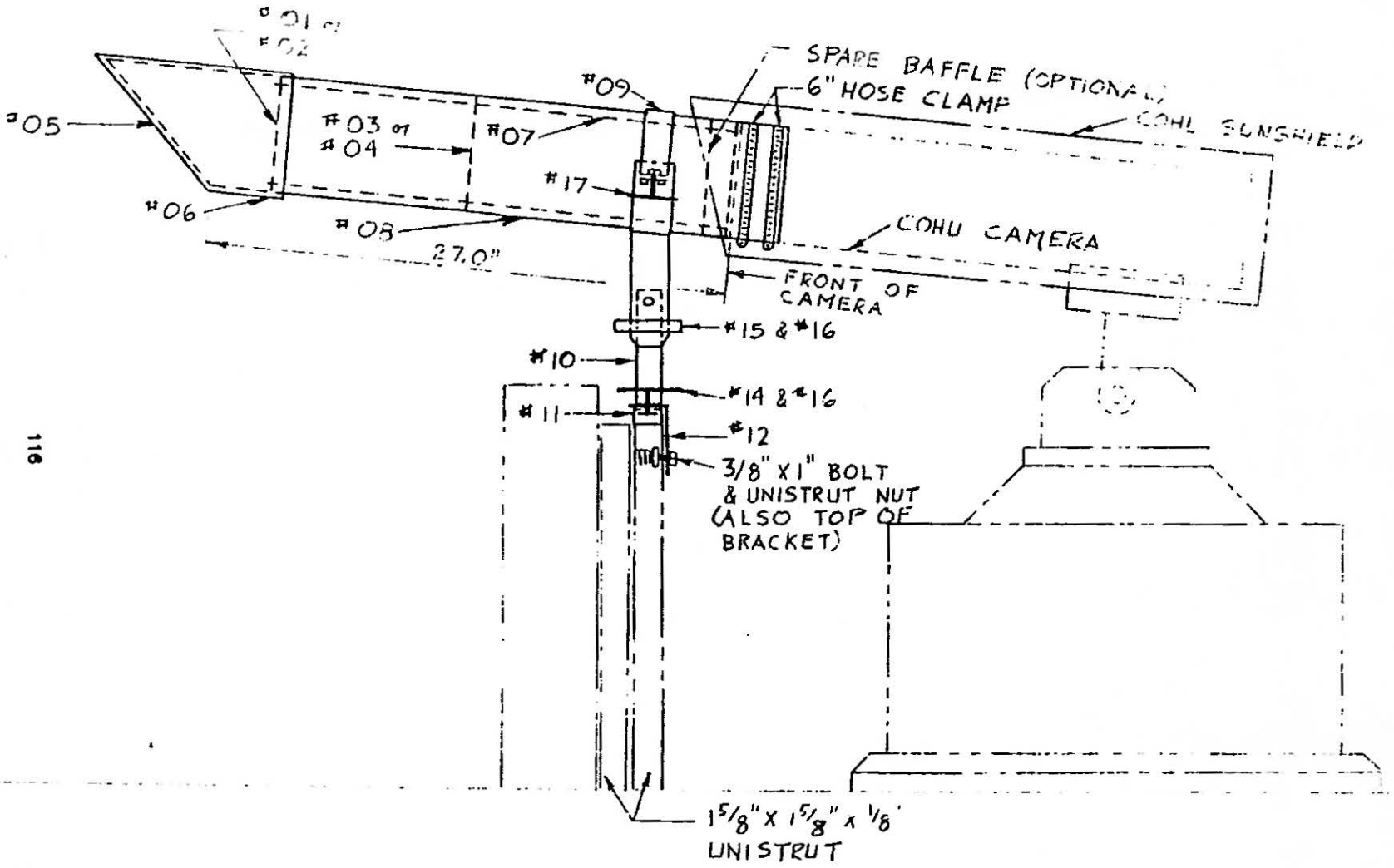

ANTI GLARE TUBE ASSEMBLY

HENDERSON & BARNES INC.

4 MAY 1983 WAB

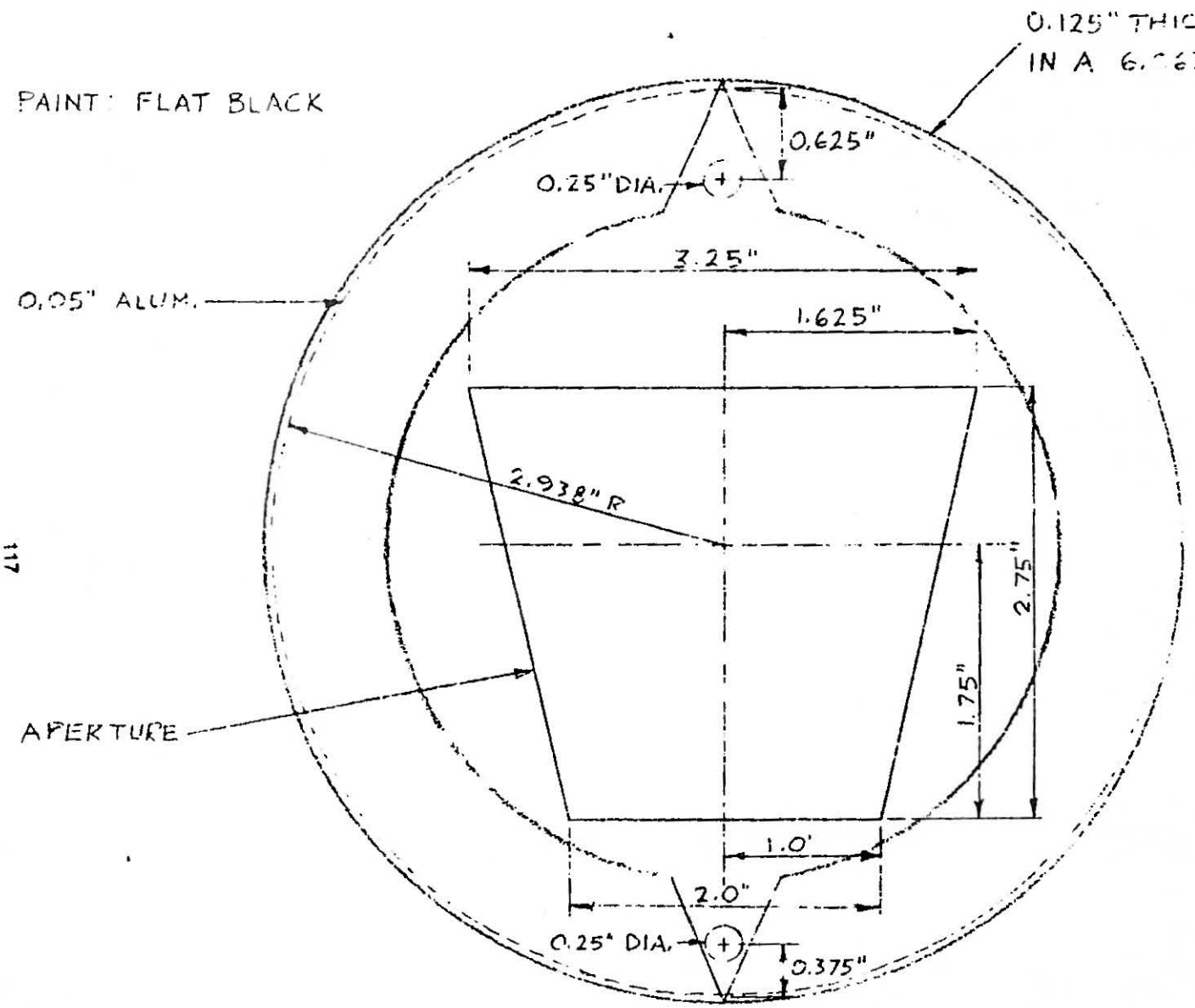

ANTI GLARE BAFFLE
EAST - WEST CAMERAS
PART NO. 01

HENDERSON & BARNES INC
3 MAY 1983 WAB 2/15

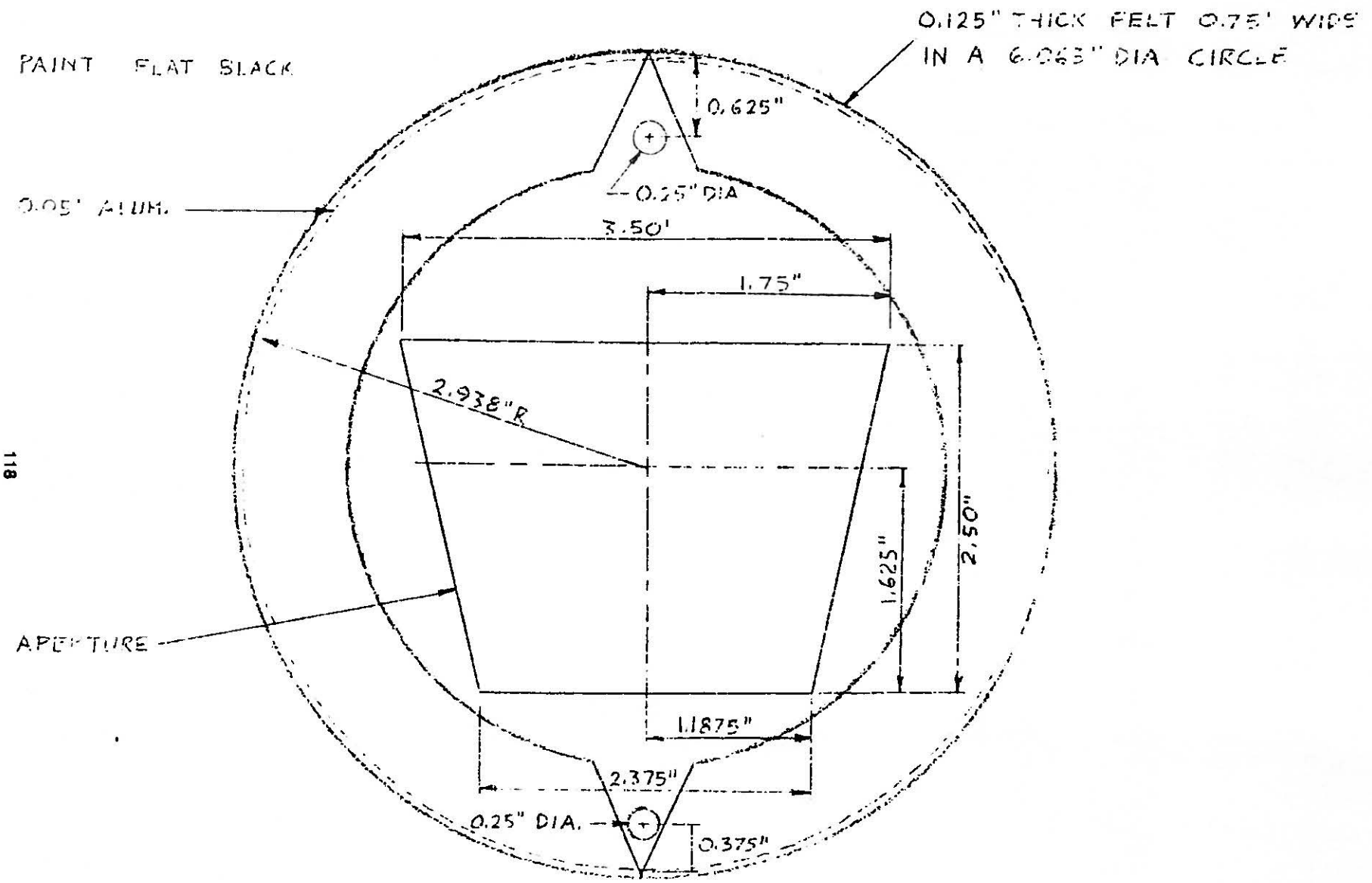

ANTI GLARE BAFFLE
NORTH-SOUTH CAMERAS
PART NO. 02

HENDERSON & BARNES INC
3 MAY 1983 WB 3 of 15

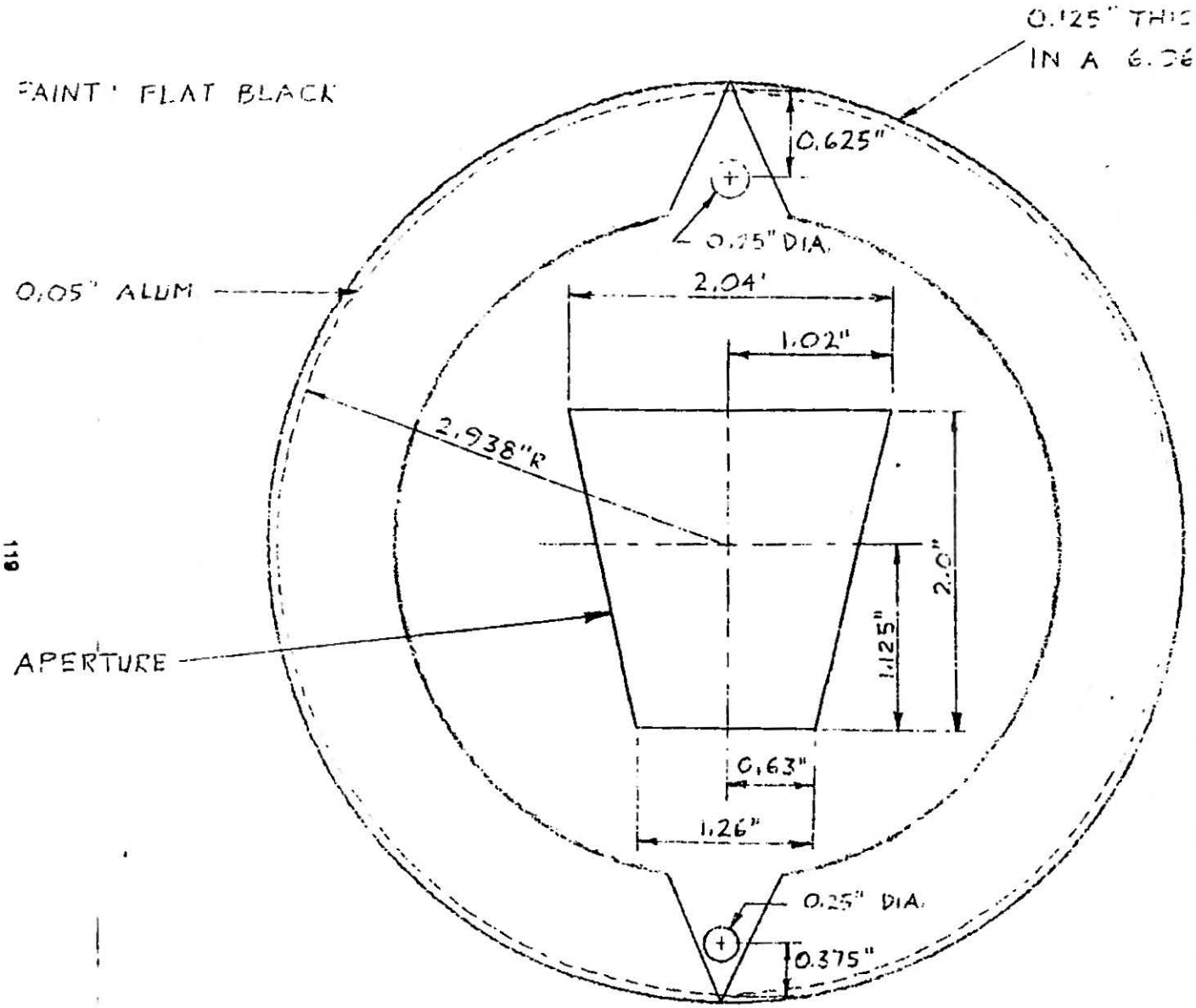

INTERIOR ANTI GLARE BAFFLE
EAST-WEST CAMERAS
PART NO. 03

HENDERSON & BARNES INC.
3 MAY 1983 WB 14 of 15

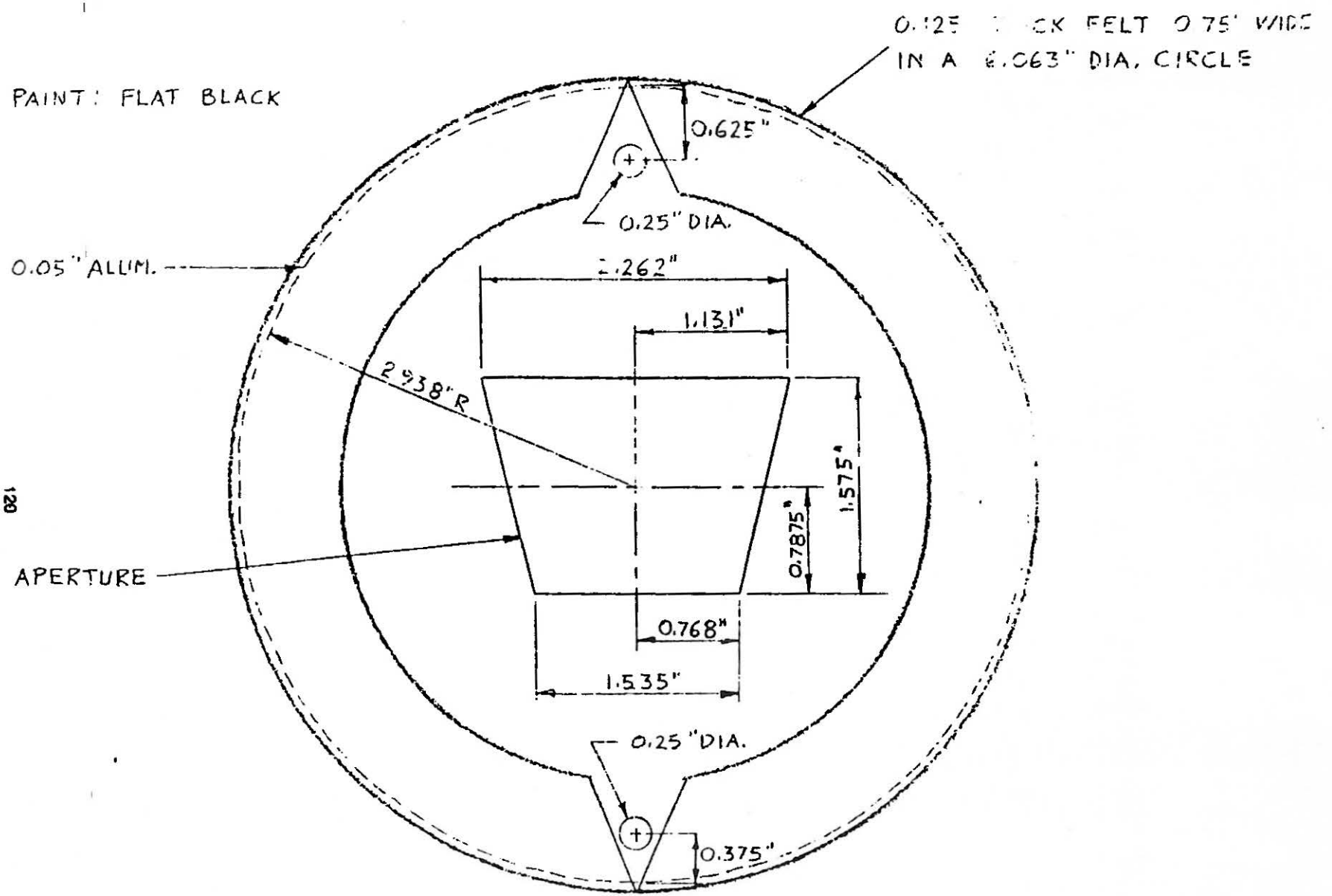

INTERIOR ANTI GLARE BAFFLE
NORTH - SOUTH CAMERAS
PART NO. 04

HENDERSON & BARNES INC
3 MAY 1983 WAB 5 of 15

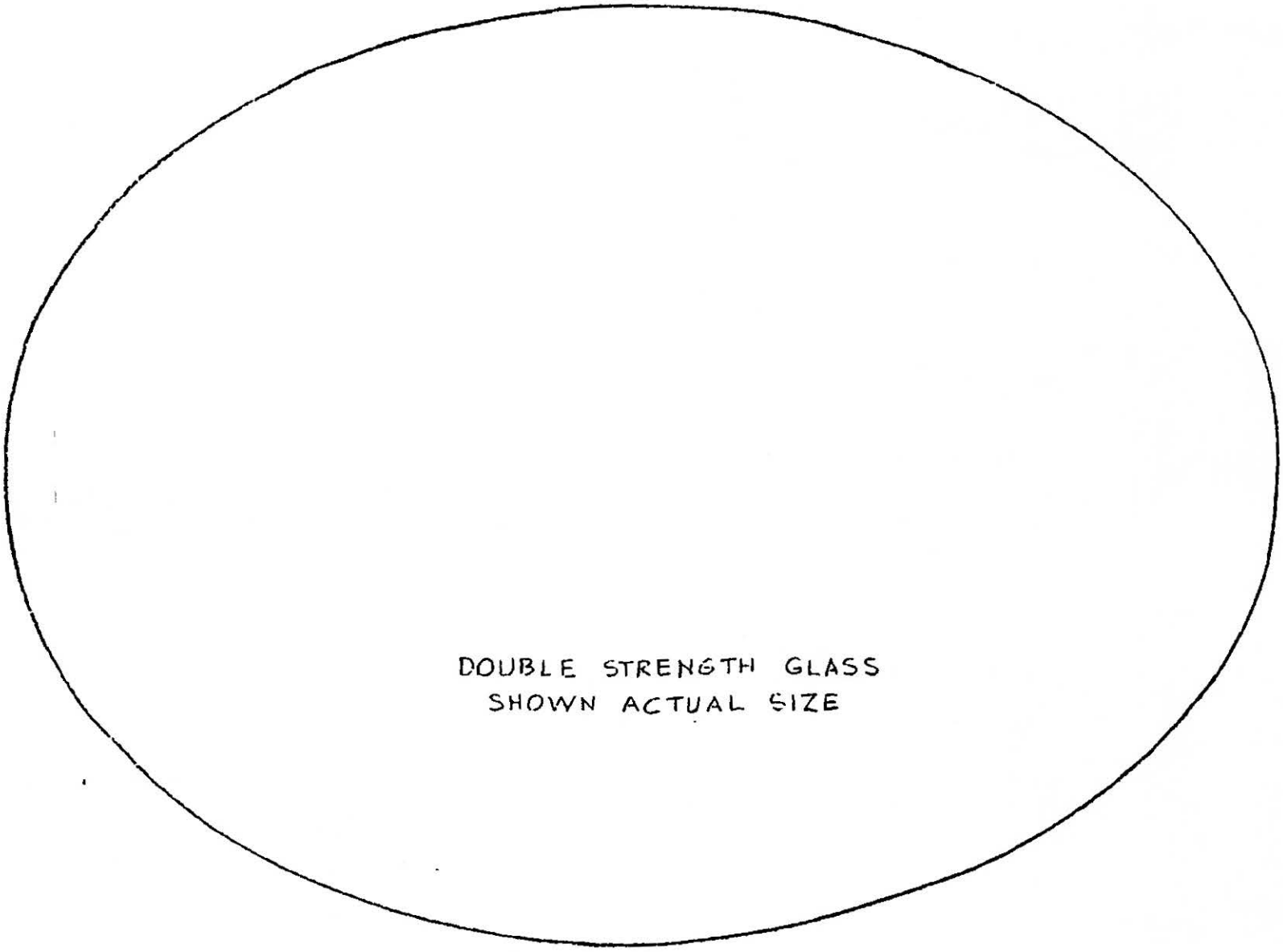

DUST COVER LENS

PART NO. 05

HENDERSON & BARNES INC.

3 MAY 1983 VAE 6 & 15

PAINT: OUTSIDE - GLOSS WHITE
INSIDE - FLAT BLACK

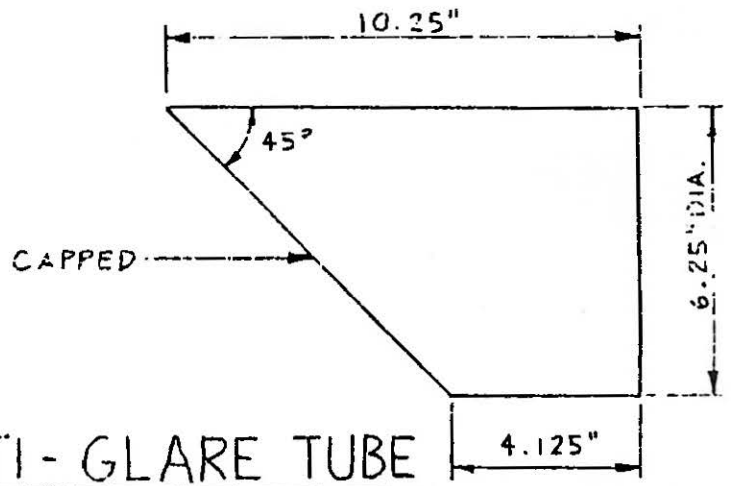

ANTI-GLARE TUBE
CAPPED DUST COVER
PART NO. 07

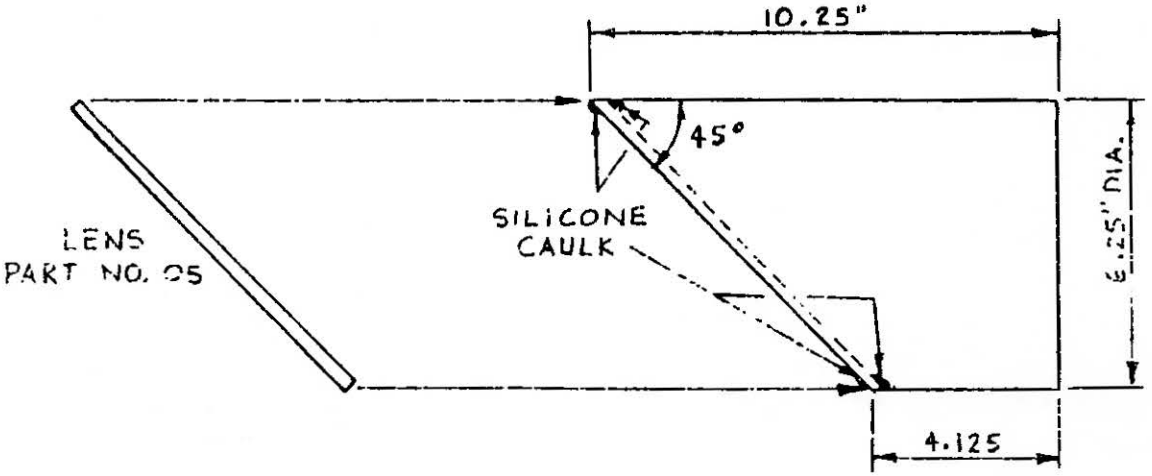

ANTI GLARE TUBE
DUST COVER
PART NO. 06

HENDERSON & BARNES INC.
3 MAY 1983 WB 7 of 15

PAINT : FLAT BLACK

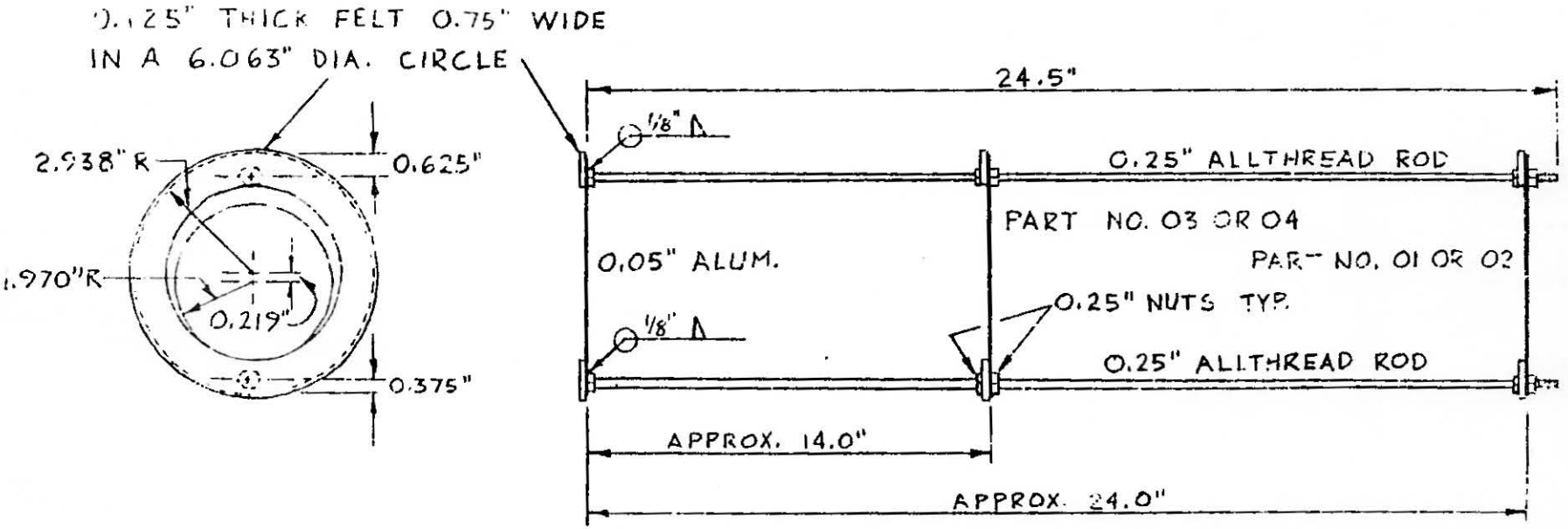

ANTI-GLARE ADJUSTABLE BAFFLE ASSEMBLY

PART NO. 08

HENDERSON & BARNES INC

3 MAY 1983 WB 8 of 15

PAINT : OUTSIDE - GLOSS WHITE
INSIDE - FLAT BLACK

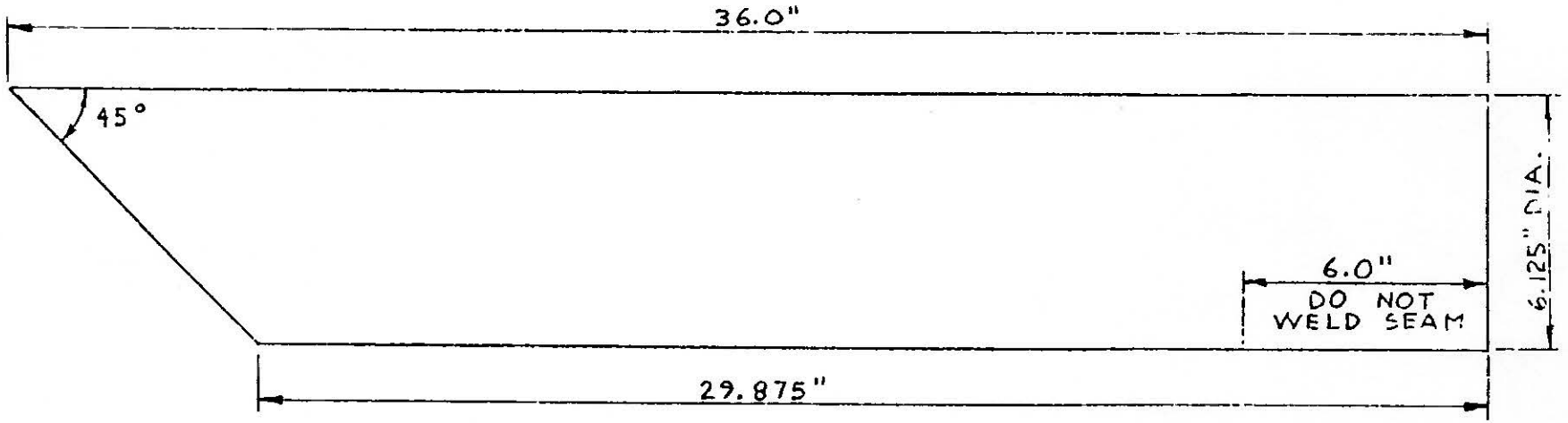

124

ANTI GLARE TUBE

PART NO. 09

HENDERSON & BARNES INC.
3 MAY 1983 WAB 9 & 15

FINISH : GLOSS WHITE

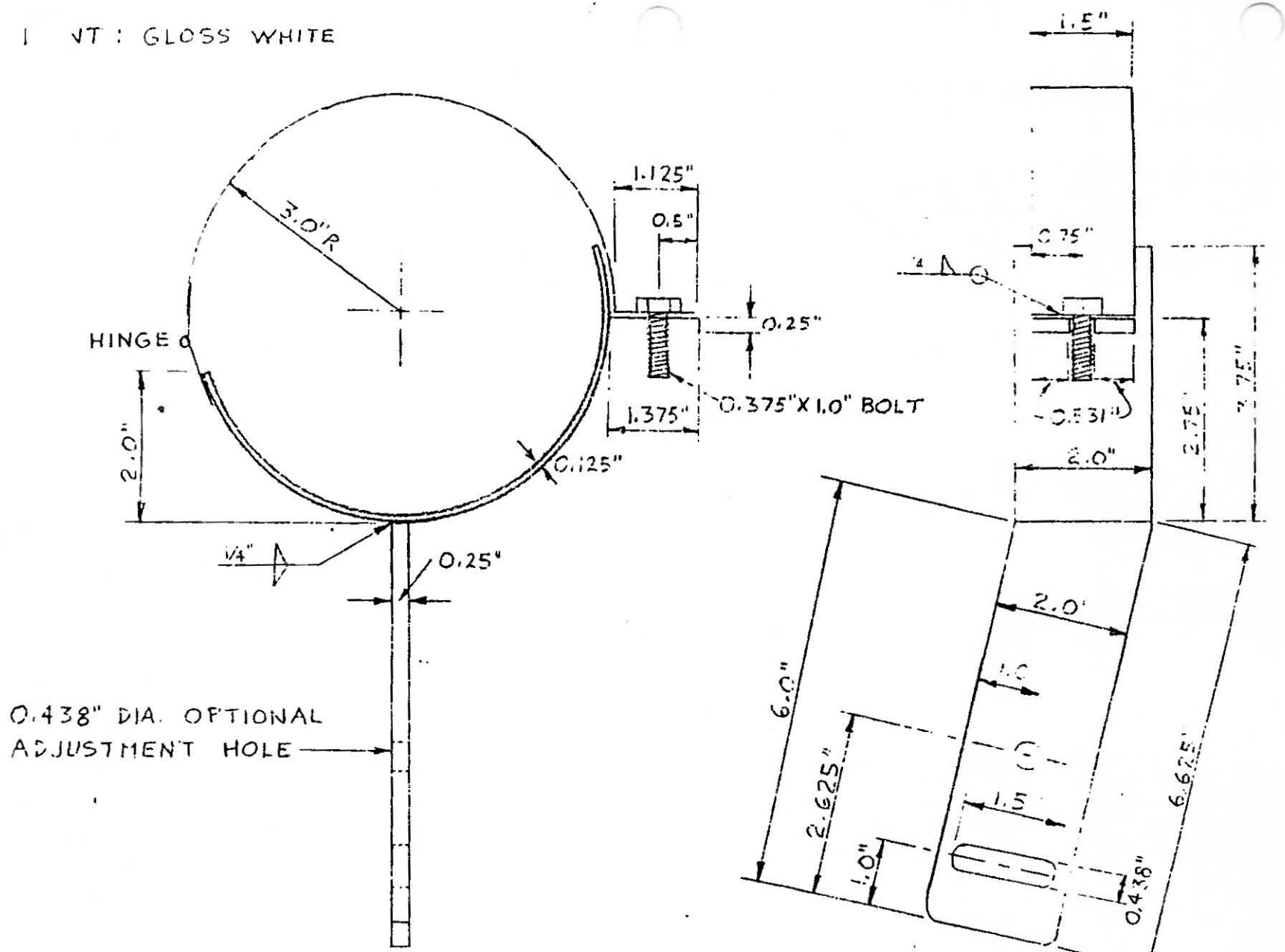

TUBE SUPPORT CRADLE

PART NO. 10

HENDERSON & EARNES INC

3 MAY 1983 WB 10 of 15

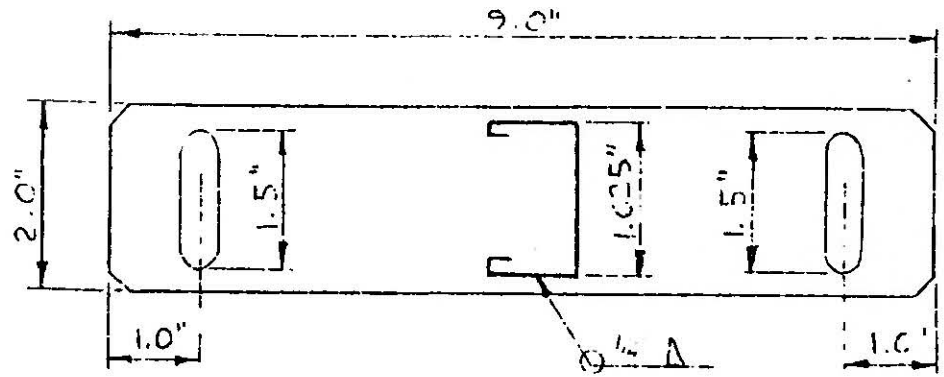

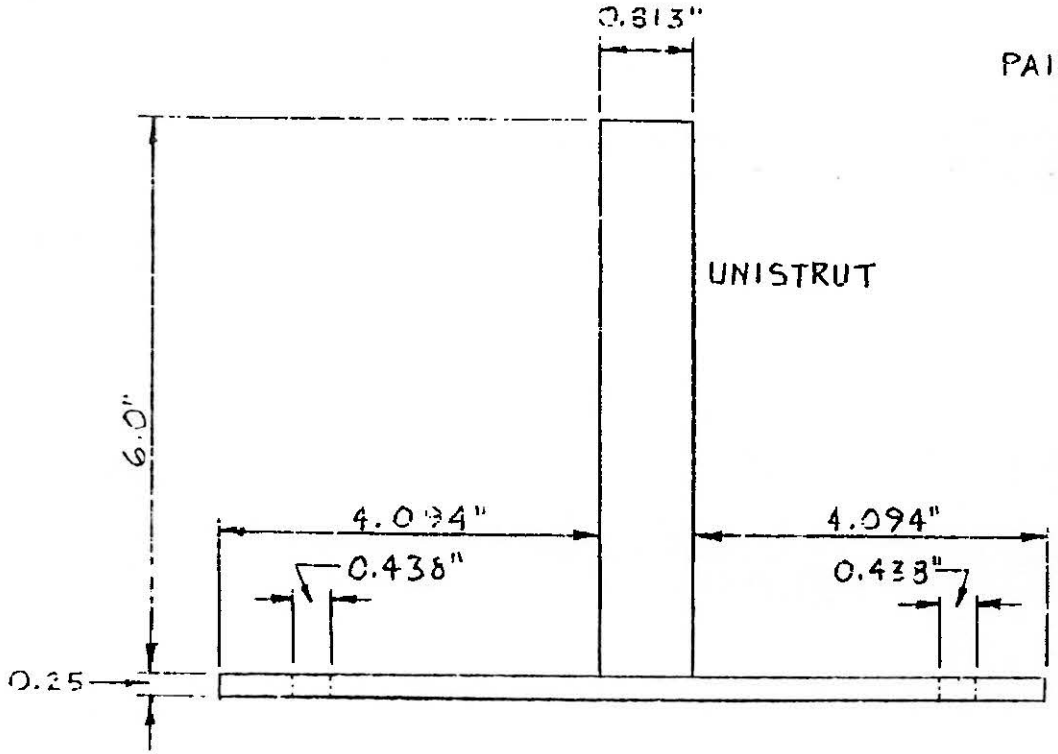

PAINT: GLOSS WHITE

VERTICAL ADJUSTMENT TRACK & SUPPORT

PART NO. 11

HENDERSON & BARNES
3 MAY 1983 WR 11 of 15

PAINT : GLOSS WHITE

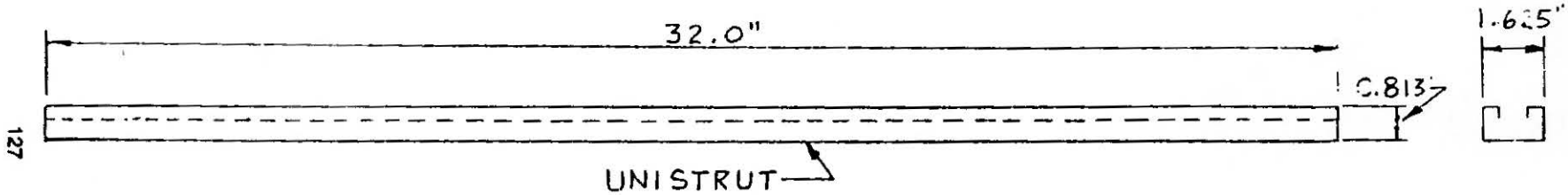

HORIZONTAL ADJUSTMENT TRACK

PART NO. 12

HENDERSON & BARNES INC.

3 MAY 1983 WAB 12 of 15

PAINT : GLOSS WHITE

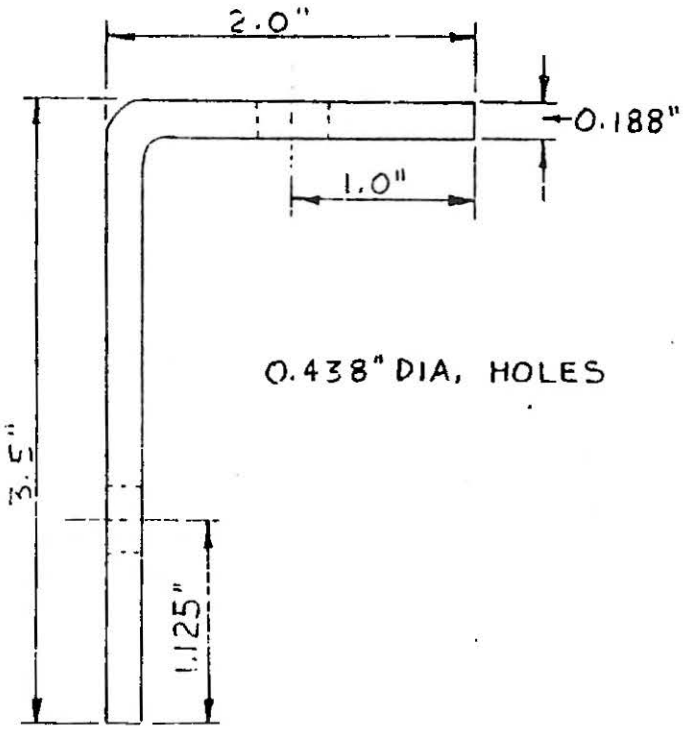

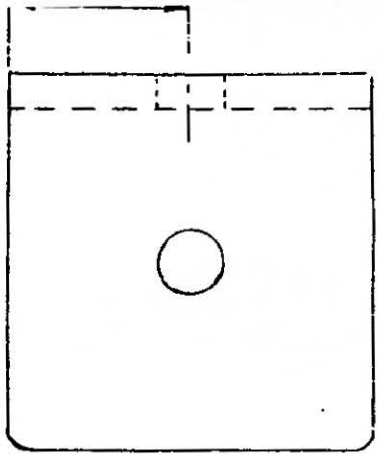

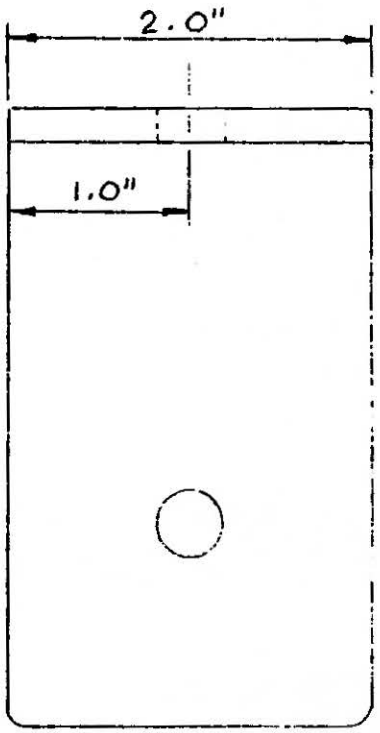

HORIZONTAL ADJUSTMENT TRACK HOLD DOWN BRACKET

PART NO. 13

HENDERSON & BARNES INC.

3 MAY 1983 WAB 13 of 15

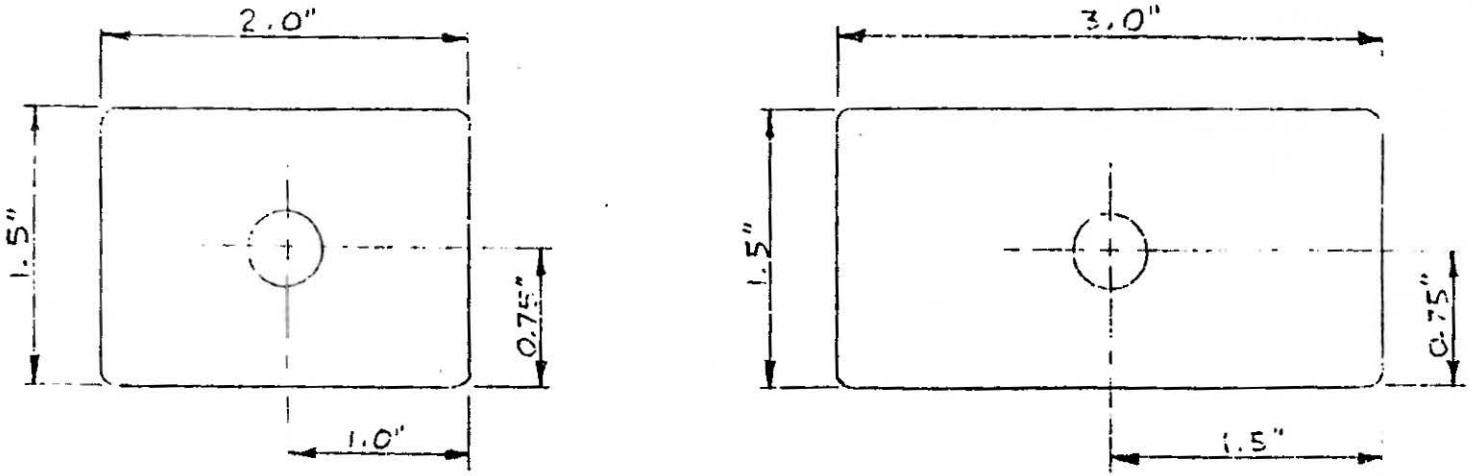

PAINT: GLOSS WHITE

128

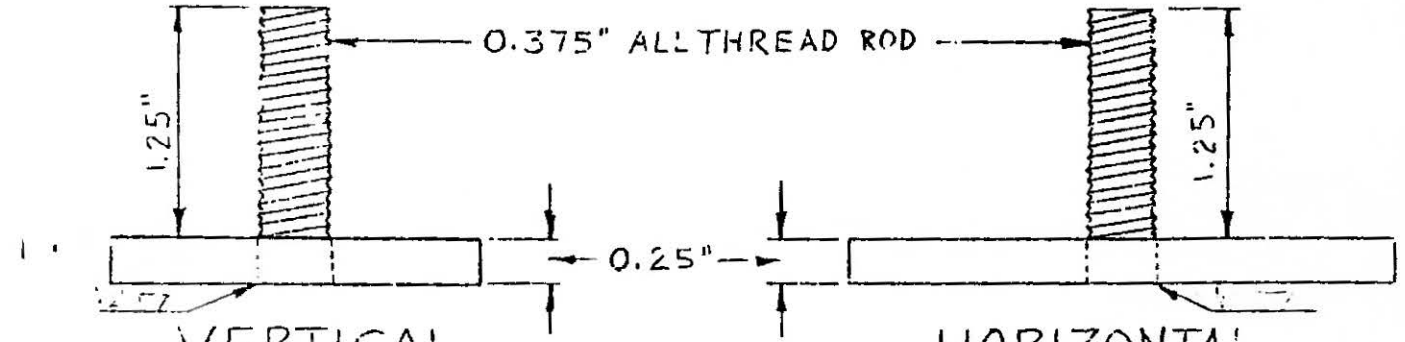

VERTICAL ADJUSTMENT CLAMP
PART NO. 15

HORIZONTAL ADJUSTMENT CLAMP
PART NO. 14

HENDERSON & BARNES INC.
3 MAY 1983 WAB 14 of 15

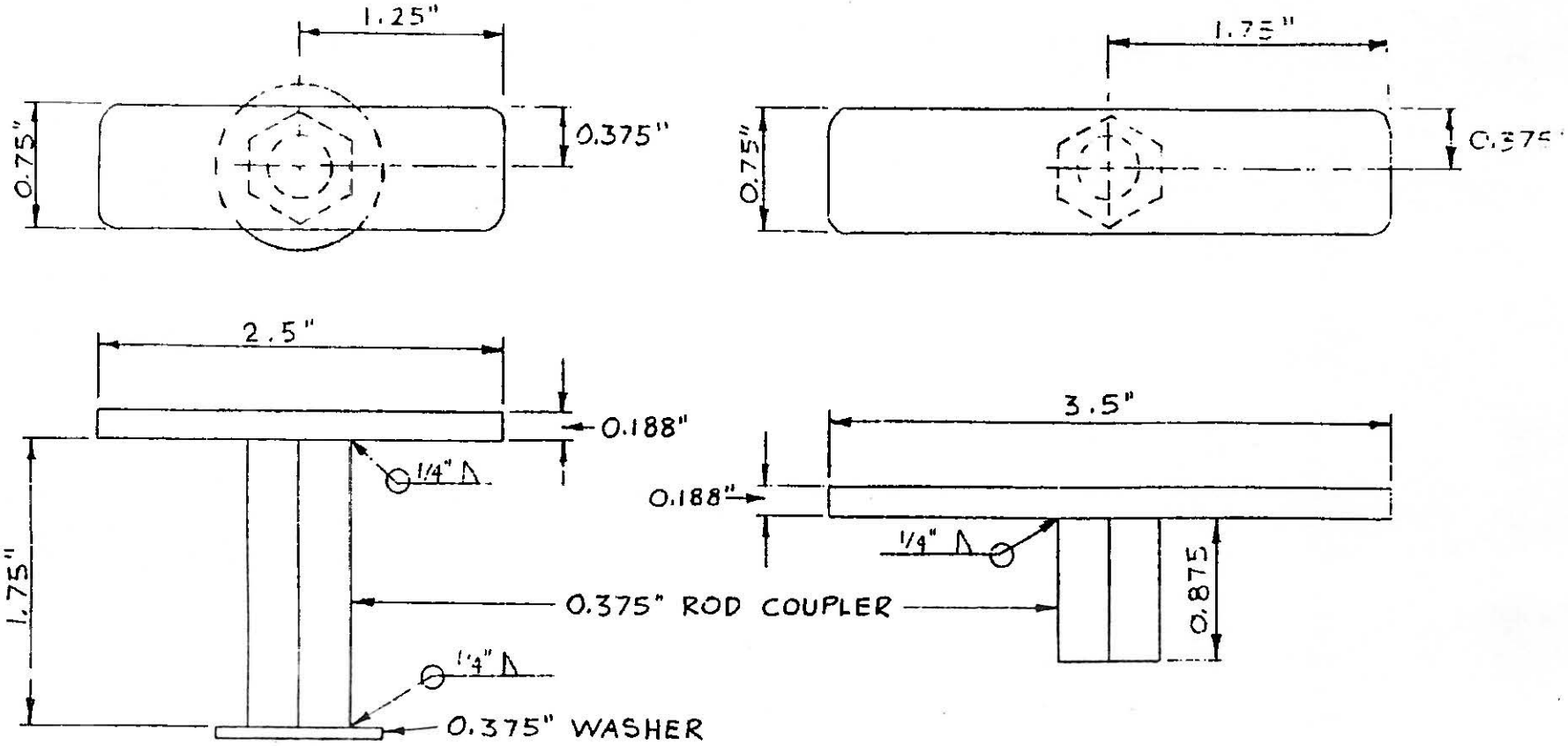

PAINT : GLOSS WHITE

CRADLE CLAMP HANDLE
PART NO. 17

HORIZONTAL & VERTICAL ADJUSTMENT CLAMP HANDLE
PART NO. 16

HENDERSON & BARNES INC.
3 MAY 1983 WAB 15 of 15

APPENDIX C

VIDEO CAMERA FOUNDATION AND MOUNT

COHU MODEL UCM-2 UNIVERSAL CAMERA MOUNT

Description

Cohu's Universal Camera Mount, Model UCM-2, is a manually adjustable pan and tilt mount for use with closed-circuit television cameras in applications in which the position of the camera will be changed infrequently. The mount can be installed in any required position on a flat surface with a single 5-1/16" bolt of suitable length. The camera can be locked in any desired panning orientation (360°) by tightening the 5/16" panning bolt; it can be tilted ±50° as required and locked in position by tighetning the tilt axis socket head bolt.

Specifications

Manual Pan Adjustment	360° arc
Manual Tilt Adjustment	100° arc (±50° with respect to plane through mounting surface)
Dimensions	
Mounting Base	1-15/16" x 3-1/2"
Tilting Platform	2-3/8" x 3"
Overall Height	2-1/2" (tilting platform and mounting surfaces parallel)
Camera Mounting	Two 1/4" holes on 1-3/8" centers
Finish	Satin-finished aluminum (clear chromate conversion coating)
Weight	10 oz.

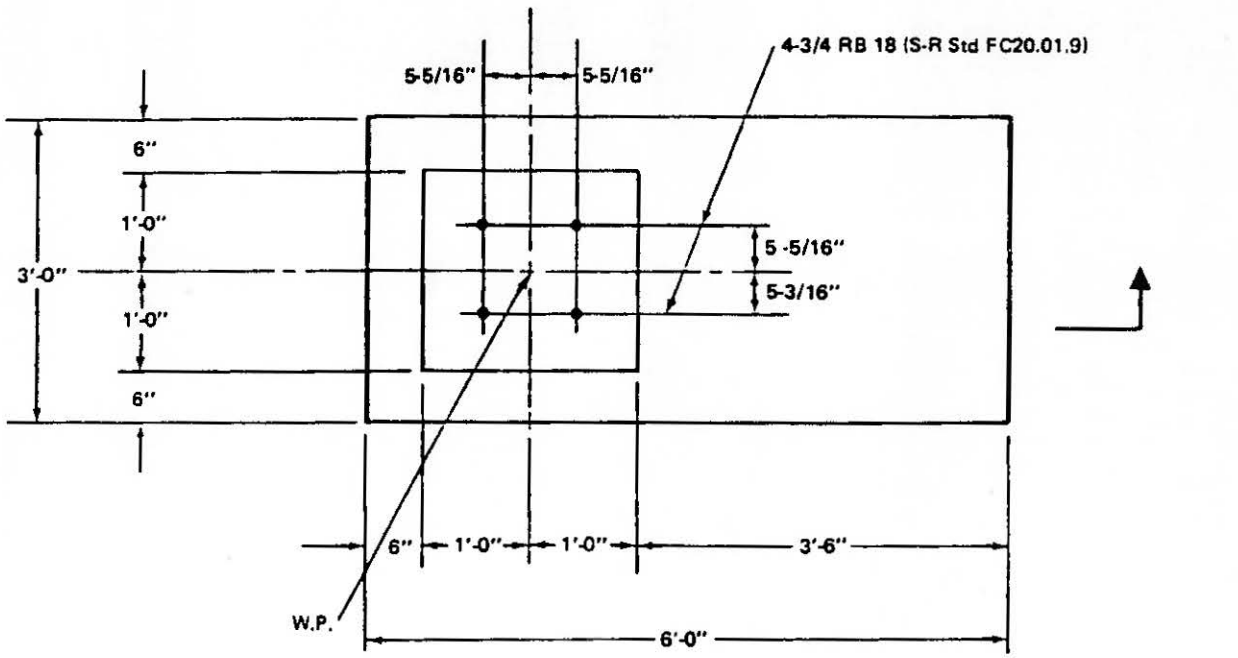

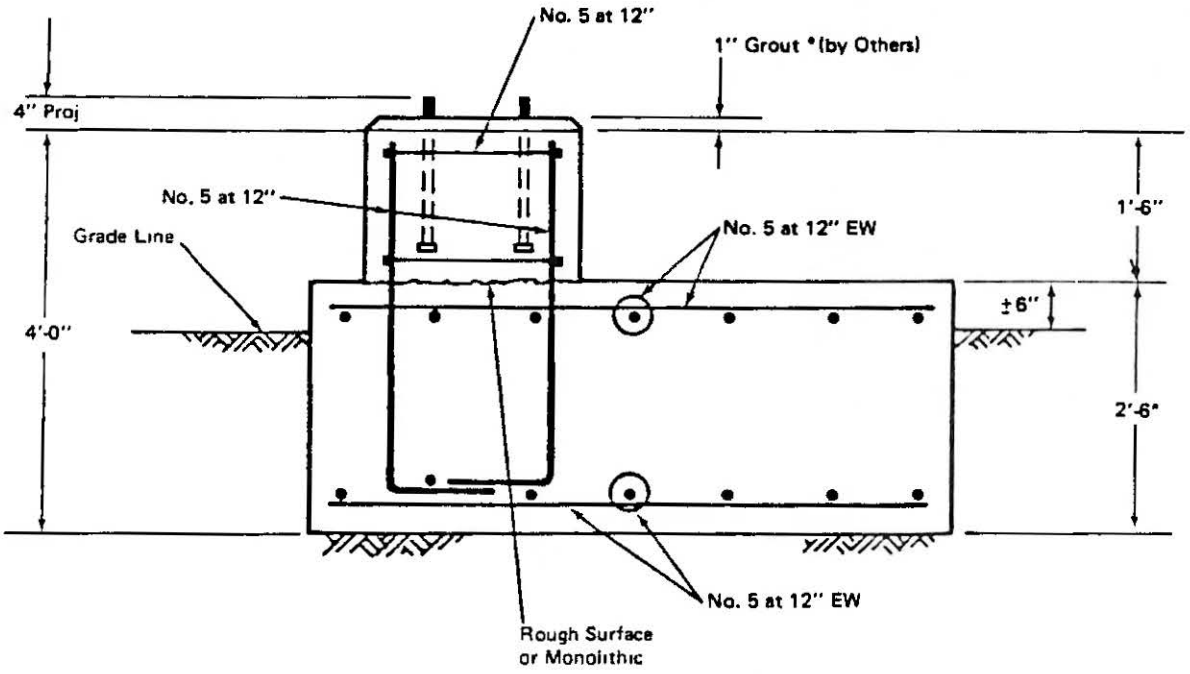

Videocamera Foundation

APPENDIX D

REMOTE CAMERA CONTROL UNIT

COHU MODEL DTMF 100/200 REMOTE CAMERA CONTROL SYSTEM

Description

The Cohu DTMF Series Remote Camera Control System provides a means to remotely control the operation of up to 100 television cameras by utilizing digital techniques and dual tone multi-frequency encoding. The basic system consists of a transmitter at the control station, with the capability of 40 different commands, and a receiver at each television camera location. The system includes: (1) a computer interface unit with a remote control interlock and remote status feedback; (2) a switcher control; (3) pre-select automatic standby or automatic off.

Signal transmission between the transmitter and receiver is over standard twisted-pair wire. The standard twisted-pair wire is branched from a central trunk.

The transmitter controls camera power; lens focus, iris and zoom. The transmitter will control 4 camera locations, one camera at a time.

When a new camera location is addressed, the previously addressed location goes to Automatic Light Control Mode (ALC) regardless of the mode it was in when last controlled. This feature serves to automatically protect the camera image tube by preventing accidental exposure to excess light.

Camera locations are addressed with a 12-key telephone-type touchpad and displayed on 2 two-digit LED readouts labeled "SELECT" and "CONTROL." The address codes are two-digit Binary Coded Decimal and the camera control codes are 4 bit. Control codes are divided into four subgroups with each subgroup capable of ten commands, this allows transmission of forty different commands.

The computer interface unit permits control of the system by computer.

Specifications

Receiver Unit DTMF-200.

Electrical

Power	105-130V 50-60 Hz or 210-260V 50-60 Hz, jumper selectable. 45W exclusive of camera and heater power
Input Signal	Level -6 to -20 dBm
Impedance	250K ohm balanced

Mechanical

Dimensions	13.5"W x 10"D x 5.25"H (34.29cm x 25.4cm x 13.33cm)
Weight	25 Lbs. (11.34kg)
Connectors (mounted on receiver)	Camera cable - conn. type MS3102E-28-21S Auxiliary outputs - conn. type MS3102E-28-12S Receiver input - conn. type MS3102E-14S-2S Video output - BNC connector

Environmental

Ambient Temperature Limits:

Operating	-40 to 60°C (-40 to 140°F)
Storage	-40 to 85°C (-40 to 185°F)
Ambient Air Pressure	Sea level to the equivalent of 10,000 feet (3,048m) above sea level (25.4cm of mercury)
Humidity	100% relative humidity (housed in NEMA-4 weatherproof box)
Vibration	5 to 30 Hz with 0.03" total excursion from 30 to 1000 Hz with peak random vibrations of 5 g's
Shock	15 g's on all axis under nonoperating conditions, MIL-E-5400R, para. 3.2.24.6

Transmitter Unit DTMF-100.

Electrical

Power	105-130V 50-60 Hz or 210-260V 50-60 Hz, jumper selectable, 20W
Output Signal	-6 dBm across 600 ohm balanced twisted-pair

Mechanical

Dimensions	3.5" (8.89cm) H x 10.5" (26.67cm) D mounted in a 19" (48.26cm) rack mount enclosure
Weight	7 Lbs. (3.18kg)
Connector	Barrier terminal strip

Environmental

Ambient Temperature Limits:

Operating	0 to 50°C (32 to 122°F)
Storage	-40 to 85°C (-40 to 185°F)
Ambient Air Pressure	Sea level to the equivalent of 10,000 feet (3,048cm) above sea level (24.4cm of mercury)
Humidity	95% relative humidity
Vibration	5 to 30 Hz with 0.03" total excursion, from 30 to 1000 Hz with peak random vibrations of 5 g's
Shock	15 g's on all axis under nonoperating conditions, MIL-E-5400R, para. 3.2.24.6

SYSTEM DESCRIPTION
POS VIDEO CAMERA SYSTEM

The system consists of:

4	2850C	Cameras with fixed gain, computer controlled iris and remote controlled zoom and focus
4	DTMF-200	Receivers
1	DTMF-100 ER-8807	Transmitter modified to decode TTL input signals for iris and switcher control
1	VS504H	Switcher with remote control capability

The DTMF-100 is modified to decode address and iris control data from a computer. The address data is on 2 lines and selects 1 of 4 switcher inputs and routes the DTMF control signals to the camera corresponding to the input selected.

A strobe output from the computer strobes the address data into a 2 bit latch in the DTMF-100. The address data must be stable for a minimum of 40 nanoseconds before the strobe becomes active; and the strobe must be active for a minimum of 140 nanoseconds.

Iris open and close commands from the computer are on two lines. Interlocking is provided to prevent simultaneous open and close commands such as could occur if the cable became disconnected. These signals activate the DTMF-100 iris open and close encoding circuits.

Decoding circuits are provided to route the DTMF control signals to the addressed camera.

A five conductor cable is provided between the DTMF-100 and the VS504H switcher. A mating connector is provided to interface with the computer.

All computer input signals are TTL levels, positive true.

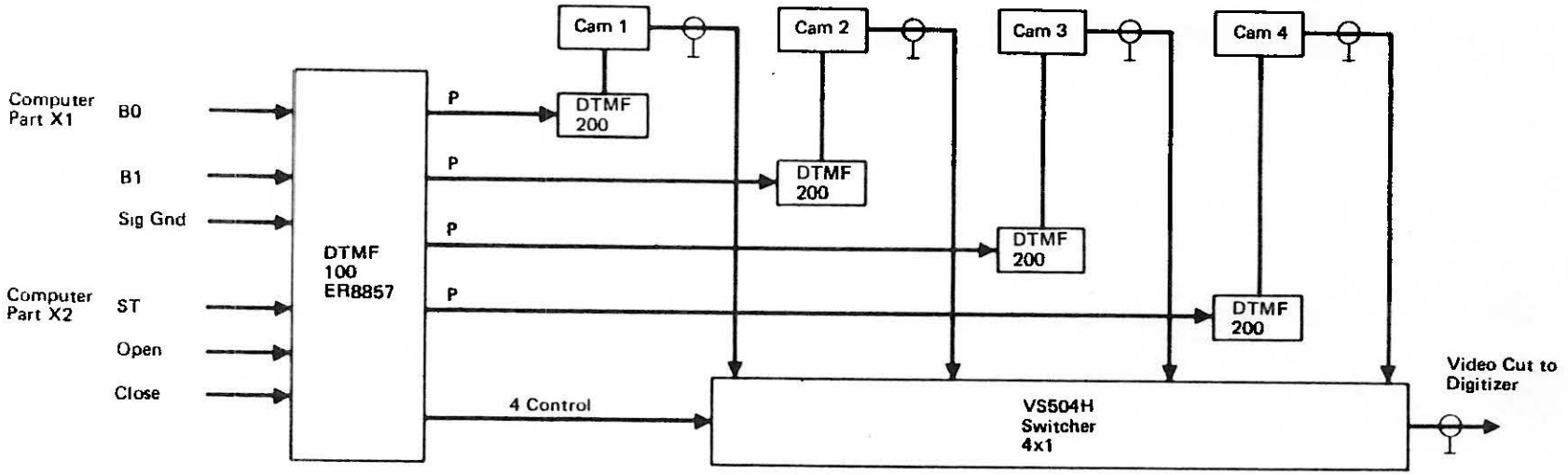

Switcher Address Timing

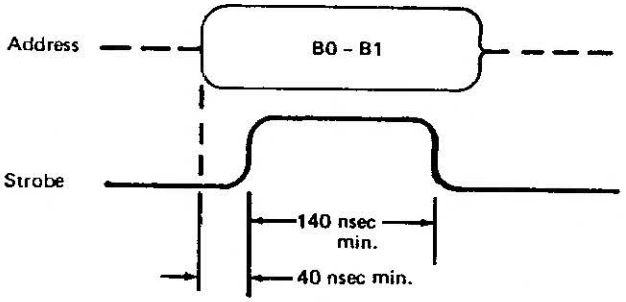

Camera Addressing

	B0	B1
Cam 1	0	0
Cam 2	0	1
Cam 3	1	0
Cam 4	1	1

Figure . BCS Video Camera System

APPENDIX E

VIDEO SWITCHING UNIT

VIDEO SWITCHING UNIT

COHU MODEL 9151 VIDEO SWITCHING MATRIX UNIT

Cohu 9151 Series Switching Matrix Unit is designed for operation in closed-circuit video systems, and is a means for flexibility interconnecting video display devices, to video sources. The unit consists of a standard 19-inch, rackmountable chassis which includes an integral power supply. Each unit is equipped with a circuit interconnection board; wiring; connectors; and plug-in, etched-circuit cards as required to perform the specified functions. Units may be used individually or interconnected to form large systems.

A standard interconnection board provides the following matrix configuration where the first number is the input and the second number is the output. This configuration indicates the maximum number of input and output channels possible for an interconnection board. Not all channels need be used. Active channels are provided by plug-in cards. Spare channels permit expansion by inserting additional plug-in cards.

Plug-in cards are of two main types: video switch cards and output amplifier cards. The unit is equipped with one switch card for each active input channel and one output amplifier card for each active output channel. Both cards may be of the nonterminated or 75-ohm terminated type.

Switch cards which are not terminated are equipped with input circuits permitting 75-ohm characteristic impedance video cables to be looped through as many as 10 switch cards.

The input circuit of the terminated switch card properly terminates the 75-ohm cable. The switch card has an input isolation amplifier, and five switching circuits each of which feeds an output amplifier input bus.

Output amplifier cards which are not terminated are equipped with output circuits permitting 75-ohm cables to be looped through other output amplifier cards. The output circuit of the terminated output amplifier properly source-terminates the 75-ohm cable.

Turn-off circuitry is provided on the output amplifier card, to minimize cross talk, when the output amplifiers are to feed a common line, as in the case of output amplifier "loop-through."

Power for controlling the matrix switch points via hard-contact circuits is provided by the power supply in the unit.

Switching may be manually or automatically controlled by remote controls such as pushbutton switches, relays and computers.

Specifications

Switching Matrix Specifications.

Type of Signals	Composite/noncomposite video (monochrome/ color)
Video Input Signal Level	2V p-p maximum
Gain	Unity
Type of Synchronization	EIA, or other compatible with rise time and levels specified herein
Switching Controls (DC logic voltage levels required to activate and deactivate)	Bipolar Control Switching Circuits: ON, +10V (at 0.5 mA) to +12V (at 0.72 mA) OFF, -7V (at 0.7 mA) to -15V (at 1.5 mA) Positive One Logic Switching Circuits: ON, +2.5V (at 0.053 mA) to +50V (at 1 mA) OFF, $0^{+0.5}_{-4}$V (at 5 to 20 µA)
Video Input Resistance	75-ohm line section for looping through up to 10 inputs
Video Output Resistance	75-ohm source terminated
Sync Input Resistance	75-ohm line section for looping through up to 20 sync inputs to output amplifiers
Sync Mixing (optional)	Capable of being switched off by external interlock signal (for EIA standard sync, per RS-170)
Frequency Response	±0.5 dB at 10 MHz ±1 dB at 20 MHz -3 dB at >32 MHz

Cross Talk	-60 dB to 10 MHz (between inputs and between outputs) -40 dB to 20 MHz
Noise and Hum	<1 mV rms in 20 MHz bandwidth
Differential Gain	<1% at 50% and 90% APL (average picture level), <1.5% at 10% APL
Differential Phase	<0.7° at 3.58 MHz at 50% and 90% APL, 1° at 10% APL
Rise Time	<15 nanoseconds
Delay (envelope)	18 to 25 nanoseconds at 3.58 MHz
Tilt	<±0.4% at 60 Hz (not applicable to cards with dc restorer)
Power Requirements	105-125V, 60 Hz, 35W
Operating Temperature	-20 to 50°C (-4 to 122°F)
Humidity	To 95%
Dimensions	19" W x 5.25" H x 19" D (48.26 x 13.33 x 48.26 cm)
Weight	30 lbs. (13.6 kg)

APPENDIX F

VIDEO DIGITIZER

VIDEO DIGITIZER

Quantex Model DS-12 Digital Image Memory/Processor

Functional Description. Incoming composite video is stripped of sync and applied to a high speed A/D converter. Data from the A/D passes through the arithmetic processor where they may be combined with memory data through hardwired arithmetic processes which include summation with data already in memory, averaging, and subtraction. The resulting data are then stored in memory.

Random access through the digital port is time-shared with a multiplexed write and read of the memory in standard TV format with the output applied to a D/A converter. Output is standard RS-170 video.

Video Input Interface — The standard DS-12 is used with the source whose video output conforms to EIA RS-170 signal standards.

Memory Quartering — Memory quartering is a standard feature in DS-12 processors. It allows the user to partition the memory into four independent memories with each having half the linear resolution of the full memory.

Selection of full or quartered memory mode and selection of quadrant can be independently selected for the write and read process. For example, the user may choose to read from Quadrant 2 while writing to Quadrant 1.

Four quarters may be displayed simultaneously; any quarter may be expanded to occupy the full screen.

When the IEEE bus interface (P/N 22-062) is installed, memory quartering is controlled by a remote computer.

IEEE Standard 488 Input/Output Interface (Order P/N 22-062) — This feature interfaces the memory and the microprocessor to the IEEE 488-1975 Interface Bus. It allows transfer of digital image data to and from memory with random

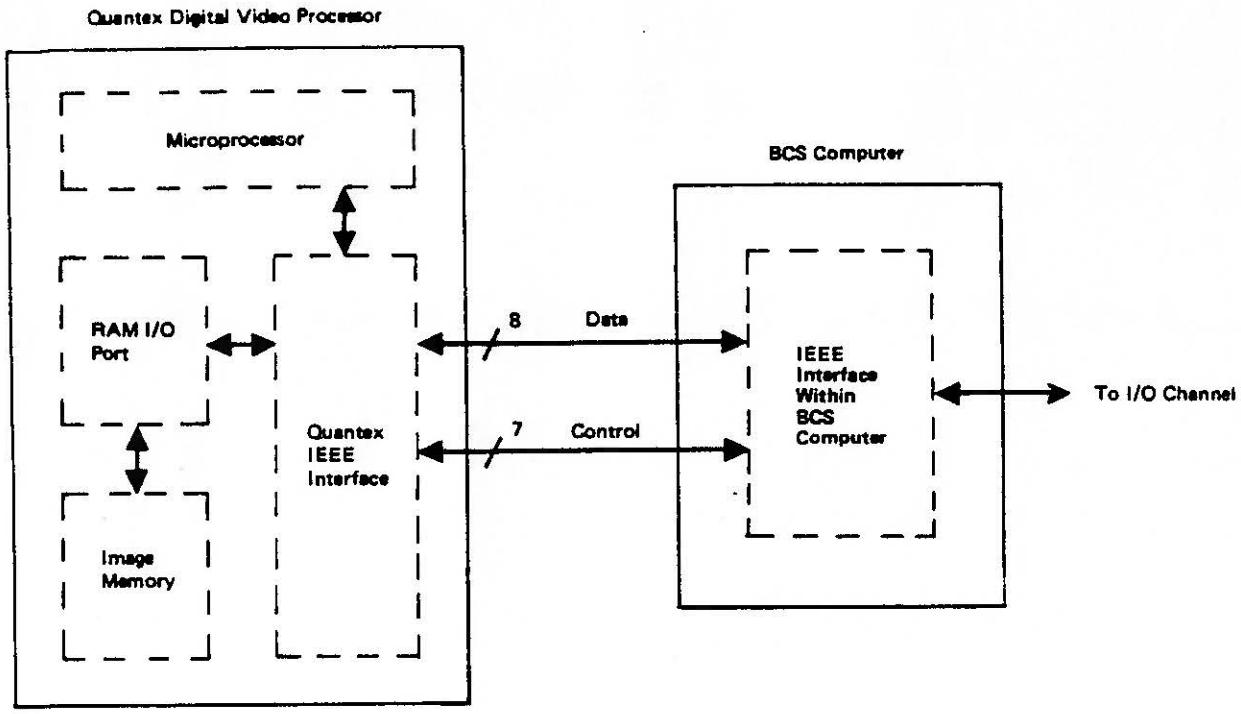

IEEE 488 Interface Block Diagram

access. It also allows control of the Quantex processor from an external computer.

This option pre-empts the Random Access I/O Port.

Digital Image Memory/Processor Specifications

Memory Size: 256 x 256 picture elements
A/D Converter Sampling Rate: 5 MHz
A/D Converter Resolution: 8 bits
Memory Word Size: 8 bits/256 levels
Random Access Cycle Time: 1.6 microseconds
Power 120 VAC, 60 Hz: Size 7" High, 17" Wide, 24" Deep, Weight 80 lbs.

APPENDIX G

TARGET SHUTTER SCHEMATIC

TARGET SHUTTER

SFDI DESIGN

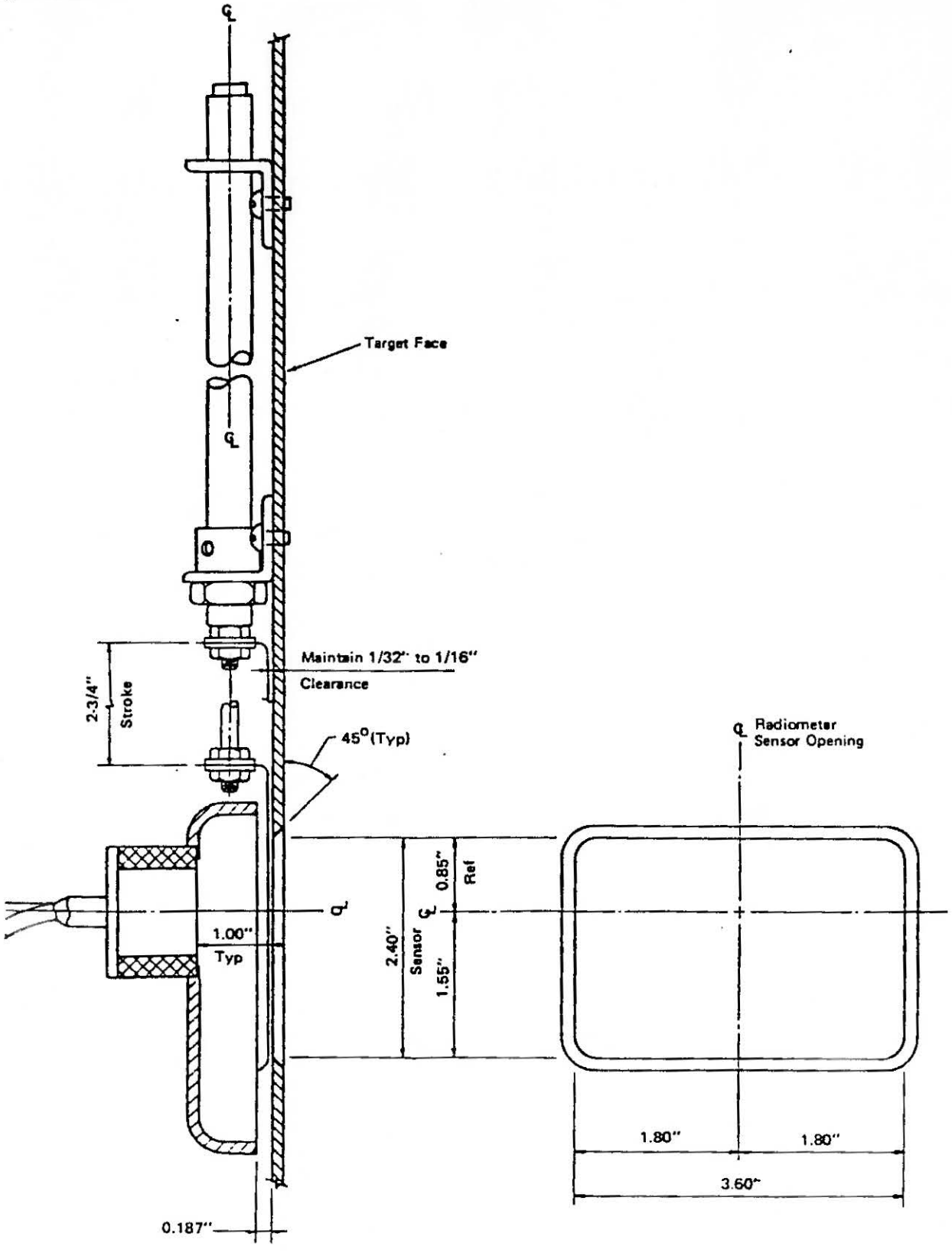

APPENDIX H

MEDTHERM RADIOMETER

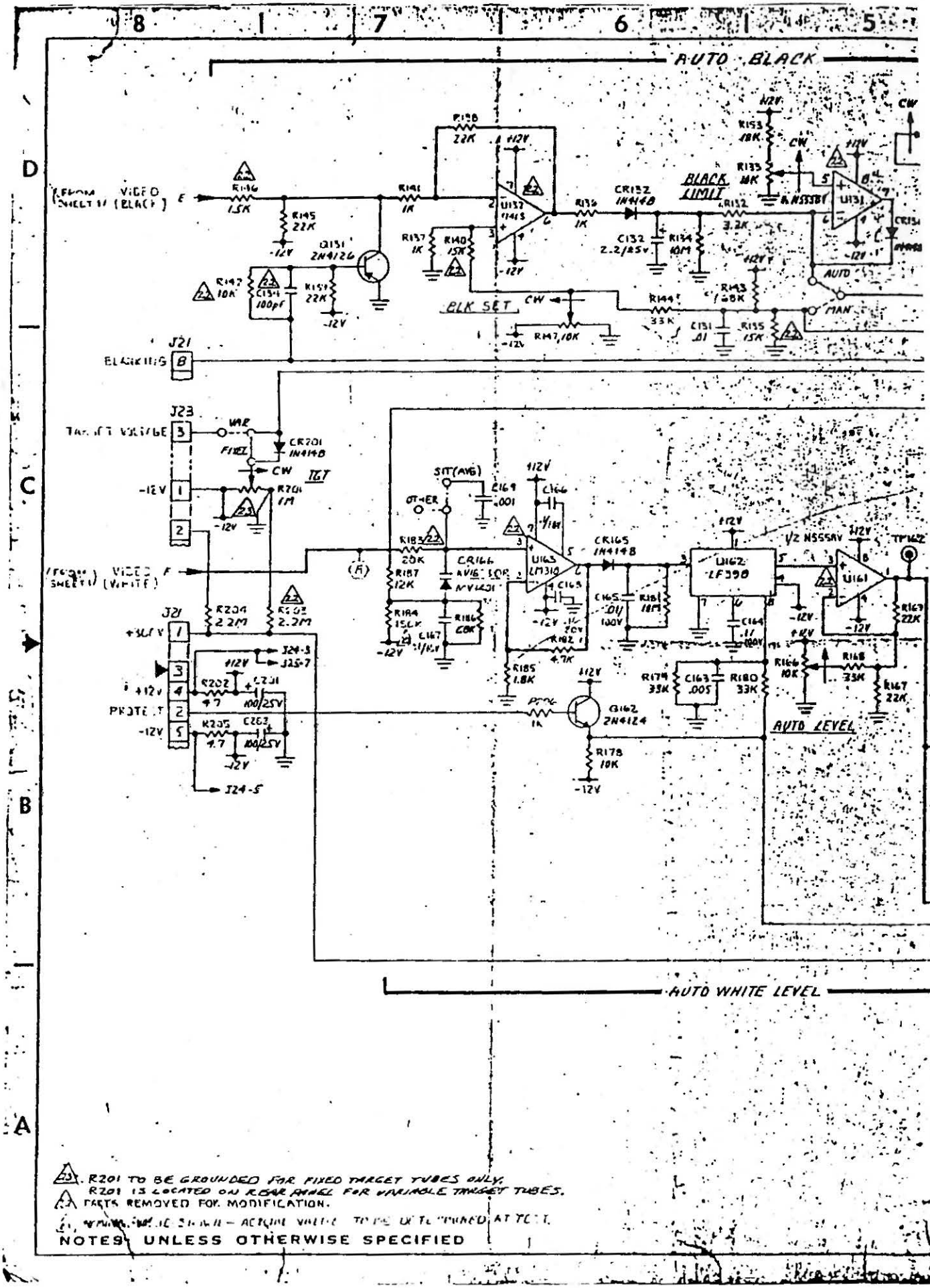

△23. R201 TO BE GROUNDED FOR FIXED TARGET TUBES ONLY. R201 IS LOCATED ON REAR ANGLE FOR VARIABLE TARGET TUBES.

△22 PARTS REMOVED FOR MODIFICATION.

△21 WHEN [illegible] IS SHOWN — ACTUAL VALUE TO BE DETERMINED AT TEST.

NOTES: UNLESS OTHERWISE SPECIFIED

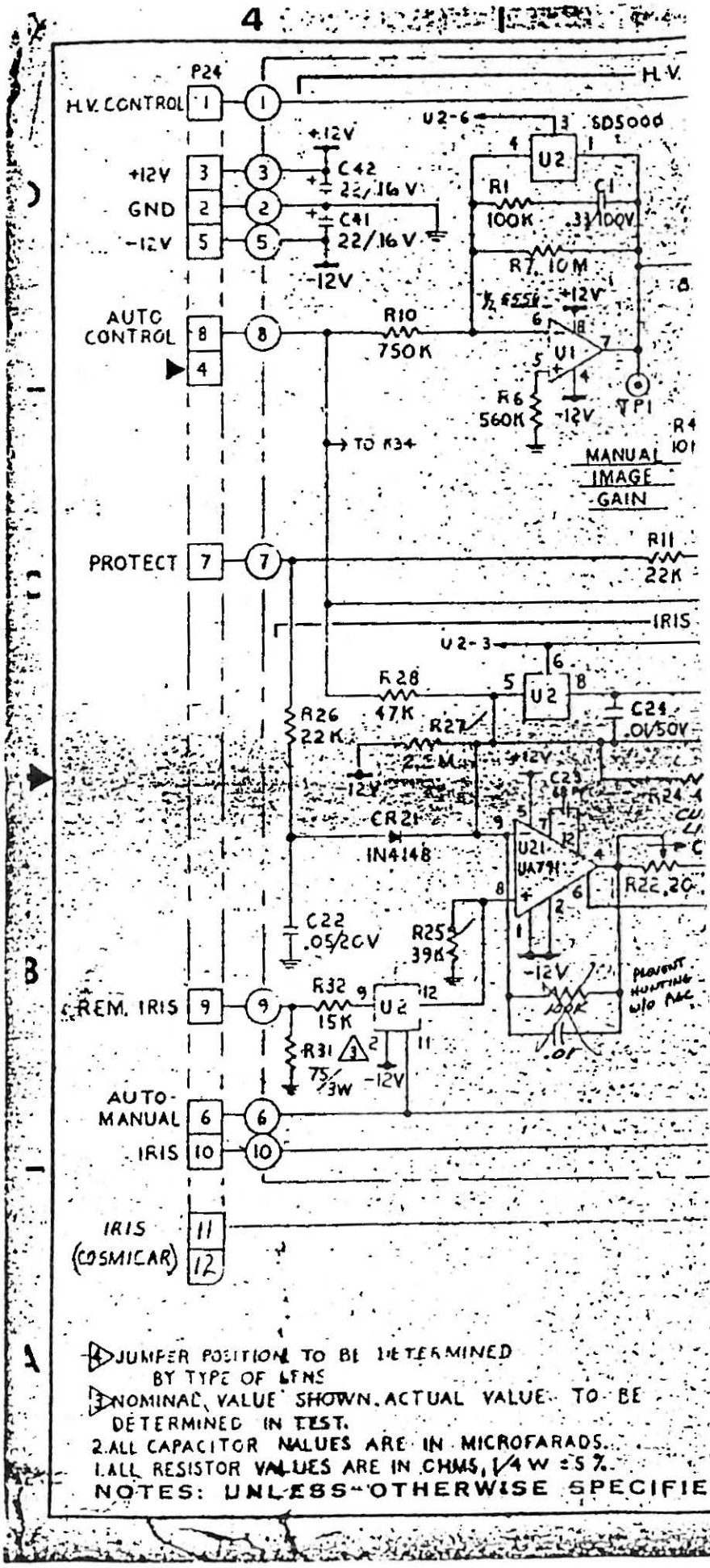
4
P24
H.V. CONTROL 1
+12V 3
GND 2
-12V 5
AUTO CONTROL 8
4
PROTECT 7
REM. IRIS 9
AUTO-MANUAL 6
IRIS 10
IRIS (COSMICAR) 11
12
H.V.
+12V
C42 22/16V
C41 22/16V
-12V
U2-6
SD5000
U2
R1 100K
C1 .33/100V
R7 10M
1/4 6556
R10 750K
U1
R6 560K
TP1
TO R34
MANUAL IMAGE GAIN
R11 22K
IRIS
U2-3
R28 47K
R26 22K
R27 2.2M
C24 .01/50V
C23
CR21 IN4148
U21 UA791
R22 20
C22 .05/20V
R25 39K
R32 15K
R31 75/3W
PREVENT HUNTING W/O AGC
100K
.05
JUMPER POSITION TO BE DETERMINED BY TYPE OF LENS
NOMINAL VALUE SHOWN. ACTUAL VALUE TO BE DETERMINED IN TEST.
2. ALL CAPACITOR VALUES ARE IN MICROFARADS.
1. ALL RESISTOR VALUES ARE IN OHMS, 1/4 W ±5%.
NOTES: UNLESS OTHERWISE SPECIFIE

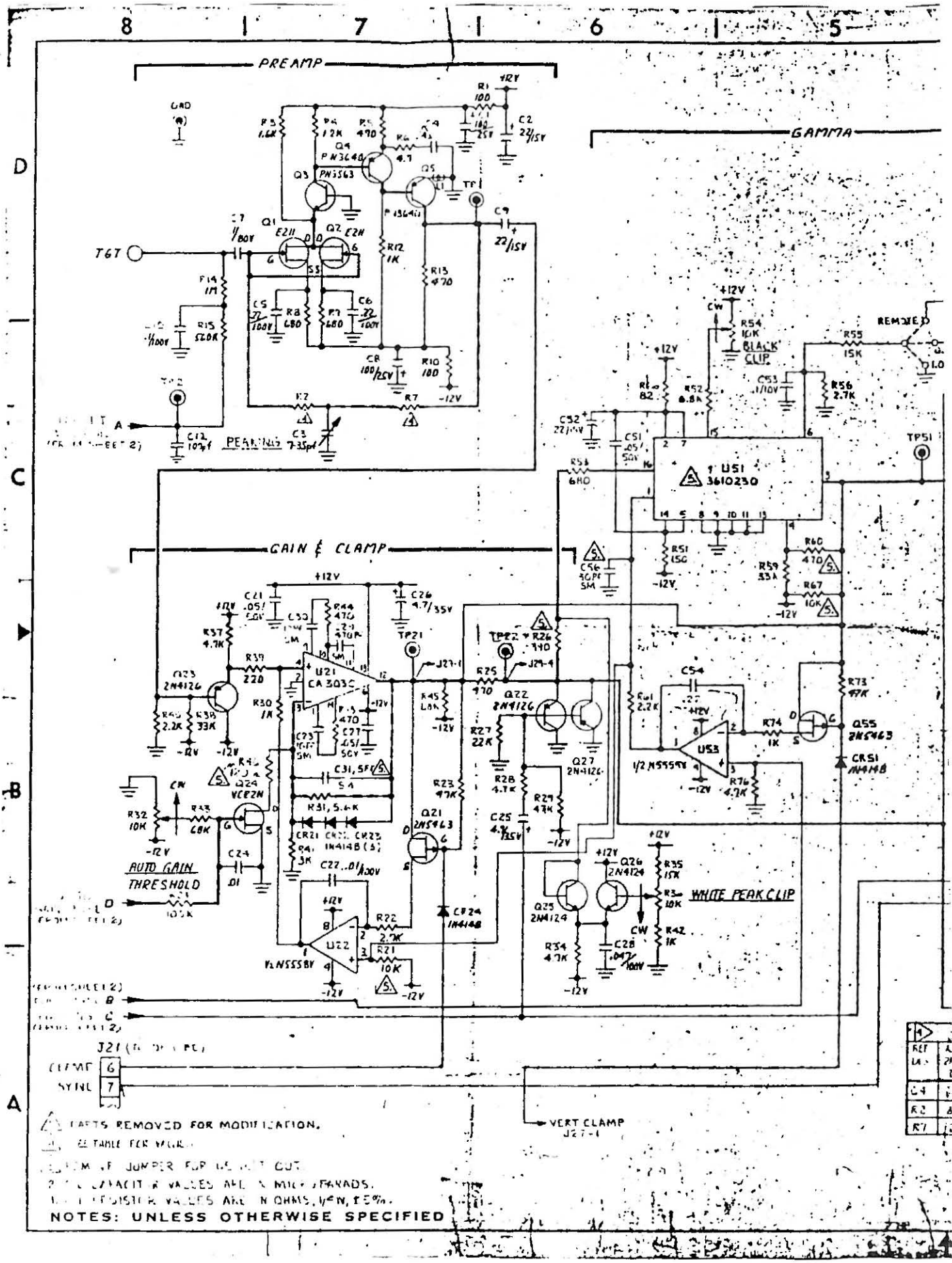
PREAMP
GAMMA
GAIN & CLAMP
PEAKING
AUTO GAIN THRESHOLD
WHITE PEAK CLIP
BLACK CLIP
REMOVED
VERT CLAMP
J27-1
J21
CLAMP
SYNC
NOTES: UNLESS OTHERWISE SPECIFIED
PARTS REMOVED FOR MODIFICATION.

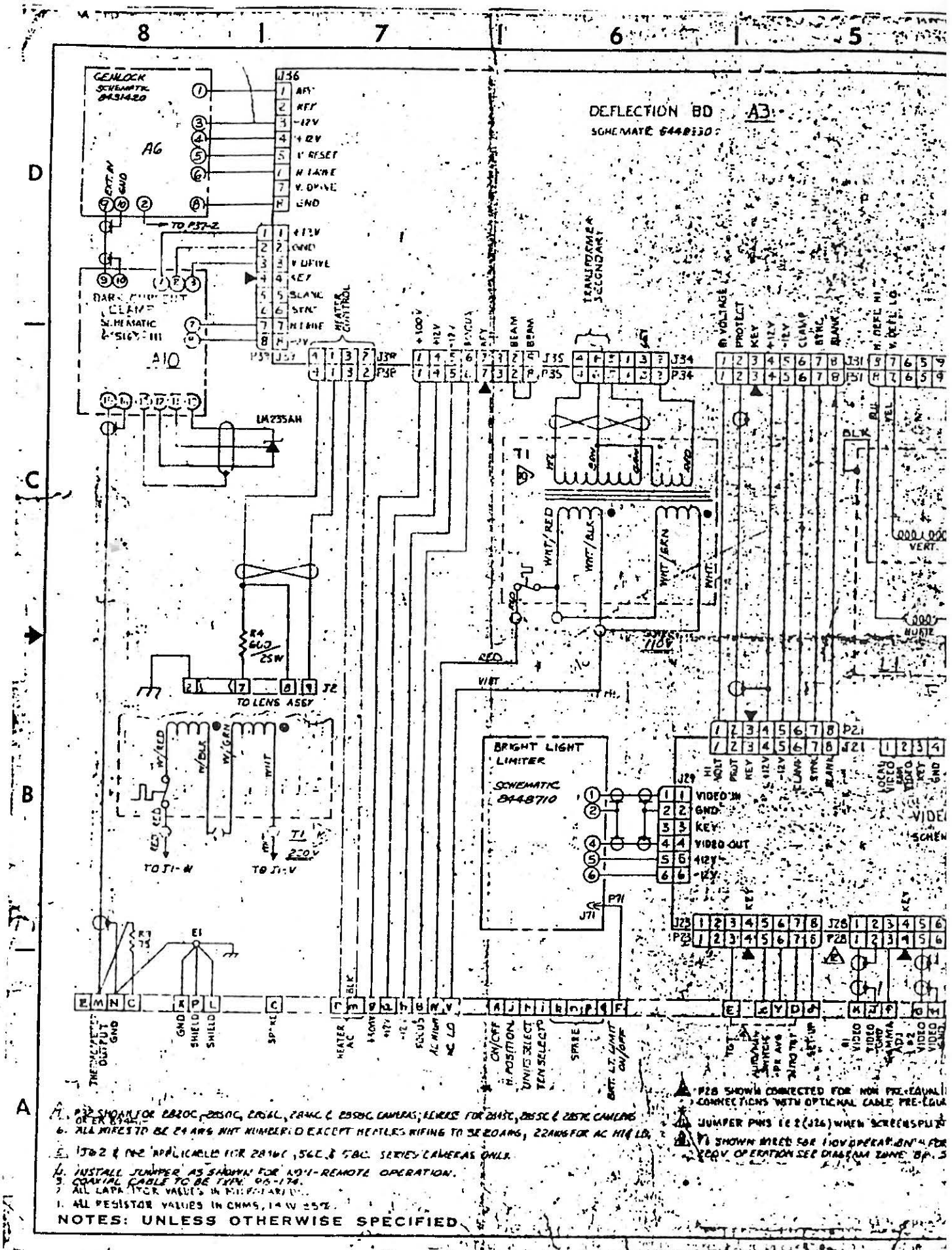
DEFLECTION BD A3
SCHEMATIC 8448530
GENLOCK SCHEMATIC 8431420
A6
J36
A10
LM235AH
R4 680 25W
J2
TO LENS ASSY
TO J1-W
TO J1-V
BRIGHT LIGHT LIMITER
SCHEMATIC 8448710
J29
P71
J71
TRANSFORMER SECONDARY
HEATER CONTROL
VIDEO IN
GND
KEY
VIDEO OUT
+12V
-12V
NOTES: UNLESS OTHERWISE SPECIFIED.
1. ALL RESISTOR VALUES IN OHMS, 1/4 W ±5%.
2. ALL CAPACITOR VALUES IN MICROFARADS.
3. COAXIAL CABLE TO BE TYPE RG-174.
4. INSTALL JUMPER AS SHOWN FOR NON-REMOTE OPERATION.
5. J3 & J42 APPLICABLE FOR 284C, 56C & 58C SERIES CAMERAS ONLY.
6. ALL WIRES TO BE 24 AWG WHT NUMBERED EXCEPT HEATERS WIRING TO BE 20 AWG, 22 AWG FOR AC HI & LO.
7. J42 SHOWN FOR 282OC, 283OC, 283SC, 284SC & 285OC CAMERAS; REVERSE FOR 284SC, 285SC & 285TC CAMERAS OR ER 8442.

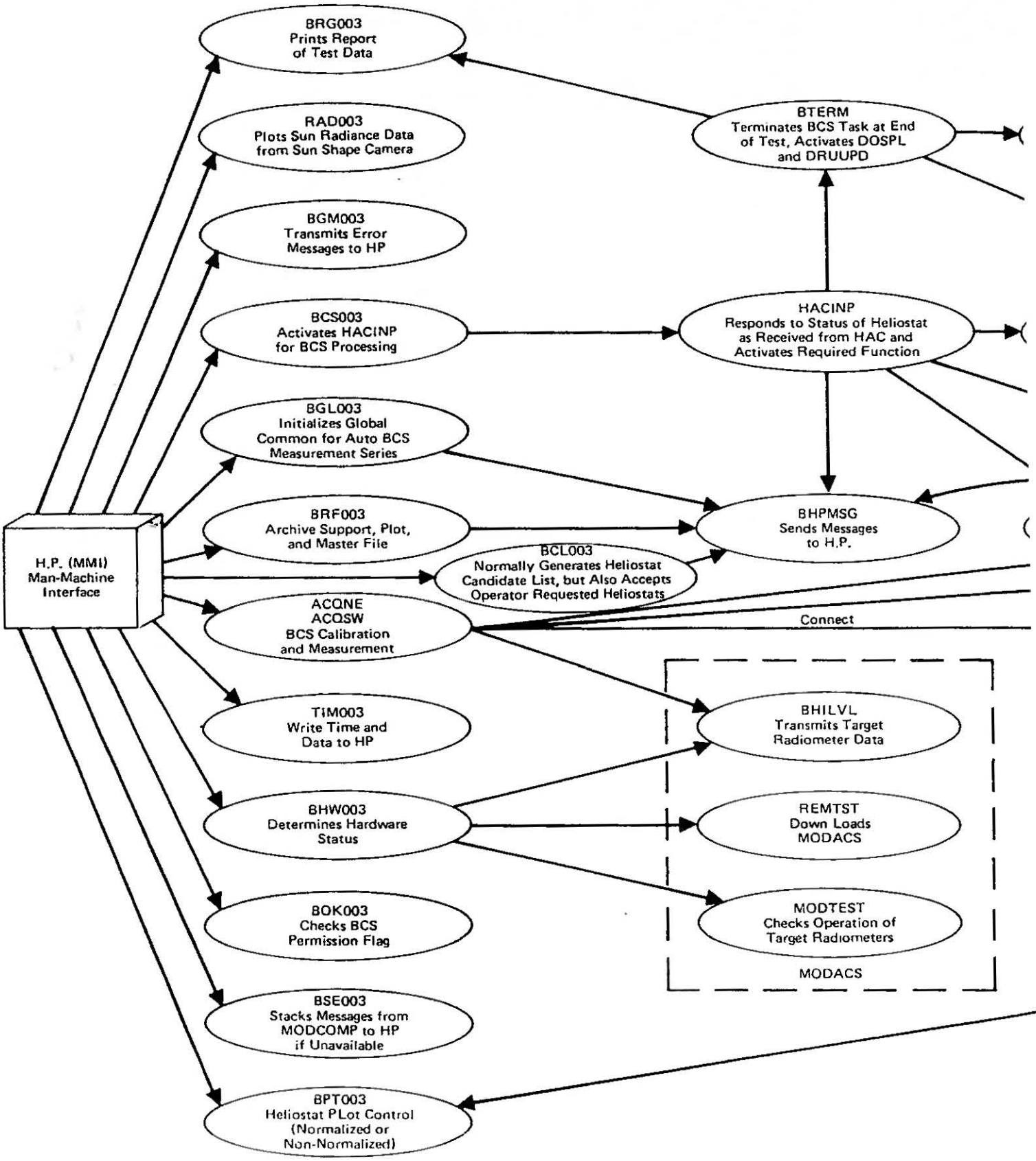
BRG003
Prints Report
of Test Data
RAD003
Plots Sun Radiance Data
from Sun Shape Camera
BGM003
Transmits Error
Messages to HP
BCS003
Activates HACINP
for BCS Processing
BGL003
Initializes Global
Common for Auto BCS
Measurement Series
BRF003
Archive Support, Plot,
and Master File
BCL003
Normally Generates Heliostat
Candidate List, but Also Accepts
Operator Requested Heliostats
ACQNE
ACQSW
BCS Calibration
and Measurement
TIM003
Write Time and
Data to HP
BHW003
Determines Hardware
Status
BOK003
Checks BCS
Permission Flag
BSE003
Stacks Messages from
MODCOMP to HP
if Unavailable
BPT003
Heliostat PLot Control
(Normalized or
Non-Normalized)
H.P. (MMI)
Man-Machine
Interface
BTERM
Terminates BCS Task at End
of Test, Activates DOSPL
and DRUUPD
HACINP
Responds to Status of Heliostat
as Received from HAC and
Activates Required Function
BHPMSG
Sends Messages
to H.P.
Connect
BHILVL
Transmits Target
Radiometer Data
REMTST
Down Loads
MODACS
MODTEST
Checks Operation of
Target Radiometers
MODACS

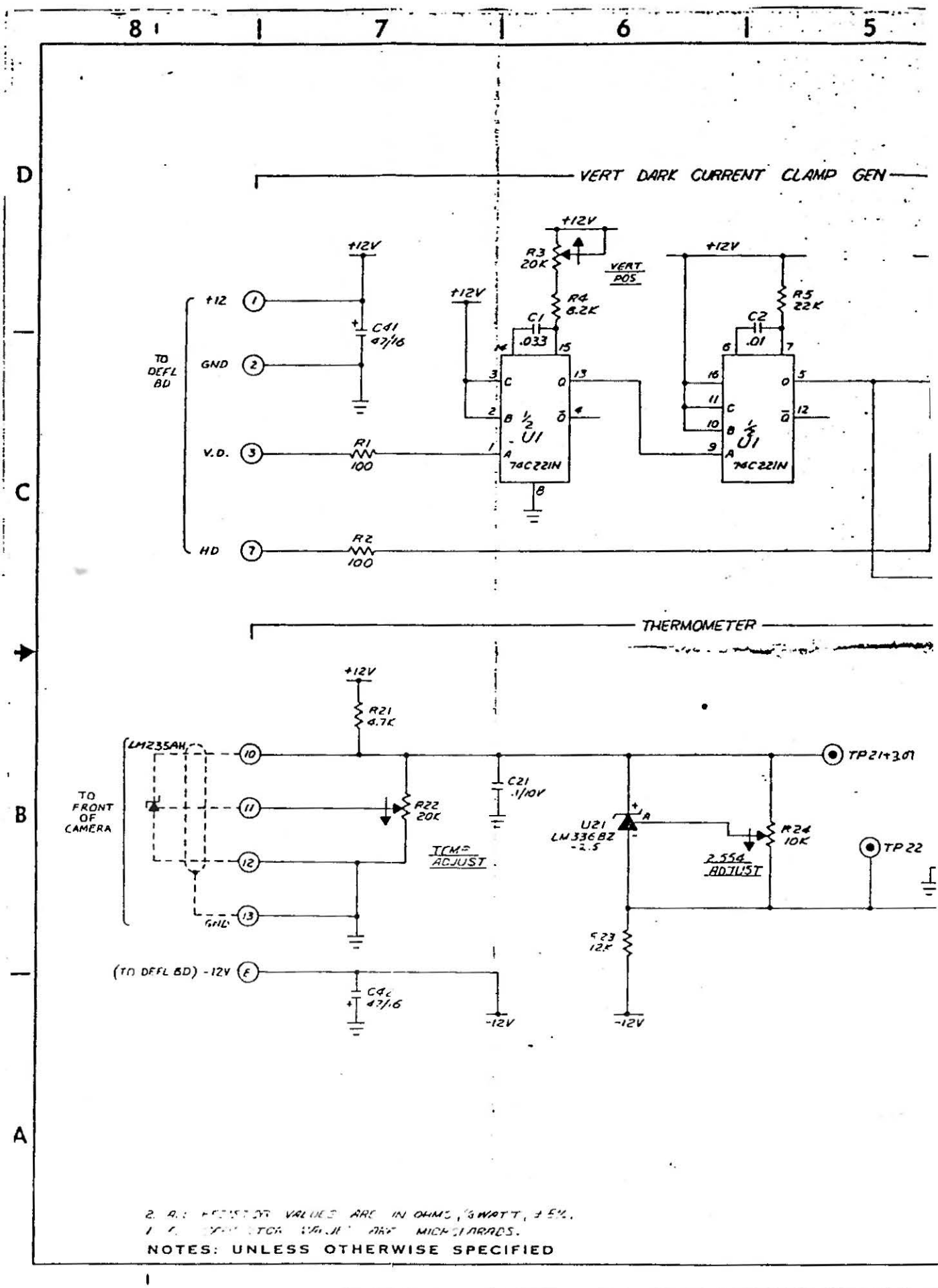
8
7
6
5
D
C
B
A
VERT DARK CURRENT CLAMP GEN
+12V
R3 20K
VERT POS
R4 6.2K
C1 .033
R5 22K
C2 .01
C41 47/16
+12
GND
V.D.
HD
TO DEFL BD
R1 100
R2 100
74C221N
U1
THERMOMETER
R21 4.7K
LM235AH
TO FRONT OF CAMERA
R22 20K
TCMS ADJUST
C21 .1/10V
U21 LM336BZ -2.5
R24 10K
2.55V ADJUST
TP21+30V
TP22
R23 12K
(TO DEFL BD) -12V
C42 47/16
-12V
2. ALL RESISTOR VALUES ARE IN OHMS, ¼ WATT, 5%.
1. ALL CAPACITOR VALUES ARE MICROFARADS.
NOTES: UNLESS OTHERWISE SPECIFIED